AD-A171 541 RESILIENT MODULUS OF FREEZE-THAW AFFECTED GRANULAR SOILS FOR PAVEMENT DES..(U) COLD REGIONS RESEARCH AND ENGINEERING LAB HANOVER NH D M COLE ET AL. JUL 86 1/1

UNCLASSIFIED CRREL-86-4 DOT/FAA/PM-84/16-1 FHWA-8-3-0187 F/G 8/13 NL

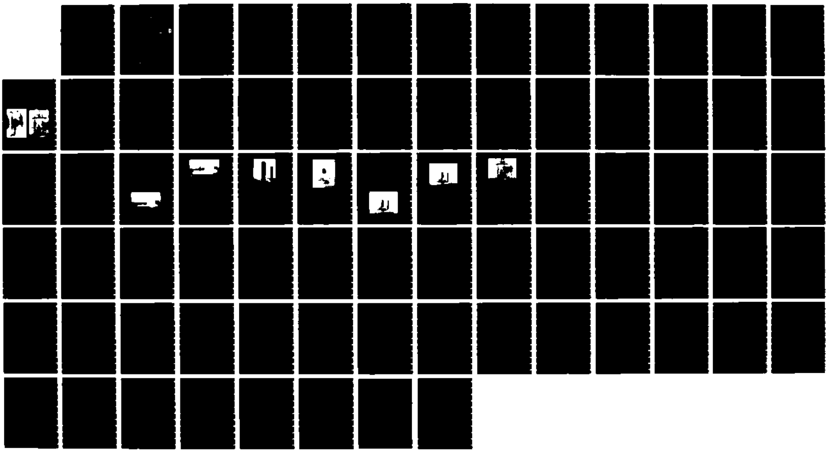

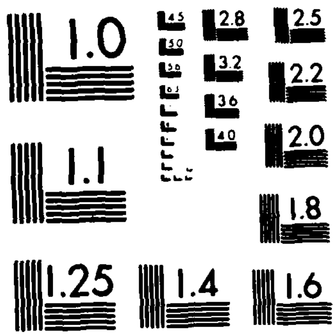

MICROCOPY RESOLUTION TEST CHART

AD-A171 541

DOT/FAA/PM-84/16,I

Program Engineering
and Maintenance Service
Washington, D.C. 20591

Resilient Modulus of Freeze-Thaw Affected Granular Soils for Pavement Design and Evaluation

Part 1. Laboratory Tests on Soils from Winchendon, Massachusetts, Test Sections

D. Cole
D. Bentley
G. Durell
T. Johnson

U.S. Army Cold Regions Research and
Engineering Laboratory
Hanover, New Hampshire 03755-1290

July 1986

This document is available to the public
through the National Technical Information
Service, Springfield, Virginia 22161

U.S. Department of Transportation
Federal Aviation Administration

86 8 ...

Technical Report Documentation Page

1. Report No.	2. Government Accession No.	3. Recipient's Catalog No.
DOT/FAA/PM-84/16, I	ADA 171541	

4. Title and Subtitle	5. Report Date
RESILIENT MODULUS OF FREEZE-THAW AFFECTED GRANULAR SOILS FOR PAVEMENT DESIGN AND EVALUATION. Part 1: Laboratory Tests on Soils from Winchendon, Massachusetts, Test Sections	July 1986
	6. Performing Organization Code
7. Author(s)	8. Performing Organization Report No.
D. Cole, D. Bentley, G. Durell and T. Johnson	CRREL Report 86-4
9. Performing Organization Name and Address	10. Work Unit No. (TRAIS)
U.S. Army Cold Regions Research and Engineering Laboratory Hanover, New Hampshire 03755-1290	11. Contract or Grant No. FHWA 8-3-0187
	13. Type of Report and Period Covered
12. Sponsoring Agency Name and Address	
U.S. Department of Transportation Federal Aviation Administration Program Engineering and Maintenance Service Washington, DC 20591	14. Sponsoring Agency Code

15. Supplementary Notes

Co-sponsored by: Federal Highway Administration, Washington, DC
Office of the Chief of Engineers, U.S. Army, Washington, DC

16. Abstract

This work is the first of a series of four reports about laboratory and field testing of various granular road and airfield subgrades. This report details the acquisition, testing and analysis of six soils from a test site in Winchendon, Massachusetts. Repeated load triaxial tests were done on frozen and thawed soils to characterize the variations in their resilient properties throughout the seasons. Linear regression yielded empirical equations relating the resilient modulus to applied stress, unfrozen water content (for frozen soils), moisture tension (for thawed soils) and density. Equipment and test procedures (given in detail) were developed that allowed simulation in the laboratory of the gradual recovery of stiffness that occurs in the field after thawing. The resilient moduli were strongly dependent on soil state, dropping at least two orders of magnitude upon thawing. For all soils the moduli increased with increasing confining stress, generally decreased with increasing principal stress ratio, and increased with increasing moisture tension levels. The resilient moduli increased by a factor of approximately two as the materials recovered from the effects of a freeze-thaw cycle. This recovery process is well modeled as a function of soil moisture tension level. The stress sensitivity did not appear to be a function of the soil moisture tension level. The report also includes tabulations of all the repeated load triaxial test data.

17. Key Words	18. Distribution Statement
Airfields, Freezing-thawing, Laboratory tests, Repeated-load-triaxial tests, Resilient moduli, Roads, Soil tests, Subgrade soils	This document is available to the public through the National Technical Information Service, Springfield, Virginia 22161.

19. Security Classif. (of this report)	20. Security Classif. (of this page)	21. No. of Pages	22. Price
Unclassified	Unclassified	75	

Form DOT F 1700.7 (8-72) Reproduction of completed page authorized

A

PREFACE

This report was prepared by David M. Cole, Research Civil Engineer, Applied Research Branch, Experimental Engineering Division; Diane L. Bentley, Research Civil Engineer, Civil Engineering Research Branch, Experimental Engineering Division; Glenn D. Durell, Mechanical Engineering Technician, Engineering and Measurement Services Branch, Technical Services Division, and Thaddeus C. Johnson, Civil Engineer and Chief of the Civil Engineering Research Branch, Experimental Engineering Division, U.S. Army Cold Regions Research and Engineering Laboratory.

This report covers certain aspects of a project partially funded by the Federal Highway Administration and the Federal Aviation Administration, and the Office of the Chief of Engineers through DA Project 4A762730AT42, *Design, Construction and Operations Technology for Cold Regions;* Task A2, *Soils and Foundations Technology/Cold Regions;* Work Unit 004, *Seasonal Change in Strength and Stiffness of Soils and Base Courses.*

The work was done at CRREL and a number of people contributed to the successful conclusion of this area of the project. The authors acknowledge in particular the assistance of E. Chamberlain who was closely involved in equipment development, D. Carbee, for his help in specimen preparation, D. Keller who assisted in field coring and sample preparation, L. Irwin for helpful discussions of the test results, J. Ingersoll who was responsible for generating the moisture characteristic curves and who assisted in the development of the tensiometer systems, and A. Tice who generated the unfrozen water content data for the test soils.

This report was technically reviewed by E.J. Chamberlain and J.A. Richter-Menge of CRREL.

CONTENTS

ILLUSTRATIONS

TABLES

NOMENCLATURE

a, b	regression constants
A_i	regression constant
c_i	regression constant
f	frequency
$f(\psi)$	$[(101.36-\psi)/\psi_o]$, moisture tension function
$f(\sigma)$	normalized stress parameter
J_1	$\sigma_1+\sigma_2+\sigma_3$, first stress invariant
J_2	$\sigma_1\sigma_2+\sigma_2\sigma_3+\sigma_1\sigma_3$, second stress invariant
K_1	coefficient of stress term in nonlinear expression for M_r; can be a function of ψ or γ_d, or both
K_2	constant, exponent of stress term in nonlinear expression for M_r
M_r	resilient modulus
T	normalized temperature
w_t	total water content
w_u	unfrozen water content
γ_d	dry density of soil
γ_o	unit density
θ	temperature
θ_o	reference temperature
μ_r	resilient Poisson's ratio
σ_0	reference stress
σ_1	first principal stress $=\sigma_3+\sigma_d$ (in these tests)
σ_3	third principal stress, confining pressure $=\sigma_2$ (in these tests)
σ_1/σ_3	principal stress ratio
σ_d	cyclic axial stress or deviator stress
τ_{oct}	$\frac{1}{3}[(\sigma_1-\sigma_2)^2+(\sigma_2-\sigma_3)^2+(\sigma_1-\sigma_3)^2]^{\frac{1}{2}}$
ψ	soil moisture tension
ψ_o	reference stress

Resilient Modulus of Freeze-Thaw Affected Granular Soils for Pavement Design and Evaluation

Part 1. Laboratory Tests on Soils from Winchendon, Massachusetts, Test Sections

D. COLE, D. BENTLEY, G. DURELL AND T. JOHNSON

INTRODUCTION

Over the past few years, CRREL has been developing a method for the design of road and airfield subgrades subjected to seasonal frost. The method addresses both the frost heave characteristics and the resilient properties of the pavement systems. In order to investigate these areas of pavement system performance, an approach of laboratory testing and field verification was adopted. For the case of the resilient properties, repeated-load triaxial tests provided laboratory data and these were verified in the field through plate loading tests.

This report discusses the methods used to generate and analyze the laboratory data from repeated-load triaxial tests. This includes retrieval and preparation of frozen and thawed cores, laboratory preparation of material that could not be cored, equipment and procedures for triaxial testing, and data reduction and analysis. The equipment and testing procedure sections detail certain unique developments in triaxial testing hardware and the use of soil moisture tension in the testing program.

The data presented in this report are for soils used in six of the pavement test sections at a Massachusetts Department of Public Works research site in Winchendon, Massachusetts. Data from several of these soils have been published elsewhere (Cole et al. 1981) but are included here for completeness. Also, since refinements have been made on previously published triaxial testing methods (Johnson et al. 1978), the most recent procedures are given in their entirety.

To make necessary distinctions among certain soil conditions peculiar to the study of frost effects, we have developed the following terminology. "Frozen" refers to material in which the soil moisture is at least partially frozen. "Thawed" indicates material that has been frozen either in nature or in the laboratory and subsequently thawed in the triaxial device, with no remolding. The thawed condition includes the post thaw period in which the resilient modulus gradually increases. "Recovered" refers to the soil state after all transient effects of a freeze-thaw cycle have abated. Soil cores taken in the fall, prior to any frost action, are thus classified as recovered.

The testing requirements call for characterizing the resilient properties of the soils under conditions representative of a full year's cycle of freeze, thaw and recovery. Wherever possible, this was done using field cores. In some cases however, most notably for the coarsest of the six soils (Dense Graded Stone), it was necessary to mold and freeze specimens in the laboratory.

For the frozen soil, we determined the resilient properties for various levels of applied stress at temperatures between about -10° to -0.5°C. For thawed and recovered soils, we varied the soil moisture tension level and the resilient properties were again determined at various levels of applied stress. The use of moisture tension as the pertinent soil characteristic stems from its importance in governing the strength-recovery phase. The use of moisture tension is convenient since it can be monitored continuously in both the field and the laboratory (see Ingersoll 1981).

Finally, we used linear regression techniques to generate empirical equations that give the resilient modulus in terms of applied stresses and either moisture tension or temperature, depending upon soil state.

BACKGROUND

A great deal of effort has been spent at CRREL in understanding the effects of freezing and thawing on the strength of soil. Work has focused on laboratory testing techniques, primarily the repeated-load triaxial test, and full-scale testing of pavement systems using surface deflection methods. As mentioned above, the field tests are used to verify the laboratory findings. A computer program for layered elastic analysis links the laboratory and field results—details of the computer program are given elsewhere (Irwin and Johnson 1981).

The use of a layered analysis program for the design or evaluation of pavements requires a model for the resilient modulus of each layer in the system (see Cole et al. 1981), and also values for Poisson's ratio, density and layer thickness. Using this input, the program calculates stresses, strains and surface deflections under a given load. A modified version of the program back-calculates layer properties given system geometry and surface deflection characteristics. The laboratory work generates models for the resilient modulus of each layer in the system. These laboratory-generated models must be valid through the complete cycle of freeze, thaw and recovery. To this end, the models must incorporate the effect of varying temperature for the frozen state, and soil moisture, stress and density for the unfrozen states.

The results of field observations provide us with information on the temperatures and moisture tension profiles of the test sections. Analysis of the frozen and recovered cores taken from the test sections provides an indication of the likely changes in density through an annual cycle. The layered elastic analysis program calculates the stress distribution throughout the soil mass under a suitable surface load and thus provides an indication of the range in stress that the laboratory test must address.

An advantage of this approach, in which moisture tension is used as a link between laboratory and field results, is that it gives us a relatively convenient means of monitoring the rate of recovery of the soil after thawing. Moisture tension is monitored in the field during recovery and the observed trends are reproduced in the laboratory specimens. Triaxial tests are conducted during this simulated recovery, and the resilient properties can thus be determined at several points during the recovery period. Tensiometers have been developed that are capable of operating in the field environment (Ingersoll 1981) and similar devices have been incorporated into our triaxial cells (Cole et al., in press).

Our method of repeated-load triaxial testing—cycling axial stress while holding the confining stress constant—has been widely used. It allows us to find the resilient modulus in a number of stress states, but does not allow for a completely accurate simulation of the actual stress path experienced by the soil in the test section (see Brown and Pappin 1981).

MODELING THE RESILIENT MODULUS

A true triaxial repeated-load test would allow independent control of the three principal stresses and would provide the most realistic simulation of the actual stress states experienced by the soil. This type of test, however, is fraught with difficulties and thus not frequently attempted. Cycling of both the axial and confining pressures in a standard repeated-load triaxial test, on the other hand, more closely approximates the in situ stress conditions we are attempting to model. Pappin and Brown (1980) have demonstrated the effect on the resilient modulus of cyclic confining pressure and have used that capability to investigate the effect of the stress path on crushed rock specimens. The result is a more generalized, and more complicated, model for the resilient response, which is suitable for numerical analyses.

In the present work, given our inability to test for resilient response under generalized conditions, we model the resilient modulus M_r in the more simple nonlinear form given in eq 1.

$$M_r = K_1[f(\sigma)]^{K_2} \tag{1}$$

where K_1 and K_2 are constants for a given soil state and $f(\sigma)$ is a stress parameter normalized to a reference stress σ_0 of 1.0 kPa.

We do, however, elaborate somewhat on the basic model by making the coefficient K_1 a function of moisture tension and, in some cases, dry density. We also take some liberty in the form of the stress function $f(\sigma)$, developing models based not only on the bulk stress (the first stress invariant) but also on a ratio of the second stress invariant to the octahedral shear stress.

The significance of moisture tension in modeling resilient response is now generally recognized (Bergen and Monismith 1973, Fredlund et al. 1975, Brown and Pappin 1981, Cole et al. 1981,

Rada and Witczak 1981). Fredlund et al. (1975) stressed the fundamental importance of including the pore air and pore water stress states as well as the applied stress in the development of a resilient modulus model. Since in a field situation the pore air pressure will tend to equal atmospheric pressure (Fredlund et al. 1975), it can be considered essentially as a constant. This leaves us to consider, apart from the externally applied stresses, only the effect of pore water pressure. Generally, negative pore water pressure is considered and referred to as moisture tension.

Examination of our data showed that the stress function exponent K_2 is statistically independent of the moisture tension (Cole et al. 1981). Furthermore, we found that the effect of moisture tension on the resilient modulus could be adequately represented by making K_1 a function of moisture tension. In the regression expressions employing the moisture tension, we use the term $f(\psi)^{A_1}$ where A_1 is a regression constant and

$$f(\psi) = \frac{101.36-\psi}{\psi_0} .$$

The value 101.36 represents atmospheric pressure in kPa, ψ is moisture tension in kPa (expressed as a positive number) and ψ_0 is a reference stress of 1.0 kPa.

Given appropriate conditions, the more frost-susceptible soils will undergo more heave. The moisture uptake associated with frost heaving generally results in a decrease in the soil density along with an increase in moisture content, possibly to the point of complete saturation. This occurred to varying degrees in the test soils, depending on their level of frost susceptibility (see Chamberlain 1983). Upon thawing, the moisture tension is generally near zero, while during subsequent recovery we find a continuing increase in ψ (decrease in the moisture content) and an increase in dry density. Densification takes place not only upon thaw as the soil consolidates and any pore water pressure dissipates, but also under the action of the cyclic loads imposed during testing. For certain soils (Ikalanian and Hart Brothers sand) it was necessary to address the effect of this density change on the resilient modulus. When this was necessary, a factor consisting of dry density raised to a power was introduced in the regression equation. We interpret this factor, when present, as a component of K_1 along with the moisture tension term.

The use of dry density in the regression equation complicates matters somewhat since it requires knowledge of the state of the subgrade that is not conveniently obtained. In the case of moisture tension, field gauges can provide year-round information and thus sensible values can be readily obtained. Such is not the case with subgrade density, however, since accurate values can only be obtained by actually sampling the soil, a task which would be unduely expensive and time consuming. As an alternative, we have used the density of the laboratory-tested soil samples to estimate the density changes expected during recovery. We will see below that it was not necessary to include the density term in many analyses since it did not change significantly for most soils tested.

TEST SECTIONS AND MATERIALS

The test soils come from experimental pavement sections at a site in Winchendon, Massachusetts, which was constructed in 1978 by the Massachusetts Department of Public Works. There are 24 test sections; each measures 2.4 m square. Table 1 gives some physical characteristics of the six soils chosen for the present study. Each section consist-

Table 1. Physical properties of test soils.

Soil	Coefficients* Cu	Coefficients* Cc	Atterberg limits LL	Atterberg limits PI	Specific gravity
Dense Graded Stone	32.8	7.1	23	3	2.81
Graves sand	39.1	1.6	0	0	2.70
Hart Brothers sand	8.0	0.92	0	0	2.76
Hyannis sand	4.7	1.2	0	0	2.67
Ikalanian sand	4.5	0.96	0	0	2.70
Sibley till	235	4.1	19	4	2.74

* Cu—coefficient of uniformity, Cc—coefficient of curvature.

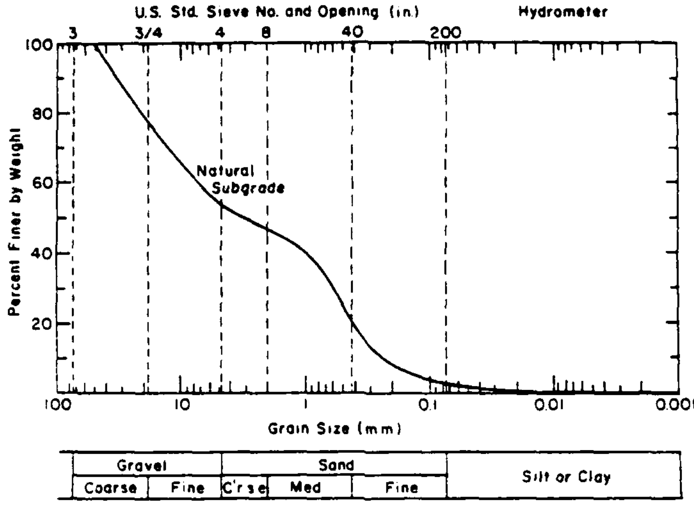

a. Natural subgrade.

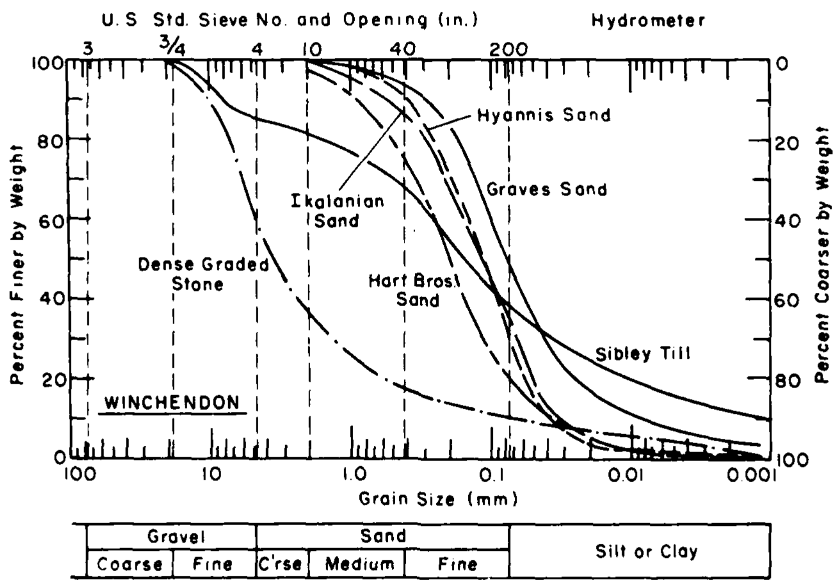

b. Six test soils.

Figure 1. Gradation curves.

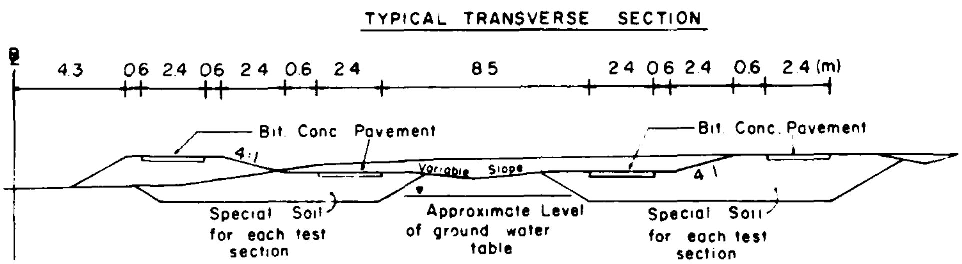

Figure 2. Cross section of the Winchendon test site.

ed of 50–90 mm of asphalt concrete and 1.5 m of the test soil overlying the natural subgrade, which was a clean, gravelly sand. Figure 1 shows gradation curves for these materials.

Figure 2 shows a cross section of the test site. Note that the construction of the test sections results in two different depths to the water table. All the sections considered in this work were from the sections having the higher elevation. For these sections, the water table is at a depth of 1.4 m below the pavement surface.

Frost penetrated the test soils to depths ranging between 0.5 and 0.8 m. Although freezing rates varied considerably, the overall average was in the range of 7.0 to 8.0 mm per day.

FIELD SPECIMEN RETRIEVAL AND PREPARATION

Most test sections were sampled in both the frozen and recovered states. Frozen cores were obtained using a double flighted auger designed at CRREL. A 150-mm-diameter core was first taken from the asphalt concrete layer. We used compressed air rather than water to clear debris from the drilling. The soil sampler fit easily through the hole thus prepared and a 50-mm-diameter frozen core of the test soil was then obtained. The core segments were generally 150–300 mm in length. They were wrapped in several layers of polyethylene film with a generous amount of snow and ice to prevent sublimation and to help maintain temperature during shipment back to the laboratory.

Cores representative of the recovered state were taken in the fall using a split tube sampler. The material was left in the 150-mm-long segments of the split aluminum sleeves and kept tightly wrapped in polyethylene film until just before trimming and testing.

Shovel samples of the natural subgrade and the Dense Graded Stone were obtained and specimens of these very coarse-grained materials were prepared in the laboratory.

LABORATORY PREPARATION OF SPECIMENS

Soil

The field cores were tested at the diameter of 50 mm resulting from the coring operation. The cores were cut approximately to length on a band saw and the ends were machined flat and parallel using a lathe. This aspect of specimen preparation is absolutely critical to the acquisition of reliable modulus values for the frozen state. Rough or unparallel specimen ends result in a nonuniform stress distribution in the material and can cause a slight rocking of the specimen when the load is applied. This rocking is detrimental to the precision of the deformation measurements.

The coarse material, which was frozen in the laboratory, required a considerable amount of preparation. The soil was molded in a 150-mm-diameter, 381-mm-high steel mold in five layers with sufficient compactive effort to achieve the estimated in situ density. A sleeve of 22-gauge aluminum, placed in the mold before compaction, provided sufficient confinement to support the specimen once the mold was removed.

For the case of the natural subgrade, which was to be tested only in the unfrozen state (this material never froze in the field test sections), the molded specimen was placed on the base of the triaxial cell. The aluminum sleeve was carefully removed and a latex membrane installed along with the top cap and O-rings. The specimen was then ready for instrumentation and testing.

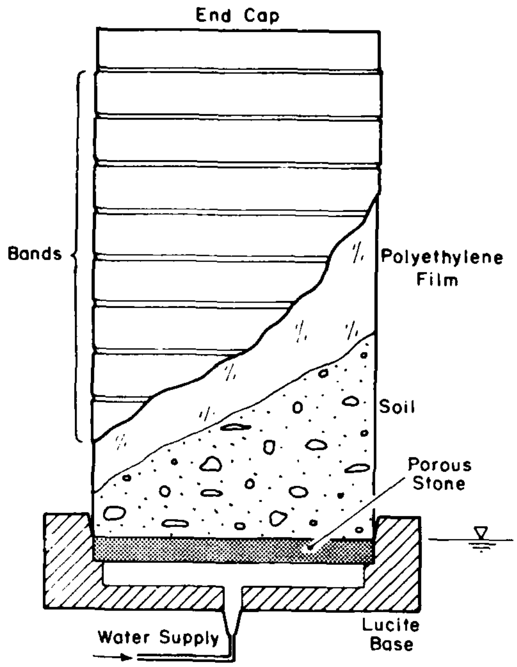

Figure 3. Mounting technique for 152-mm-diameter specimens to be subjected to unidirectional, open system freezing.

The Dense Graded Stone, which was tested in the frozen state, required further attention (Fig. 3). The molded specimen was placed on a special lucite base equipped with a porous stone and a water supply inlet. The sleeve was removed and polyethylene film was wrapped around the specimen several times. Then, specially prepared aluminum belts were placed about the circumference of the specimen and secured by rubber bands. The belts were coated on the inside with an adhesive-backed Teflon film and on the outside with standard duct tape. The polyethelene film prevented evaporation of s. l moisture and the rings provided sufficient lateral confinement to prevent specimen degradation during subsequent handling and freezing. The coatings on the approximately 40-mm-wide belt segments were designed to prevent both side wall friction if there was any heaving and to inhibit unwanted advancement of the freezing front along the sides of the specimen during freezing.

The specimens were frozen unidirectionally at about 25 mm/day in insulated cabinets (see Chamberlain and Carbee 1981) using open-system freezing, i.e., a constant head water supply to the base of the specimen. Once completely frozen, the specimen was removed to a coldroom and the ends were prepared for testing in the following manner. We made a slurry from a portion of the material from which the large aggregates had been removed. The ends of the frozen specimen were then capped employing the same equipment used to cap concrete specimens with a molten sulfur compound. The slurry was placed in the base of the capping jig and allowed to freeze to the soil specimen. This method resulted in smooth, flat specimen ends.

Once the frozen tests were completed, the specimen was thawed in the triaxial device and then retested according to the method given in the *Testing Sequence* section.

Asphalt concrete

In the initial laboratory investigations for this phase of the work, the resilient modulus of the asphalt concrete was measured in indirect tension. Cores 102 mm in diameter were tested in repeated indirect tension at two load durations and at a range in temperature from approximately -10° to 32°C.

To perform cyclic load tests under uniaxial compression, a suitable length-to-diameter ratio was required. We accomplished this by forming a composite cylindrical specimen from three of the 102-mm-diameter, 50- to 90-mm-long cores, yielding a test specimen 200 to 250 mm long. Each core was machined on the top and bottom on a precision grinder so that the ends were smooth and parallel. The ends were then cemented together with a thin layer of asphalt emulsion. Once the composite specimen was assembled, it was bonded and excess emulsion was extruded by applying an axial compressive stress. Five specimens were thus constructed.

These specimens were then tested in unconfined compression at temperatures of -10°, 5°, 25° and 39°C and cyclic axial stresses of 69.0, 103.4, 137.9, 172.4 and 241.3 kPa. Two hundred cycles were applied at each stress level. Three loading wave forms were used: a 1-second pulse applied every 3 seconds, which simulates the load pulse of the repeated plate bearing device; a continuous haversine wave form at 1, 4 and 16 Hz according to ASTM standards (D3497-76T) for testing (ASTM 1981); and a 28-ms haversine pulse every 2 seconds, which simulates the load pulse of the falling weight deflectometer. Tests were performed on the same closed-loop, electro-hydraulic testing machine used for the soil tests. Load was monitored by a load cell mounted on the testing machine piston. Deformation was monitored by two

Linear Variable Differential Transformers (LVDTs) mounted on circumferential clamps at third points along the specimen length. Load and deformation were recorded simultaneously on a strip chart recorder.

EQUIPMENT AND PROCEDURES FOR TRIAXIAL TESTING

Triaxial cells

Special triaxial cells were constructed to accommodate the instrumentation used to monitor load and deformation (see Cole et al., in press). Cells for both the 50- and 150-mm-diameter specimens are shown in Figure 4. In both cells, the top and bottom plates and the cylinder may be removed from the cell base. This facilitates the testing sequence, which calls for several tests on any given specimen. With this arrangement, a specimen need not be disturbed by removing it from its base between tests. Each specimen can remain on its base, with end caps and membranes in place, while the cell and all instrumentation are removed and installed on the next specimen and base. In this way, up to six 50-mm-diameter specimens could be mounted and tested in a rotating sequence without requiring any remounting or handling of the specimen. As will be explained in more detail later, we did several tests on each specimen in order to obtain its resilient properties at several levels of soil moisture tension.

A miniature, high-precision load cell mounted in the triaxial cell on the loading piston monitors the load applied to the specimen and also acts as a feedback source for the testing machine used in this program.

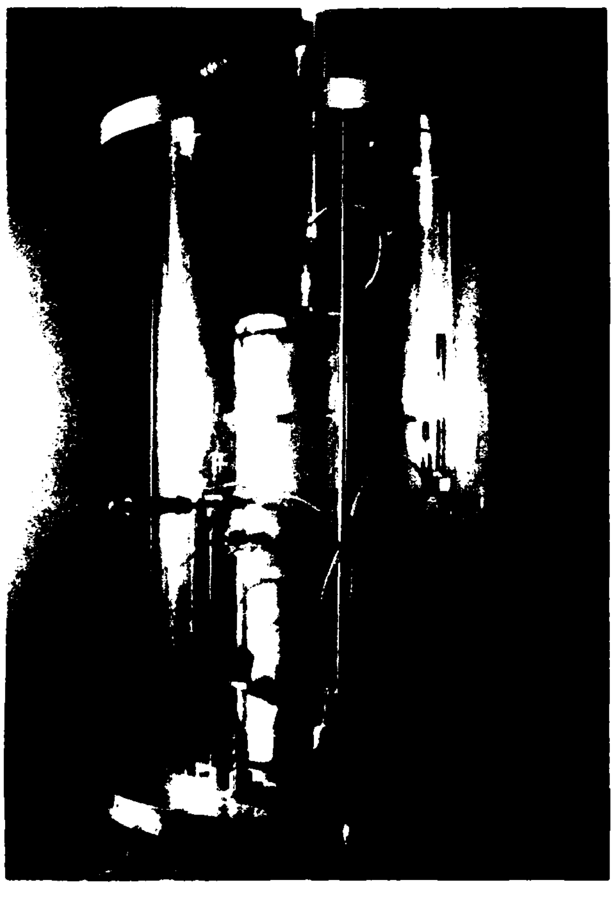

a. 152-mm-diameter specimen in the large triaxial cell.

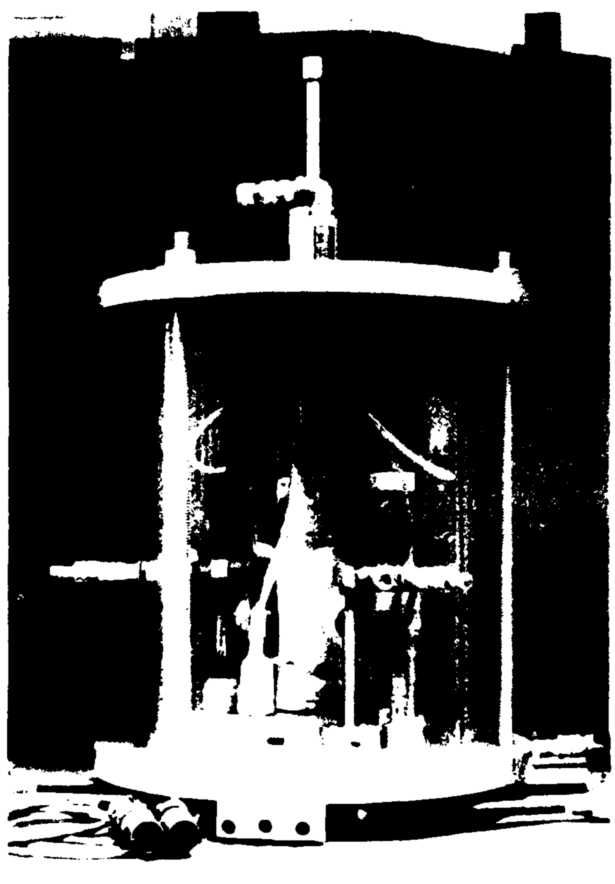

b. 50.8-mm-diameter specimen in the small triaxial cell.

Figure 4. Specimens fully mounted for testing.

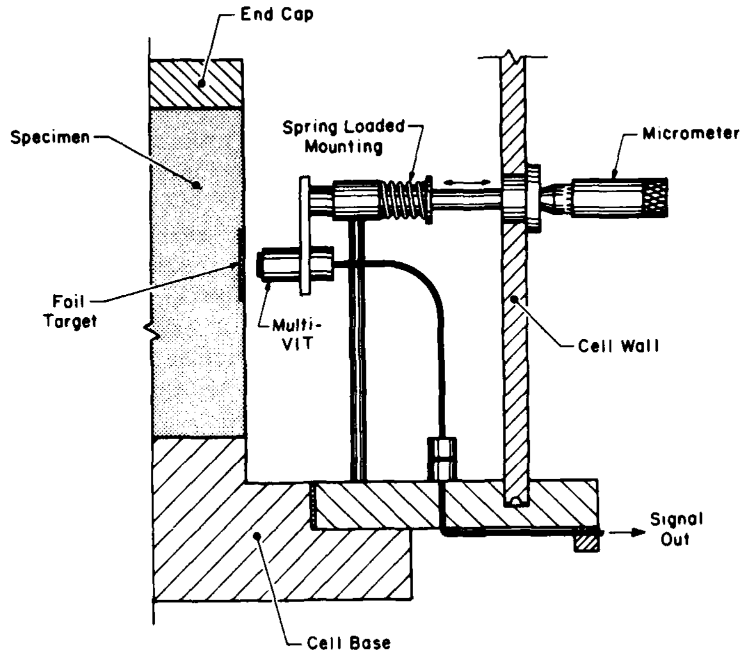

Figure 5. Detail of the multi-VIT mounting. Variable Impedance Transducer is positioned with micrometer.

The axial strain is monitored using four LVDTs mounted on hinged arms. The LVDT cores are mounted on two spring-loaded circumferential rings on the specimen. This system has been described in detail elsewhere and remains unchanged in this work (see Johnson et al. 1978). Some improvements have been made, however, in the system of noncontacting displacement transducers used to measure radial deformation (presented by Cole 1978). As seen in Figure 5, the multi-VITs (Variable Impedance Transducers) are no longer mounted directly on the micrometers located on the cell wall, but are now mounted on standards that bolt to the floor of the triaxial cell. The location of each transducer is still adjusted by a micrometer, which now reacts against the spring-loaded rod to which the transducer is affixed. These devices and the testing and calibration procedures are fully documented in Appendix A.

As mentioned earlier, moisture tension is monitored in these tests as a means of linking laboratory and field results. To facilitate the laboratory triaxial tests across the range of moisture tensions encountered in the field, we developed a special base for the triaxial cell.

Soil moisture is sensed through an element of porous ceramic protruding from the center of the pedestal on which the specimen is mounted (see Fig. 6). These porous tips typically have an air entry value of 100 kPa. A very small diameter duct through the base connects the porous tip to a larger tube on which a vacuum gauge is mounted. The tip and duct system, which has an associated branch that permits flushing to remove air bubbles, is in effect a tensiometer. Once the tip is in contact with the pore water of an unsaturated soil, the stress state of that pore water is transferred to the tensiometer system and registers on the vacuum gauge. In this manner, we continuously monitor the stress state of the soil moisture. This stress increases as water content decreases according to a relationship of the type shown in Figure 7. Moisture retention curves for all test soils appear in Appendix B. Field work indicates that as a soil recovers from a freeze-thaw cycle, it drains and consolidates, and the moisture tension level rises accordingly. This tensiometer system allows us to simulate a controlled recovery period in the triaxial cell by merely draining the specimen until a desired moisture tension level is reached. At that point, the specimen is tested to determine the resilient properties associated with the prevailing moisture tension value; the process is repeated several times, until the highest moisture tension level experienced in the field has been reached. Note that at no time during this testing sequence is it neces-

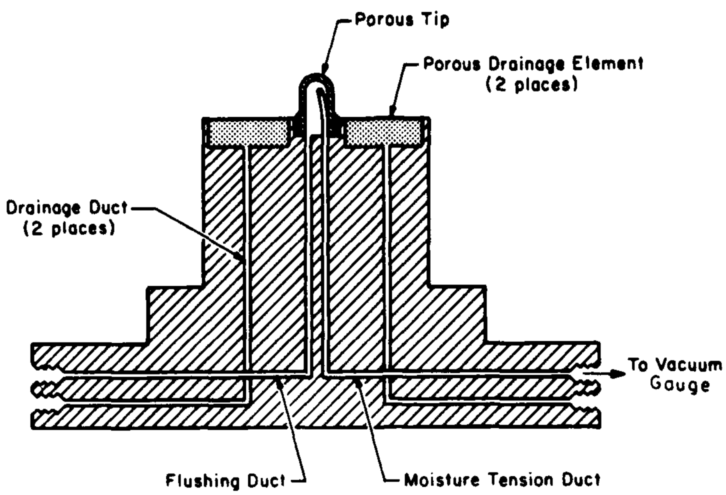

Figure 6. Cross section of small triaxial cell base. Vacuum gauge continuously monitors moisture tension level. System may be flushed to expell gas bubbles.

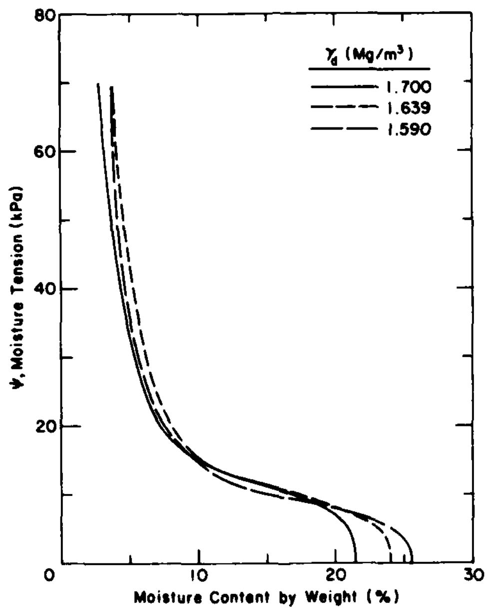

Figure 7. Moisture retention curve for Ikalanian sand.

sary to remove the specimen from its base since all cell components may be removed from the base without disturbing the mounted specimen. Additional details on the performance of this system are given in Appendix A along with testing and calibration procedures.

Waveform of applied stress

Two waveforms were used in the laboratory testing that simulate the loading conditions associated with field testing devices (Fig. 8). The pulse designated as RPB simulates the load pulse generated by the Repeated Plate Bearing apparatus. The pulse is approximately 1 second on and 2 seconds off. The waveform designated FWD simulates the pluse generated by a Falling Weight Deflectometer. This waveform is a 28-ms haversine pulse repeated every 2 seconds.

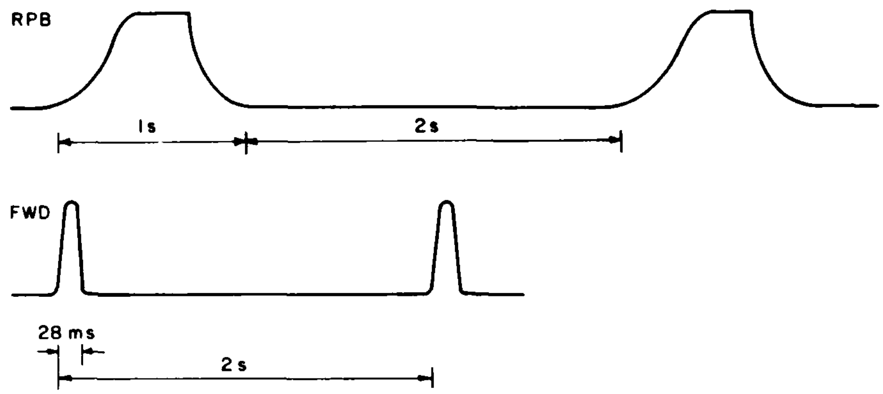

Figure 8. Waveforms of the Repeated Plate Bearing (RPB) apparatus and Falling Weight Deflectometer (FWD).

Testing sequence

Once mounted and instrumented, the specimen is tested in repeated-load triaxial compression using a closed-loop, electro-hydraulic testing machine according to the sequence of stresses given in Table 2.

Upon thawing, specimens were generally highly saturated, corresponding to the most severely thaw-weakened state in the field. Low moisture tension levels (or possibly pore water pressure) and low modulus values characterize this state. Often the complete schedule of stresses given in Table 2b could not be applied without causing excessive damage to the specimen, a circumstance to be avoided since each specimen was retested several times. Thus, it was necessary for the operator to exercise judgment in proceeding with the stress levels, avoiding those that could render the specimen unusable for subsequent testing.

As mentioned previously, the thawed testing sequence called for a series of tests at successively higher levels of moisture tension. Field tensiometer data provided the limits of moisture tension values in these tests. A set of tensiometers at varying depths in each field test section provided a continuous record of the stress state of the soil moisture. These values gave the necessary link between field and laboratory data in the following way.

Surface deflection measurements, made at various times throughout the year, generated data on the test section's performance. We recorded both temperature and moisture tension profiles in the section when doing these tests. We tested the validity of the laboratory results by using them in a

Table 2. Applied stress levels.

Static axial stress, σ_1 (kPa)	*Static confining stress, σ_3 (kPa)*	*Cyclic axial* stress, σ_d (kPa)*	σ_1/σ_3
	a. Frozen specimens		
—	69	60	—
—	69	138	—
—	69	207	—
—	69	276	—
—	69	345	—
—	69	482	—
—	69	620	—
—	69	827	—
	b. Thawed and recovered specimens		
—	6.9	3.4	1.5
—	13.8	6.9	1.5
—	27.6	13.8	1.5
—	48.3	24.1	1.5
—	69.0	34.5	1.5
—	6.9	6.9	2.0
—	13.8	13.8	2.0
—	27.6	27.6	2.0
—	48.3	48.3	2.0
—	69.0	69.0	2.0
—	6.9	10.3	2.5
—	13.8	20.7	2.5
—	27.6	41.4	2.5
—	48.3	72.4	2.5
—	69.0	103.4	2.5
	c. Natural subgrade material		
13.8	5.5	3.4	—
27.6	11.0	6.9	—
55.2	22.1	13.8	—

* Deviator stress.

layered elastic analysis of the test sections. Laboratory-determined moduli and Poisson's ratio characterize the resilient properties for each layer of the analysis. Since the moduli are moisture-tension dependent (or temperature dependent if frozen), appropriate values of these variables must be used in the regression equations to generate realistic moduli for comparison with the field results. The field data taken at the time of the surface deflection test provided us with these appropriate values of moisture tension and temperature.

As might be expected, the specimens densified to varying degrees during this testing sequence. We applied approximately 200 cycles at each load level, so a given specimen was subjected to thousands of load cycles by the end of its use. This situation caused an undesired bias in the results by generating a covariance between density and moisture tension. That is, the results contained data sets that always showed moisture tension and density increasing together, and the subsequent statistical analysis was incapable of separating the effects of the two variables. To avoid this circumstance, we resaturated the test specimens after the highest moisture tension level had been reached. This gave additional data points with low moisture tension but high density values. The covariance inherent in the first part of the sequence was thus eliminated and the effects of the two variables were more easily separated.

In most of these tests, we applied a vacuum to the specimen through the drainage system of the cell equal to the moisture tension level at the start of testing. This assured the maintenance of a constant level of tension in the specimen as testing proceeded.

As can be seen in the stress table (Table 2), the tests began at low levels of confining and deviator stress and proceeded to high stress levels. Thawed soil tests generally began producing measurable results at stress levels near 3.5- to 7.0-kPa deviator stress and 7.0-kPa confining stress, since their moduli are very low and the deformation is correspondingly high and easy to measure. The frozen tests, however, presented difficultes in this respect. Since the moduli are up to two orders of magnitude greater, the strains can be about two orders of magnitude smaller than the thawed case for a given stress. These small strains became very difficult to measure and, consequently, we applied significantly greater stresses in the frozen tests in order to produce deformations that could be accurately measured. Hence the rather large deviator stress levels given in Table 2a. The modulus of the frozen material becomes a strong function of temperature for temperatures approaching the melting point. At high temperatures, then, it was generally possible to obtain valid results for a range of stresses that overlapped that of the thawed tests, thus providing some continuity in stress level over the transition between the frozen and thawed states.

DATA REDUCTION AND ANALYSIS

For each set of applied deviator and confining stresses, we recorded the resilient and permanent axial and radial strains and can thus calculate a resilient modulus and a resilient Poisson's ratio. The resilient modulus is defined as the applied deviator stress divided by the strain recovered upon unloading for a representative loading cycle, and the resilient Poisson's ratio is defined as the recoverable radial strain divided by the recoverable axial strain. The recoverable strains generally stabilized within 10–20 cycles and the permanent strains, for all but the highest stress levels, became virtually imperceptible within the first 50 cycles. Thus, our measurements taken near the 200-cycle mark represent an approximately steady state condition for the prevailing stress levels.

After several specimens from a given test section had been tested, the data were tabulated and entered into a computer. Entries consisted of confining stress, deviator stress, resilient axial strain, resilient radial strain, density and moisture tension or temperature. The tables in Appendix C contain these data along with the calculated results, as discussed below.

We performed linear regression analyses on these data with various forms of stress, density and moisture tension used as independent variables and either resilient modulus or Poisson's ratio as the dependent variable. The frozen material was analyzed in terms of either unfrozen water content or temperature.

Stress functions used either the first stress invariant $J_1(=\sigma_1+\sigma_2+\sigma_3)$ or a ratio of the second stress invariant to the octahedral shear stress J_2/τ_{oct} to help characterize the stress dependence of the material. The use of J_1 is traditional in such analyses. The use of J_2/τ_{oct}, while somewhat unorthodox, has proven valuable in some cases since it reflects the tendency of the modulus to increase with confining stress but to decrease with increasing principal stress ratio. Details on this stress function may be found elsewhere (Cole et al.

1981). It may be calculated from the confining stress σ_3 and the deviator stress σ_d by the following formula:

$$J_2/\tau_{oct} = \frac{9\sigma_3^2 + 6\sigma_3\sigma_d}{\sqrt{2}\,\sigma_d}\,. \qquad (2)$$

As noted earlier, the nonlinear form given in eq 1 was used to represent the modulus in this analysis.

The coefficient K_1 is often a function of other test parameters such as moisture tension or density and has the units of stress. Moisture tension ψ is incorporated through the term $[(101.36-\psi)/\psi_0]$ where ψ is expressed in kPa and ψ_0 is a reference stress of 1 kPa. The expression $(101.36-\psi)$ then represents the deviation from atmospheric pressure of the soil moisture stress state; A_1 is determined in the regression analysis.

In analyzing the results of frozen tests, the modulus can be expressed either directly in terms of temperature or in terms of the unfrozen water content. Initially, a second order expression using temperature appeared sufficient in most cases. During the course of this work, however, experimental data on the unfrozen water content of the Winchendon soils became available,* which provided an alternative means of accounting for temperature effects (see Cole 1984). The expressions for unfrozen water content are of the form

$$W_u\% = a(-\theta)^{-b} \qquad (3)$$

where θ is temperature (°C) and a and b are constants.

The constants were determined for a range of initial water contents that could be expected in the field. Although there is a hysteresis effect between the warming and cooling temperature paths, the values of a and b did not change significantly for the range of conditions considered here, and were thus assumed constant. Dimensional considerations prompted some changes in the form of these equations. The temperature is normalized to a unit value $\theta_0 = 1.0$°C and the constant a is divided by 100.0 to yield values of W_u in decimal form rather than as a percent. The resulting expressions used for each soil are given in Table 3. It was necessary to assume values for a and b in the case of the Dense Graded Stone since the large aggregate size prevented testing in the nuclear magnetic resonance apparatus used to determine unfrozen water content.

The expressions for the resilient modulus in terms of unfrozen water content tend to be simpler than those in terms of temperature or temperature and water content. However, an additional calculation is required in order to obtain the unfrozen water content prior to evaluation of the modulus.

The data sets upon which the frozen state equations are based include several points from the thawed data. These points have very low moisture tension values and are thus representative of the condition of the soil upon thaw. The inclusion of

Table 3. Expressions for unfrozen water content (θ_o = 1°C, W_u expressed as a decimal).*

Material	*Equation*	*Equation number*
Ikalanian sand	$W_u = 1.43\times10^{-2}\,(-\theta/\theta_o)^{-0.214}$	1
Graves sand	$W_u = 3.06\times10^{-2}\,(-\theta/\theta_o)^{-0.309}$	2
Hart Brothers sand	$W_u = 1.81\times10^{-2}\,(-\theta/\theta_o)^{-0.340}$	3
Hyannis sand	$W_u = 2.23\times10^{-2}\,(-\theta/\theta_o)^{-0.415}$	4
Dense Graded Stone	$W_u = 2.00\times10^{-2}\,(-\theta/\theta_o)^{-0.400}$†	5
Sibley till	$W_u = 4.29\times10^{-2}\,(-\theta/\theta_o)^{-0.305}$	6

* Based on unpublished equations from A. Tice (CRREL).
† Assumed since test data were not available.

* Personal communication with A. Tice, CRREL, 1983.

these points extends the range of validity of the frozen state equations to the completely thawed condition and thus helps maintain continuity between the frozen and thawed state results.

The regression equations are used in the computer analysis to predict deflection basins in the pavement system (see Johnson et al., in prep.). It is noted here that for the Ikalanian and Graves sands, equations in the form of eq 3 were not developed at the time the deflection basins were being computed. Instead, equations based only on frozen-soil data points and employing a second order expression in terms of temperature were used in the computer analysis. Equations based on unfrozen water content and including thawed-soil data points were eventually developed but we did not rerun the computer analysis with the updated modulus expressions since the equations based on temperature led to satisfactory results.

RESULTS AND DISCUSSION

General

The results of the laboratory tests for all soils are tabulated in Appendix C. The tables in Appendix C give values for all the relevant parameters at each data point. We tested the specimens according to the stress sequences shown in the first two columns. The strain values were calculated using the deformation measurements described earlier divided by the instantaneous gauge length of the measurement in question. Dry densities were generally back-calculated after testing, using specimen weights and permanent deformation records. Moisture content and density were determined at the end of testing for a given sample, and moisture contents corresponding to each level of moisture tension employed during testing were found from the moisture retention characteristic curves for each soil.

Resilient modulus

Table 4 shows the results of the regression analysis performed on these test data. The results of tests on the asphalt concrete are also given here for completeness: these equations give moduli values for several different load pulse wave forms. The asphalt equation for the FWD pulse was derived from the haversine pulse equation with an appropriate value substituted for frequency f.

The number n in Table 4 refers to the number of points evaluated in the analysis. A given sample is subjected to a series of confining and deviator stresses for each moisture tension level. Each stress combination at a given level of moisture tension results in one data point; thus, a single specimen gives rise to many data points. Generally, the regression equations presented are based on from four to six specimens. Tests in the recovered state have the fewest data points since they were tested at only one level of moisture tension.

The coefficients of determination (R^2) for these analyses are, for the most part, very good. The standard error given in Table 4 applies to the natural logarithm of the modulus because each equation was linearized by taking the log of each side. Thus, regression coefficients were found for equations of the form

$$\ln M_r = A_0 + A_1 \ln[f(\psi)] + A_2 \ln[f(\sigma)]. \quad (4)$$

The regression program established a standard deviation for eq 4, so care must be taken in applying this to the exponentiated form of the equations given in Table 4.

The significance of an independent variable was established on the basis of F- and t-tests made during the regression analysis. In order to examine the influence of all variables, the F-level for acceptance into the analysis was set at an extremely low value. An insignificant variable was subsequently rejected on the basis of the t-test. Additionally, in the interest of keeping the equations as simple as possible, marginally acceptable variables were ignored if they failed to increase the R^2 value by more than 0.02.

In some cases, the regression analysis did not reveal any strong trends in the data when certain independent variables were used. For example, use of the stress function J_2/τ_{oct} resulted in at least marginally acceptable values of the correlation coefficients (0.65) for the thawed Hyannis sand. However, an unacceptable correlation coefficient ($R^2 < 0.5$) resulted when J_1 was used as the stress parameter. Such equations were not deemed useful and are thus not given in Table 4.

Figure 9 shows modulus versus temperature for all six frozen soils using regression equations developed from tests in which the RPB waveform was used. As seen in the equations given in Table 4, the modulus is primarily a function of unfrozen water content. Deviator stress level is relatively insignificant and consequently was rejected by the regression analysis and thus does not appear in several of the equations plotted in Figure 9.

Stress and density terms were occasionally accepted into the regression equations for the frozen

Table 4. Results of regression analysis.

Material	Load pulse	Regression equation	n	R^2	Std. error	Eq. no.
Asphalt concrete						
	RPB	$M_r(\mathrm{MPa}) = \exp[9.204-5.552\times10^{-2}T-9.744\times10^{-4}T^2]$	85	0.97	0.287	1
	Haversine	$M_r(\mathrm{MPa}) = \exp[9.183-7.47\times10^{-2}T]\,f^{0.1777}$	158	0.81	0.469	2
	FWD	$M_r(\mathrm{MPa}) = \exp[9.429-7.47\times10^{-2}T]$	—	—	—	3
Natural subgrade						
	RPB and FWD	$M_r(\mathrm{MPa}) = 8.829\,f_1(\sigma)^{0.708}$	65	0.67	0.235	4
	RPB and FWD	$M_r(\mathrm{MPa}) = 20.74\,f_2(\sigma)^{0.352}$	65	0.76	0.201	5
Graves sand						
Frozen	RPB	$M_r(\mathrm{MPa}) = \exp(9.677-1.0314T-0.0708T^2)(\tau_{oct}/\sigma_o)^{-0.682}$	56	0.88	0.332	7
	RPB	$M_r(\mathrm{MPa}) = 39.1(w_u/w_t)^{-1.79}$	95	0.91	0.502	8
	FWD	$M_r(\mathrm{MPa}) = 32.14(w_u/w_t)^{-1.96}$	73	0.95	0.446	9
Thawed	RPB	$M_r(\mathrm{MPa}) = 2.139\times10^6\,f(\psi)^{-2.7925}\,f_1(\sigma)^{0.462}$	186	0.76	0.209	10
	FWD	$M_r(\mathrm{MPa}) = 9.27\times10^5\,f(\psi)^{-2.60}\,f_1(\sigma)^{0.477}$	222	0.71	0.224	11
	RPB	$M_r(\mathrm{MPa}) = 6.68\times10^4\,f(\psi)^{-2.2948}\,f_2(\sigma)^{0.414}$	186	0.89	0.144	12
	FWD	$M_r(\mathrm{MPa}) = 1.47\times10^6\,f(\psi)^{-2.75}\,f_2(\sigma)^{0.413}$	222	0.86	0.157	13
Recovered	RPB	$M_r(\mathrm{MPa}) = 6.89\,f_1(\sigma)^{0.418}$	36	0.76	0.247	14
	RPB	$M_r(\mathrm{MPa}) = 4.80\,f_2(\sigma)^{0.4046}$	36	0.87	0.185	15
Ikalanian sand						
Frozen	RPB	$M_r(\mathrm{GPa}) = \exp[13.74-(0.820)T-(0.0538)T^2-(0.8378)w + (0.04416)w^2](\tau_{oct}/\sigma_o)^{-0.382}$	62	0.90	0.308	16
	RPB	$M_r(\mathrm{MPa}) = 86.4(w_u/w_t)^{-1.32}$	87	0.92	0.749	17
Thawed	RPB	$M_r(\mathrm{MPa}) = 8.129\times10^4\,f(\psi)^{-3.324}\,f(\gamma)^{11.578}\,f_1(\sigma)^{0.490}$	119	0.84	0.323	18
	RPB	$M_r(\mathrm{MPa}) = 3.021\times10^4\,f(\psi)^{-3.266}\,f(\gamma)^{11.634}\,f_2(\sigma)^{0.442}$	119	0.89	0.276	19
Recovered	RPB	$M_r(\mathrm{MPa}) = 5.69\times10^6\,f(\psi)^{-3.118}\,f_1(\sigma)^{0.537}$	38	0.88	0.205	20
	RPB	$M_r(\mathrm{MPa}) = 2.405\times10^6\,f(\psi)^{-2.918}\,f_2(\sigma)^{0.442}$	38	0.84	0.238	21
Hart Brothers sand						
Frozen	FWD	$M_r(\mathrm{MPa}) = 38.28(w_u/w_t)^{-1.782}$	88	0.95	0.53	22
	RPB	$M_r(\mathrm{MPa}) = 4.085\times10^1\,(w_u/w_t)^{-1.59}$	99	0.92	0.623	22
	FWD	$M_r(\mathrm{MPa}) = 8.05\times10^{-2}\,f(\gamma_d)^{7.64}\,f_2(\sigma)^{0.365}\,(w_u/w_t)^{-1.97}$	88	0.97	0.445	23
	FWD	$M_r(\mathrm{MPa}) = 4.689\times10^{-1}\,f_1(\sigma)^{0.484}\,(w_u/w_t)^{-1.38}$	88	0.96	0.464	25
Thawed	RPB	$M_r(\mathrm{MPa}) = 2.97\times10^5\,f(\psi)^{-3.063}\,f(\gamma)^{5.986}\,f_2(\sigma)^{0.453}$	174	0.71	0.280	26
	RPB	$M_r(\mathrm{MPa}) = 1.269\times10^5\,f(\psi)^{-3.089}\,f(\gamma)^{7.023}\,f_2(\sigma)^{0.453}$	174	0.87	0.185	27
	FWD	$M_r(\mathrm{MPa}) = 3.93\times10^4\,f(\psi)^{-2.67}\,f(\gamma)^{6.18}\,f_1(\sigma)^{0.457}$	164	0.67	0.292	28
	FWD	$M_r(\mathrm{MPa}) = 3.81\times10^4\,f(\psi)^{-2.817}\,f(\gamma)^{7.43}\,f_2(\sigma)^{0.375}$	164	0.67	0.292	29
Hyannis sand						
Frozen	RPB	$M_r(\mathrm{MPa}) = 0.68\,f(\gamma)^{11.0}\,(w_u/w_t)^{-2.12}$	69	0.96	0.536	30
	RPB	$M_r(\mathrm{MPa}) = 33.45(w_u/w_t)^{-2.03}$	69	0.95	0.617	31
Thawed	FWD	$M_r(\mathrm{MPa}) = 7.147\times10^4\,f(\psi)^{-1.782}\,f_2(\sigma)^{0.264}$	128	0.71	0.129	32
	FWD	$M_r(\mathrm{MPa}) = 3.57\times10^7\,f(\psi)^{-3.276}\,f_1(\sigma)^{0.3628}$	61	0.74	0.194	33
Dense Graded Stone						
Frozen	RPB	$M_r(\mathrm{MPa}) = 82.27(w_u/w_t)^{-2.03}$	32	0.97	0.413	34
Thawed	RPB	$M_r(\mathrm{MPa}) = 1.56\times10^5\,f(\psi)^{-1.76}\,f_2(\sigma)^{0.136}$	64	0.65	0.202	35
	RPB	$M_r(\mathrm{MPa}) = 7.17\times10^4\,f(\psi)^{-1.589}\,f_2(\sigma)^{0.1725}$	64	0.65	0.203	36
Sibley till						
Frozen	RPB	$M_r(\mathrm{MPa}) = 1.01\times10^2(w_u/w_t)^{-3.446}$	108	0.87	0.71	37
Thawed	RPB	$M_r(\mathrm{MPa}) = 7.47\times10^6\,f(\psi)^{2.829}\,f_2(\sigma)^{0.192}$	118	0.63	0.283	38
	RPB	$M_r(\mathrm{MPa}) = 1.29\times10^7\,f(\psi)^{-2.84}$	118	0.54	0.313	39

NOTES:

$f_1(\sigma) = (J_1/\sigma_o)$ $\quad$ $f_2(\sigma) = [(J_2/\tau_{oct})/\sigma_o]$ $\quad$ $f(\psi) = [(101.38-\psi)/\psi_o]$

$\gamma_o = 1\ \mathrm{Mg/m^3}$ $\quad$ $f(\gamma) = \gamma/\gamma_o$ $\quad$ $\sigma_o = 1\ \mathrm{kPa}$

$\psi_o = 1\ \mathrm{kPa}$ $\quad$ $T = \theta/\theta_o$ $\quad$ $\theta_o = 1\,^\circ\mathrm{C}$

w_u = unfrozen water content $\quad$ w_t = total water content $\quad$ n = number of points

RPB = Repeated Plate Bearing apparatus waveform

FWD = Falling Weight Deflectometer waveform

f = load wave frequency

M_r = resilient modulus

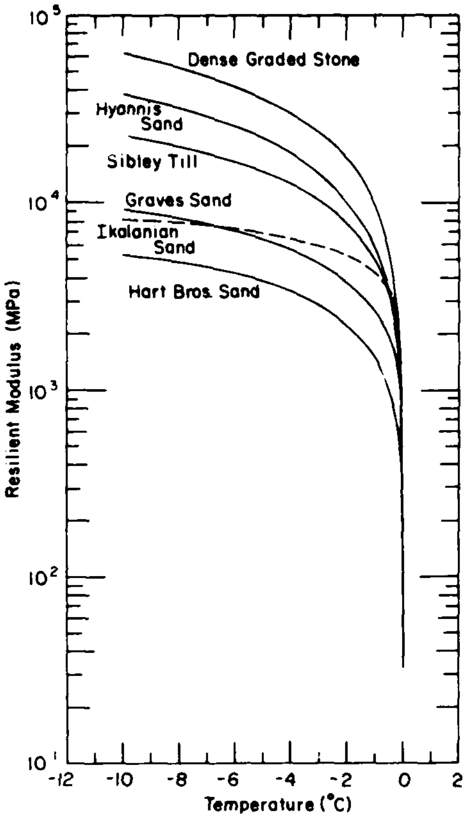

Figure 9. Resilient modulus versus temperature for all test soils.

state. The incorporation of dry density γ_d in the expression for frozen Hyannis sand gives a slight improvement in accuracy. However, the simpler expression (eq 31, Table 4) is sufficient and requires only one variable for the modulus determination.

In examining the regression results, several other points require mention. We were not always successful in sampling material in the recovered state; in fact, only specimens from the Ikalanian sand and Graves sand sections proved useful for this characterization. For all other soils, we used the thawed state equations, evaluated at suitably high moisture tension levels, to represent the recovered state.

The "recovered" cores taken from the Ikalanian sand section possessed a sufficient range in moisture tension to allow that variable into the regression equation. This was not the case for the Graves sand, where the moisture tension in the cores varied little, and it was thus rejected as a significant variable in the regression analysis.

Additionally, in examining Table 4, the use of the two load pulse waveforms does not appear to be completely systematic. This happened because many of these tests were performed in a period when we were changing from the Repeated Plate Bearing (RPB) device to the Falling Weight Deflectometer (FWD) in the field verification work.

The Ikalanian sand, under all conditions, and the recovered Graves sand were subjected only to the RPB pulse. In the other tests, we applied both waveforms. If there was a significant difference between the results from the two waveforms, analyses from both are given. For the thawed Sibley till, the two waveforms resulted in virtually identical moduli values, as determined by several comparisons made early in the load cycling. Only the RPB pulse was applied in subsequent testing. The results given are assumed valid for the FWD pulse as well. The stiffness of Hyannis sand, Dense Graded Stone and frozen Sibley till resulted in excessive vibrations when the fast FWD pulse was applied. Since this made the deformation measurement very difficult, we decided to use only the RPB pulse in these cases. Finally, the thawed Hyannis sand data from the RPB pulse did not respond acceptably to the regression analysis and thus an equation is not presented. We believe that data scatter, coupled with a relatively low sensitivity to stress, brought this about.

Interestingly, in the Hart Brothers sand analysis, unfrozen water content was the only significant variable for results obtained wth the RPB waveform, whereas unfrozen water content, density and stress were all found to be significant for the same soil tested under the FWD waveform.

Poisson's ratio

The measurement system described earlier allowed us to calculate Poisson's ratio directly in all tests. We performed regression analyses similar to those done with the resilient modulus data on the results in an effort to correlate values with the pertinent variables. Unfortunately, these analyses proved unsuccessful. Correlation coefficients did not exceed 0.42 and in most cases were very near zero. Consequently, no stress- or moisture-tension-dependent model of Poisson's ratio emerged from these analyses. Table 5 gives the average values obtained for each soil under various conditions.

No values are presented for the frozen case since the radial deformations encountered in those tests were too small to be measured reliably.

Table 5. Average values of Poisson's ratio.

Material		*Load pulse waveform**	μ_r
Dense Graded Stone	Thawed	RPB	0.31
Graves sand	Recovered	RPB	0.23
	Thawed	RPB	0.25
Hart Brothers sand	Recovered	RPB	0.30
		FWD	0.29
	Thawed	RPB	0.37
Hyannis sand	Recovered	RPB	0.15
	(Remolded)	RPB	0.35
		FWD	0.33
	Thawed	FWD	0.25
Ikalanian sand	Recovered	RPB	0.25
	Thawed	RPB	0.26
Sibley till	Thawed	RPB	0.42

* RPB—Repeated Plate Bearing apparatus waveform.
FWD—Falling Weight Deflectometer waveform.

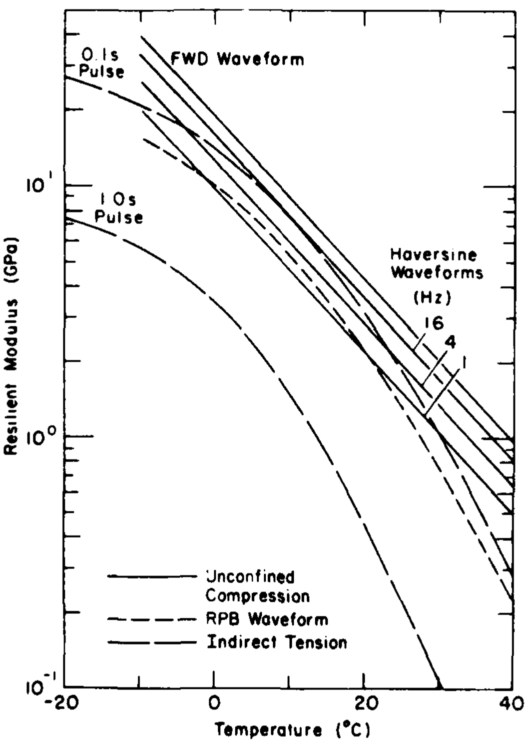

Figure 10. Resilient modulus versus temperature for the asphalt concrete (RPB—Repeated Plate Bearing apparatus; FWD—Falling Weight Deflectometer).

Asphalt concrete

Equations 1-3 in Table 4 give the results of regression analyses of the cyclic loading tests on the asphalt concrete. This material was found to be insensitive to the level of deviator stresses applied for each waveform. For the slower RPB waveform (1 second on, 2 seconds off), the resilient modulus M_r was a function of temperature only, as seen in eq 1 of Table 4. For the haversine loading according to ASTM standards, M_r was a function of both temperature and frequency (see eq 2 of Table 4). Here, a given load was applied at three frequencies: 1, 4 and 16 Hz. The modulus increases with increasing frequency of loading. Representative results are plotted in Figure 10, where the lines are generated by the regression equations.

We carried out a second set of tests in repeated uniaxial compression on the same composite specimens mentioned above in order to characterize in the laboratory the asphalt concrete under the FWD load waveform. These tests included the same RPB and haversine load waveforms as well as the FWD waveforms. The M_r results were internally very consistent for these data, but were noticeably low relative to the M_r values obtained using previously untested specimens. We believe that the previous repeated load testing of these specimens resulted in fatigue damage, which lowered the resilient modulus.

It was noted in this second data set, for the damaged samples, that the values of M_r resulting from the FWD waveform differed by an almost constant factor of 1.5 from the 4-Hz-haversine waveform results over the full range in temperatures. Based on this observation, the same factor of 1.5 was applied to the 4-Hz-haversine results from the original tests on undamaged samples to obtain an estimate of the FWD results on the specimens in their original condition.

Natural subgrade

Regression equations 4 and 5 in Table 4 are for the natural subgrade material. The use of the stress function J_2/τ_{oct} instead of J_1 results in a significant increase in the correlation coefficient. The results for both the FWD and RPB waveforms were merged when we found that there was no statistically significant difference between the two data sets. Plots of the regression equations are given in Figure 11.

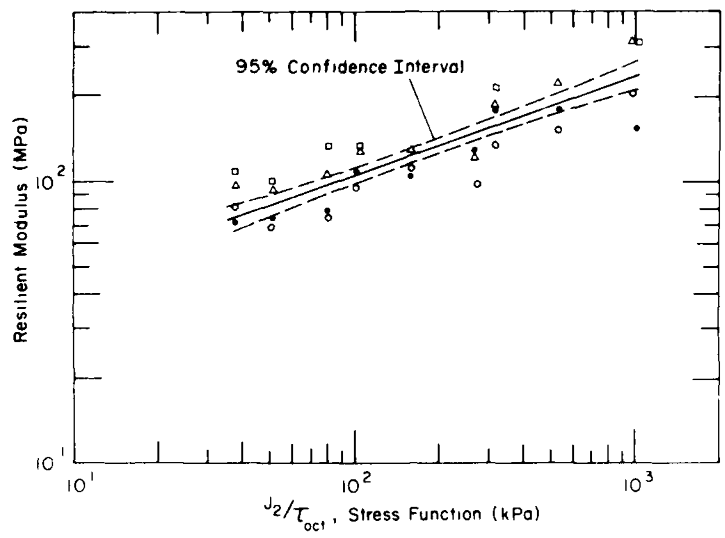

Figure 11. Resilient modulus versus stress function J_2/τ_{oct} for the natural subgrade.

K_1 values for thawed soils

Figure 12 shows how the coefficient K_1 changes over the expected range of moisture tension ψ. The current interpretation sets K_1 equal to the product of all terms before the stress function in the regression equations. Thus, for a given moisture tension value (and γ_d value where applicable) the equations reduce to the form

$$M_r = K_1[f(\sigma)]^{K_2}$$

where

$$K_1 = C_0[f(\psi)]^{C_1}$$

or

$$K_1 = C_0[f(\psi)]^{C_1}(\gamma_d/\gamma_0)^{C_2}.$$

and C_0, C_1 and C_2 are the constants from the regression equation and γ_0 is unit density.

The values of K_1 are given over the range of ψ used in the laboratory tests and this range brackets the moisture tension values determined by the field measurements. So, for a given stress state, these curves show the relative stiffness of the soils as well as the sensitivity of K_1, and thus the resilient modulus, to changes in moisture tension. In the cases where γ_d occurs in the expression for K_1, typical values (1.6 Mg/m³ for Ikalanian Sand, 1.8 Mg/m³ for Hart Brothers sand) are used.

The curves in Figure 12 also give an indication of the increase in stiffness of the soils as recovery proceeds. Values along the y-axis, where $\psi = 0$, indicate K_1 values upon thaw. Recovery may be viewed as a steady progression to higher ψ levels as the soil drains, and K_1 steadily increases as a result.

The power to which the moisture tension function is raised gives an indication of how strongly the resilient modulus depends on moisture tension. Values of this exponent range from -1.57 for the Dense Graded Stone to -3.324 for the Ikalanian sand. For a given soil, there is only a small change in the moisture tension exponent when the modulus is expressed in terms of J_1 rather than J_2/τ_{oct}.

The slope of the K_1 versus ψ curves would be steeper if, for equations possessing a γ_d term, an increase in dry density were considered along with an increase in moisture tension. K_1 would then reflect the stiffening effect of both factors, and the resulting rate of strength recovery after thawing would be correspondingly greater.

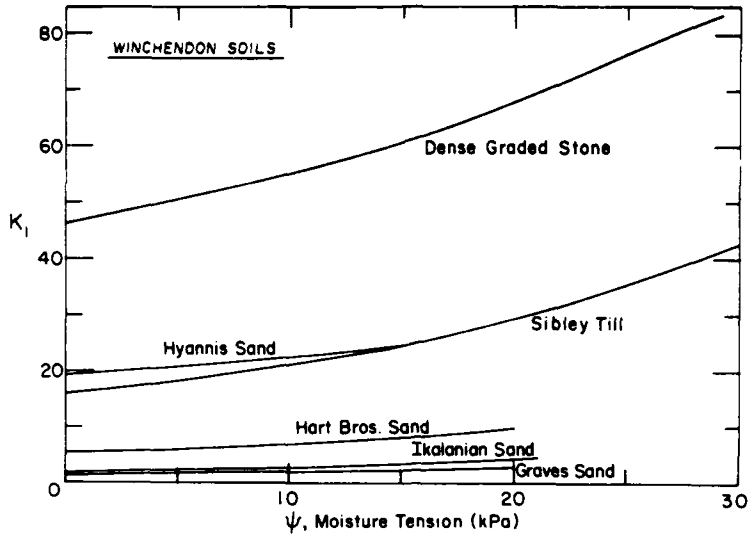

a. J_2/τ_{oct} *model.*

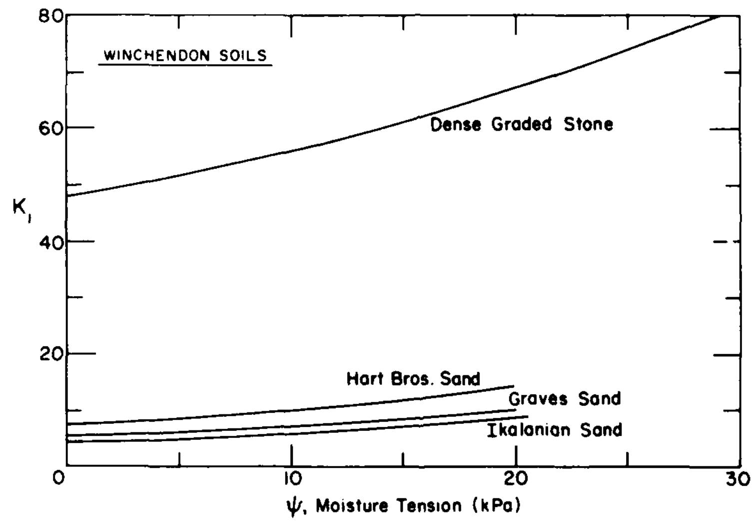

b. J_1 *model.*

Figure 12. K_1 *versus moisture for all test soils.*

K_2 values for all soils

Table 6 shows the values of K_2, the exponent of the stress function, for all soils. Hyannis sand, Dense Graded Stone and Sibley till show the lowest values, indicating the least stress-sensitivity. The other soils are in the range of 0.418 to 0.531 when J_1 is used and from 0.365 to 0.453 when J_2/τ_{oct} is used. For a given soil, K_2 generally tends to be somewhat lower when the stress is expressed in terms of J_2/τ_{oct}.

It is interesting that in the case of frozen Hart Brothers sand, where stress was found to be a significant factor, the exponent K_2 was close to the value found for the thawed state.

The frequency of loading, which varied significantly between the two load pulses, apparently has little effect on the value of K_2 when J_1 is considered for the stress function. The Hart Brothers sand data show a decrease in K_2 from 0.453 to 0.375 with an increase in the frequency of loading when J_2/τ_{oct} is considered.

Table 6. Stress function exponents (K_2) from regression analyses.

		Stress function		
		τ_{oct}	J_1	J_2/τ_{oct}
Ikalanian sand	Frozen	-0.382	†	†
	Thawed		0.490	0.442
	Recovered		0.537	0.442
Graves sand	Frozen	-0.682	†	†
	Thawed		0.462	0.414
	Recovered		0.418	0.4046
Hart Brothers sand	Frozen	† *	0.484*	0.365*
	Thawed		0.453	0.453
	Thawed		0.457*	0.375*
Hyannis sand	Thawed		0.3628	0.264*
Dense Graded Stone	Thawed		0.1725	0.136
Sibley till	Thawed	†	0.192	

* Falling weight deflectometer (all others repeated plate bearing apparatus).

† Stress function not accepted into analysis.

Earlier work (Cole et al. 1981) demonstrated that K_2 does not change appreciably with increasing values of K_1 (i.e., for a given soil, increasing moisture tension and density, where applicable, does not influence the value of K_2 significantly).

It is possible that this would not always be the case, and that the stress function exponent could change with, say, increasing levels of moisture tension. Thus, data sets should be examined closely, and if need be, K_2 should be expressed as a function of the appropriate independent variable.

Comparison of stress functions

The stress function J_2/τ_{oct} proved more effective than J_1 in some cases and equally effective in others. Three soils showed the most dramatic increases: natural subgrade (where R^2 increased from 0.67 to 0.76), thawed Graves sand (R^2 increased from 0.76 to 0.89) and thawed Hart Brothers sand (R^2 increased from 0.71 to 0.87). J_2/τ_{oct} produced marginally acceptable results for thawed Hyannis sand and thawed Sibley till where the use of J_1 did not result in acceptable correlation coefficients.

In the cases where J_2/τ_{oct} proved successful, the soil showed a marked trend toward a decrease in resilient modulus with an increase in principal stress ratio σ_1/σ_3, as well as the typical trend for an increase in modulus with bulk stress at a constant principal stress ratio.

Figure 13 demonstrates the response of the test data to the two stress functions. Figure 13a shows modulus as a function of J_1 for data from thawed Hart Brothers sand with ψ = 5 kPa. The applied stresses result in principal stress ratios of 1.5, 2, 2.5 and 3. Each cluster of points on the graph represents data obtained in tests where the confining pressure was held constant and the cyclic deviator stress σ_d was changed incrementally to achieve these four stress ratios. In this case as σ_d increases, σ_1/σ_3 and the bulk stress J_1 also increase, but, as seen in Figure 13, the modulus generally decreases. If, on the other hand, σ_d remains constant while σ_3 increases, σ_1/σ_3 decreases, J_1 increases and the modulus increases.

Given this behavior, we see that an adequate model of resilient modulus in terms of applied stresses must reflect the effect of stress ratio as well as bulk stress. The function J_2/τ_{oct} addresses this pattern in behavior as seen in Figure 13b. This figure shows the data from Figure 13a replotted in terms of J_2/τ_{oct}. It is evident that this stress function all but eliminates the systematic trends observed when J_1 is employed. Again, the utility of the function J_2/τ_{oct} stems from its sensitivity to the principal stress ratio as well as the bulk stress. Although we do not suggest that this stress function is of extremely wide applicability, it adequately represents soils exhibiting the observed behavior trends.

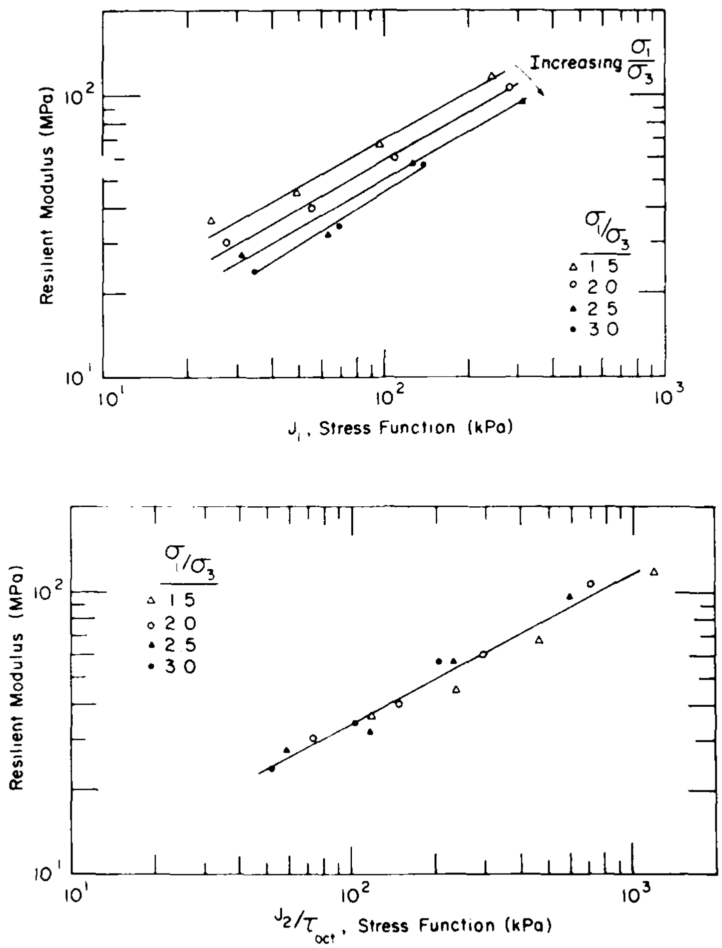

Figure 13. Resilient modulus versus the two stress functions for Hart Brothers sand, specimen HB-4-2, γ = 5 kPa.

Data from soils that either do not exhibit the above mentioned trends or have sufficient scatter to obscure these trends, respond equally as well to both J_1 and J_2/τ_{oct} for the most part. One case, recovered Ikalanian sand, showed a slight drop (0.88 to 0.84) in correlation coefficient with the use of J_2/τ_{oct}.

SUMMARY

This paper presents methodology developed to evaluate the resilient characteristics of soils intended for use as road or airfield subgrades. Results from repeated-load triaxial tests in the laboratory lead to empirical relationships between the resilient modulus and the imposed stress state. These relationships also account for the effects of soil moisture as well as density and temperature where applicable.

Appropriate laboratory testing techniques allow for modeling the changes in resilient behavior that occur during the freeze–thaw–recovery cycle common to cold regions. This work details the equipment, testing methods and analytical techniques employed in all phases of this modeling process.

Appendices include a complete description of the repeated load triaxial testing procedure as well as the results from six soils from the road test sections of the Department of Public Works at Winchendon, Massachusetts. Laboratory characterization of the asphalt concrete and natural subgrade materials is also included.

A method used to characterize the strength recovery period by testing each specimen at successively higher levels of moisture tension is also given. Of particular importance to laboratory work are the triaxial cells developed for this work. The cells feature detachable bases that allow for retesting without remounting the specimen. The

cells are also equipped to monitor the moisture tension level in the soil. This work uses moisture tension as the primary variable affecting a given soil's response to stress in the thawed state. Since moisture tension can be monitored in the field as well, it provides a convenient link between in situ observations and laboratory results.

CONCLUSIONS

The laboratory testing methods detailed in this report allow the determination of the resilient response of granular soils throughout a freeze, thaw and recovery cycle. Soil moisture tension proved to be a suitable quantity with which to monitor this recovery phase. The resilient modulus in the frozen state is a strong function of unfrozen water content, and applied stress becomes significant at temperatures close to the melting point. Most of the soils tested exhibited a significant loss of strength upon thaw, but strength was gradually regained as moisture drained from the soil during the recovery period.

The resilient response can be modeled by equations of the form

$$M_r = K_1[f(\sigma)]^{K_2}$$

using linear regression techniques to determine K_1 and K_2. The coefficient K_1 is often found to be a function of soil moisture and occasionally dry density while K_2 is considered constant for a given soil. The analyses use either J_1 or J_2/τ_{oct} as the stress function $f(\sigma)$. In general, higher correlation coefficients resulted with the use of J_2/τ_{oct} because of its sensitivity to the influence of the principal stress ratio.

LITERATURE CITED

Bergan, A.T. and C.L. Monismith (1973) Characterization of subgrade soils in cold regions for pavement design purposes. Transportation Research Board Record 431, pp. 25–37.

Brown, S.F. and J.W. Pappin (1981) Analysis of pavements with granular bases. Transportation Research Board Record 810, pp. 17–22.

Chamberlain, E.J. (1983) Frost susceptibility of Soil. Review of index tests. USA Cold Regions Research and Engineering Laboratory, Monograph 81-2.

Chamberlain, E.J. and D.L. Carbee (1981) The CRREL frost heave test. *Frost i Jord,* NR22, pp. 55–62.

Cole, D.M. (1978) A technique for measuring radial deformation during repeated load triaxial testing. *Canadian Geotechnical Journal,* **15**: 426–429.

Cole, D.M., L.H. Irwin and T.C. Johnson (1981) Effect of freezing and thawing on resilient modulus of a granular soil exhibiting nonlinear behavior. Transportation Research Board Record 809, pp. 19–26.

Cole, D.M. (1984) Modeling the resilient behavior of frozen soil using unfrozen water content. Presented at the Third International Cold Regions Engineering Specialty Conference, April 4–6, Edmonton, Alberta. American Society of Civil Engineers (unpublished).

Cole, D.M., G. Durell and E.J. Chamberlain (In press) Repeated load triaxial testing of frozen and thawed soils. *Geotechnical Testing Journal.*

Fredlund, D.G., A.T. Bergan and E.K. Sauer (1975) Deformation characterization of subgrade soils for highways and runways in northern environments. *Canadian Geotechnical Journal,* **12**(2): 213–223.

Ingersoll, J. (1981) Laboratory and field use of soil tensiometers above and below 0°C. USA Cold Regions Research and Engineering Laboratory, Special Report 81-7.

Irwin, L.H. and T.C. Johnson (1981) Frost-affected resilient moduli evaluated with the aid of nondestructively measured pavement surface deflections. Presented at the Transportation Research Board Task Force Meeting on Nondestructive Evaluation of Airfield Pavements (unpublished).

Johnson, T.C., D.M. Cole and E.J. Chamberlain (1978) Influence of freezing and thawing on the resilient properties of a silt soil beneath an asphalt concrete pavement. USA Cold Regions Research and Engineering Laboratory, CRREL Report 78-23.

Johnson, T.C., D. Bentley and D. Cole (In prep.) Resilient modulus of freeze-thaw affected granular soils for pavement design and evaluation. Part 2. Field validation tests at Winchendon test sections. USA Cold Regions Research and Engineering Laboratory, CRREL Report.

Pappin, J.W. and S.F. Brown (1980) Resilient stress-strain behavior of a crushed rock. In *Proceedings of the International Symposium on Soils Under Cyclic and Transient Loading, 7-11 January, Swansea, Wales,* pp. 169–178.

Rada, G. and M.W. Witczak (1981) Comprehensive evaluation of laboratory resilient moduli for granular material. Transportation Research Board Record 810.

APPENDIX A: DETAILED TESTING PROCEDURES

This Appendix provides details of the testing equipment, calibration procedures, test operation and data reduction. A basic understanding of the principles of operation of a closed-loop, electro-hydraulic test machine is required for a thorough understanding of some of the following methods. However, the bulk of the material deals with the triaxial cell set-up and specimen instrumentation. Specifications appear in English units since virtually all of the electronic devices and the testing machine itself are calibrated in that system. An English–SI conversion chart appears at the end of this appendix for the reader's convenience.

System overview

Figure 1 in the main text shows the two triaxial cells that were built for the repeated load tests. The large cell (Fig. 1a) provides for testing 6-in.-diameter, 15-in.-high specimens, while the small cell (Fig. 1b) is used for 2-in.-diameter, 5-in.-high specimens. The radial and axial deformation measuring systems, as well as the miniature load cells, are interchangeable. The load cells are of 200-, 500- or 10,000-lb capacity. The size and state (frozen or thawed) of the soil specimen determines the appropriate capacity load cell.

A system of four Linear Variable Differential Transformers (LVDTs) measures axial deformation. The cores of the LVDTs are mounted on miniature universal joints, which are in turn affixed to spring-loaded circumferential clamps. There are two clamps placed at the third points along the specimen length and two LVDTs measure the excursion of each clamp during load cycling. The outputs of each pair of LVDTs are averaged electrically and the resulting averages are combined to give a single output for the differential clamp movement. Resilient axial strain is then calculated by dividing this deformation by the distance between the two clamps. The sensitivity of this system may be adjusted in order to accommodate a range of material stiffnesses.

A system of three noncontacting displacement transducers (multi-VITs [Variable Impedance Transducers]) measures radial deformation at points about the center of the specimen. The three transducer outputs are added and recorded along with the axial deformation. This information allows the calculation of radial strain and hence Poisson's ratio.

The cell bases are equipped with a system for measuring soil moisture tension, as mentioned earlier in the text. This system provides a continuous monitor of the moisture tension. It must be kept free of entrapped air bubbles in order to perform properly, and the porous ceramic tip must remain saturated at all times.

A pressurized air system provides the confining pressure. It is regulated by a bleeding-type pressure regulator (accurate to 0.01 lb/in.^{2}) and monitored by a dial type pressure gauge (accurate to 0.1% full-scale).

Testing is done on an MTS machine in LOAD control. The miniature load cell mounted in the triaxial cell serves as the machine's feed-back source. The machine receives a command signal from either the electro-mechanical device (Data Trak) or a digital function generator. The former device supplies the RPB (Repeated Plate Bearing device) waveform and the latter provides the FWD (Falling Weight Deflectometer) and haversine waveforms.

The axial and radial deformations and the axial load are all recorded on a multi-channel strip chart recorder. Representative loads and deformations are then taken for each set of test conditions from the strip chart recording. Stress and resilient strain levels are calculated from this information and these results are then tabulated, entered in a computer and analyzed by linear regression.

Calibration

Load cells

The miniature load cells should be calibrated periodically using a standard calibration load cell. Care should be taken to properly match the range of the calibration load cell with the cell to be calibrated. The sensitivities of the three cells are shown in Table A1.

Table A1. Load cell sensitivity.

Cell capacity (lb)	*MTS range*	*Load range (lb)*	*Factor (mV/lb)*
200	I	0–200	50
500	I	0–500	20
10,000	III	0–2000	5

PREVIOUS PAGE IS BLANK

Note that range III for the 10,000-lb cell gives 20% of the cell's capacity as full-scale, whereas range I gives 100%.

Before the calibration load cell and the test load cell are fastened securely to the MTS piston, make sure that the correct range card is in the load dc conditioner. Each load cell has a range card associated with it to ensure the proper gain for each load cell. Follow the calibration procedure for the MTS model 440.21 dc conditioner located in the appropriate MTS manual.

LVDTs

The LVDTs that measure axial displacement are calibrated individually. Each pair shares a Shaevitz carrier amplifier, but each individual LVDT has a separate gain pot located in the averager circuit chassis. A calibration jig with a large micrometer head, accurate to 0.0001 in., is used to calibrate the LVDTs (Fig. A1a).

Place one LVDT from the upper pair in the calibration jig. Connect the pair to the cable marked no. 1. On the adder circuit box, move the no. 1 (upper) switch to "on" and the no. 2 (lower) and zero switches to "off." This isolates the output of the LVDTs to be calibrated. Connect the output from the adder to a digital voltmeter. Slide the core into the barrel of the LVDT in the jig and adjust for 0 V output. Adjust the core with the micrometer until the desired full-scale displacement is obtained. Adjust the pot on the averager circuit that corresponds to the LVDT to obtain 2.5 V. If there is not enough adjustment in this pot, the gain adjust on the Shaevitz carrier amplifier must be adjusted. In this case, use the carrier amplifier gain for a coarse adjustment and the averager circuit pot for fine adjustment. Check several increments during calibration, such as 0.125 in., 0.075 in., 0.025 in., 0.005 in., to determine if the system is linear and adjust the averager pot to compensate for any discrepancies. Recheck full-scale displacement again. Repeat the operation for the second LVDT in the pair but do not adjust the carrier amplifier gain again since it will change the calibration of the first LVDT. Adjust only the pot on the averager circuit. Note that for the pair of LVDTs being calibrated, the core must be removed completely from the LVDT not mounted in the calibration jig.

The lower pair is calibrated exactly as was the upper pair. Hook the lower pair connector to the no. 2 output cable and turn the no. 2 switch on the adder circuit to "on," and the no. 1 and zero switches to "off." It is necessary to adjust all

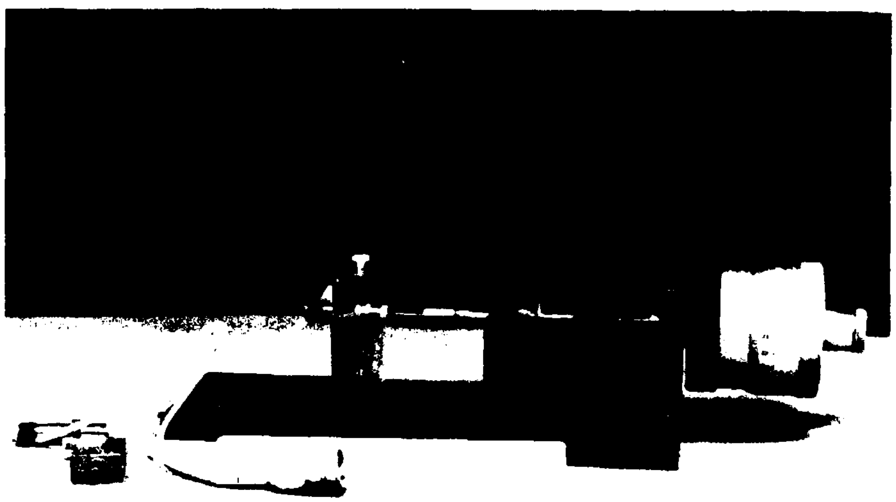

a. LVDTs.

Figure A1. Calibration jigs.

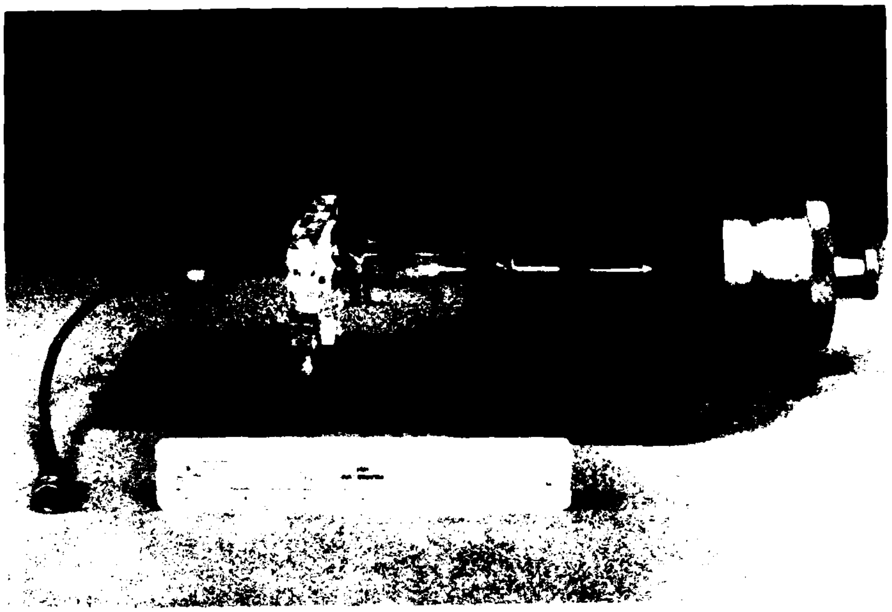

b. Multi-VITs.

Figure A1 (cont'd). Calibration jigs.

LVDTs to exactly the same calibration factor. Each LVDT has its own core and they must not be interchanged or the sensitivity will change. The LVDTs must be calibrated frequently since they have a tendency to shift. It is good practice to calibrate them before each day's testing.

Multi-VITs

The radial displacement measuring devices maintain their calibration very well. They should be checked monthly, however, using the same calibration jigs that were used for the LVDTs. Since the target must be of the same shape and of the same material as that used during testing, use a plexiglass target with aluminum foil glued to it (Fig. A1b). Targets with either a 1- or 3-in. radius of curvature are used, depending on whether the 2- or 6-in. diameter samples are being tested. Adjust each multi-VIT to 1×10^{-4} in./mV using the calibration procedure given in the Kaman Sciences instruction manual.

Mounting specimen and installing instruments

The tests of both frozen and thawed soils employ essentially the same equipment, except that a cell base without a built-in porous ceramic tip is used for the frozen samples. This second type of base has a thermocouple in place of the porous tip for directly monitoring the specimen temperature.

Before mounting, carefully measure and weigh the specimens. Drill a ¼-in. hole, approximately ½ in. deep, in the center of the bottom surface of the specimen to receive the porous tip. Carefully place the sample on the pedestal. Place a top cap on the sample. Next, install a latex membrane on the entire sample by first stretching the membrane on the inside of a 3-in. by 6-in. plexiglass cylinder and applying a vacuum to draw the membrane onto the walls of the cylinder; then slide the cylinder membrane over the sample. Releasing the vacuum will cause the membrane to fit tightly against the sample.

Remove the cylinder and secure the membrane to the top cap and the pedestal with O-rings. Set the triaxial cell base on the pedestal and set the Multi-VITs with mounts in their proper mounting bases. Place three 1- × 2-in. aluminum foil targets on the sample so that the multi-VITs are centered on the targets. Applying silicone grease to the back of the target material sticks the targets to the membrane. Remove the multi-VITs and the cell base. Place another membrane on the sample in the same manner as the first, being careful not to disturb the multi-VIT targets. Place two more O-rings to secure the second membrane to the ped-

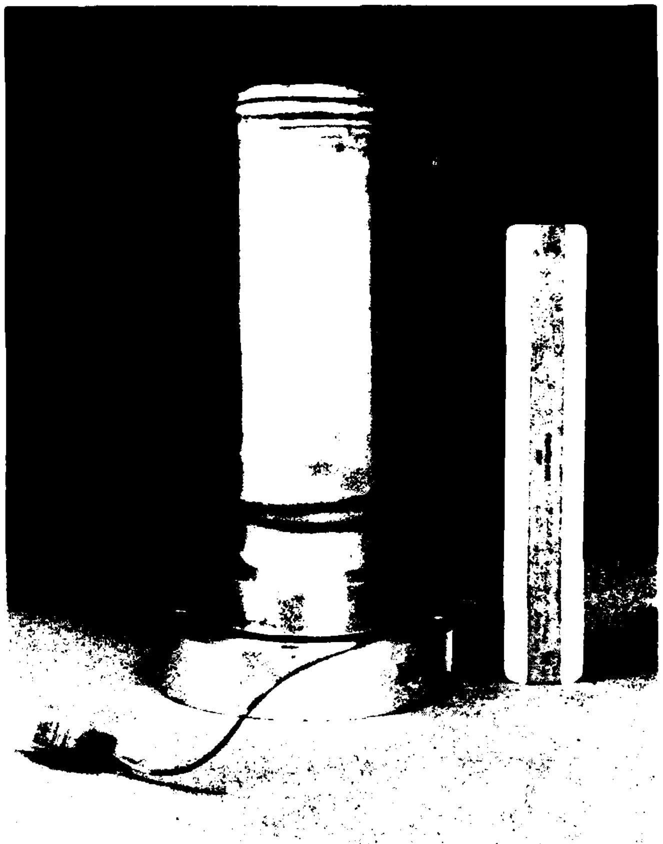

Figure A2. Specimen mounted on pedestal with membrane and multi-VIT targets in place.

estal and top cap. The sample is now ready for instrumenting (Fig. A2).

As noted above, the frozen 2-in. samples are to be mounted on solid aluminum pedestals that have thermocouples through their centers to monitor temperature. Drill a small hole in the center of the sample base and place the sample on the pedestal, aligning the thermocouple and the hole in the bottom of the sample. With a squirt bottle, apply a small quantity of water around the base of the sample to bond the frozen sample to the pedestal. Avoid saturating the sample. Place the top cap on the sample and then apply water along the top cap/soil interface. Allow the water to freeze for a few minutes and then place the membranes, O-rings and multi-VIT targets as on the thawed sample.

Keeping the pedestal clean helps to avoid any air leaks when the confining pressure is applied.

Cell assembly and instrumentation

Place an O-ring in the O-ring groove of the pedestal and install the base plate of the cell on the pedestal, aligning the three bolt holes. Secure with three allen-head bolts, tightening equally.

Screw the LVDT cores onto their respective stems on the LVDT clamps. These stems are connected to miniature universal joints which accommodate tilting of the circumferential clamps and thus prevent binding between the LVDT core and barrel. Place the two LVDT mounting rods into the mounting holes on the cell base. Place the two clamps around the sample, keeping each clamp at least 1 in. from the specimen end.

Placement of the clamps is critical (Fig. A3). It is important to leave enough space between them to get a gauge length of about 2 in. but also to keep them far enough away from the top cap and the pedestal to avoid end effects. A good rule of

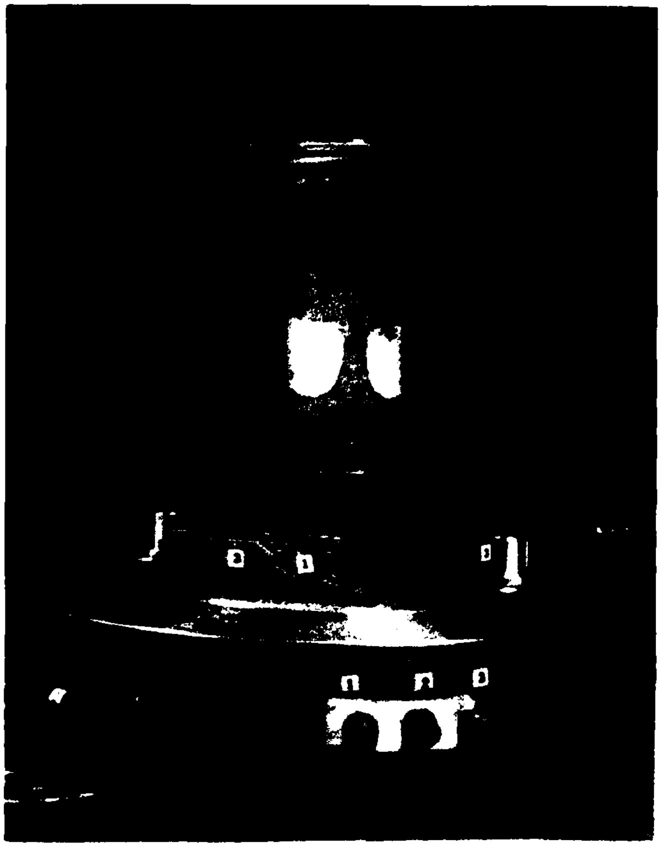

Figure A3. Installation of cell base and LVDT core clamps.

thumb is to keep a 3-in. gauge length on a 5- to 6-in.-long, 2-in.-diameter sample, and a 9- to 12-in. gauge length on a 16- to 18-in.-long, 6-in.-diameter sample.

The clamps are held onto the sample with springs. Choose the stiffest spring that will not damage the sample. Use a vernier caliper to make fine adjustments to the clamp to achieve a uniform gauge length. Record this gauge length along with the sample measurements (see Fig. A4). Stagger the LVDT cores close to the LVDT mounting rods so that the double-hinged barrel mounts can easily reach the cores. The double hinged barrel mounts employ miniature ball bearings and precision-ground steel shafts. They allow complete freedom of movement in the horizontal plane but do not move vertically. Thus, as the specimen deforms and the LVDT cores move laterally, the barrels move laterally as well. Thus, alignment is maintained and binding between the core and barrel is avoided.

Install the bottom LVDT barrels onto the mounting rods, matching the serial number of the core to that of the barrel. Slide the barrel over the core using caution not to disturb the circumferential clamps. There is a mark on the stem that the core is screwed into which is approximately the LVDTs' electrical zero. Slide the barrel to this point and tighten the set screw on the barrel mount, ensuring that the two hinges of the barrel mounts are able to rotate freely. Attach the LVDT connector to the corresponding connector on the cell base. Repeat the procedure for the upper LVDTs (Fig. A5).

Install the multi-VIT mounting rods in the numbered holes in the cell base that corresponds to the multi-VIT number. Adjust the multi-VITs so that they are perpendicular to the targets on the sample and tighten the set screw at the base of the multi-VIT mounting rod. Install the twin BNC connector for each multi-VIT in the cell base. The sample is now fully instrumented (Fig. A6). Be-

LVDT FACTOR: 5×10^{-5} in./mV

L_o = 3.150 in.

D_o = 1.969 in.

A_o = 3.043 in.^{2}

SAMPLE #: TW13 Subgrade 1A

DATE: 28 June 83

TEMPERATURE: Room

MOISTURE TENSION: 5 cbar

Nominal stress (lb/in.^{2})	Residual deformation chart reading	(x10^{-4} in.)	Gauge length L_g (in.)	Resilient deformation chart reading	(x10^{-4} in.)	Resilient strain (x10^{-4})	
σ_3 = 1	3 mV	2	D_o = 1.969	0.5 mV	0.333	ε_r = 0.169	μ_r = 0.237
σ_d = 0.5	2 mV	1	L_o = 3.150	4.5 mV	2.250	ε_A = 0.714	M_r = 7.36x10^3 lb/in.^{2}
							M_r = 50.75 MPa

(P = 1.16 lb, A_o = 3.043 in.^{2}, σ_d = 0.526 lb/in.^{2}, σ_d = 3.625 kPa)

Figure A4. Repeated load triaxial test data sheet.

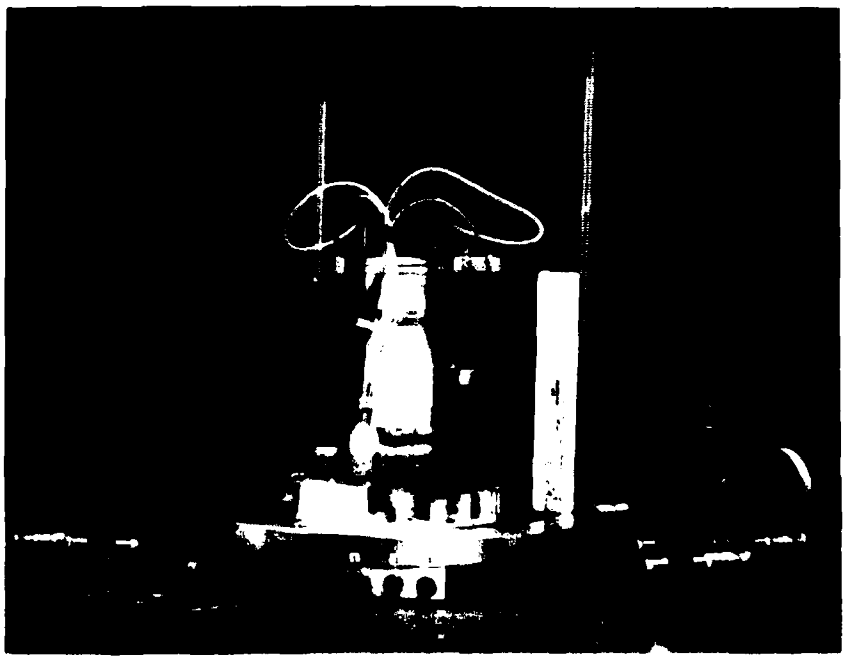

Figure A5. Installation of LVDT barrels.

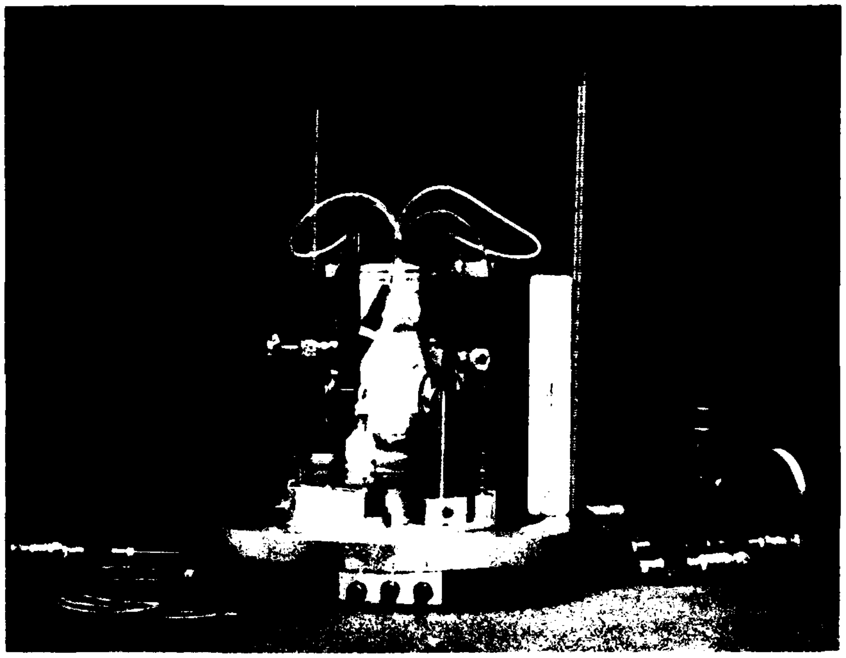

Figure A6. Installation of multi-VITs.

fore placing the cell cylinder over the sample, check that the LVDT wires do not restrict the motion of the LVDTs in any way.

Final cell assembly

Retract the three micrometers in the wall of the plexiglass cylinder. Install an O-ring in the groove of the cell base and place the cylinder over the sample and onto the base. Align the micrometers to the butt end of the multi-VIT mounts. Screw the three long-threaded rods into the outside rim of the cell base.

A miniature load cell that is capable of measuring the maximum load expected for the test is now bolted onto the loading piston of the top plate. Install a load button on the load cell and connect the load cell output to the bulkhead connector in the top plate. Place an O-ring in the O-ring groove of the top plate and place the top plate on the plexiglass cylinder, aligning the three holes with the threaded rods. Carefully seat the top plate on the cylinder and uniformly tighten three nuts on the threaded rods (see Fig. A7).

Adjust the micrometer in the cylinder wall to bring the multi-VITs toward the target on the sample. The multi-VITs are calibrated for a range of 0.10 in. but they are most linear over the first 0.05 in. Turn the micrometer to place each multi-VIT approximately 0.05 in. from the target.

This completes the specimen mounting and cell assembly procedure. It is essentially the same for the frozen and thawed cases, with the exception of the type of pedestal used. For the frozen specimens, all hardware should be brought to the test temperature before the specimen is mounted.

Allow 12 to 24 hours for temperature equilibration between frozen tests, depending upon the magnitude of the temperature change. Generally, begin testing at the lowest temperature indicated in the field test results.

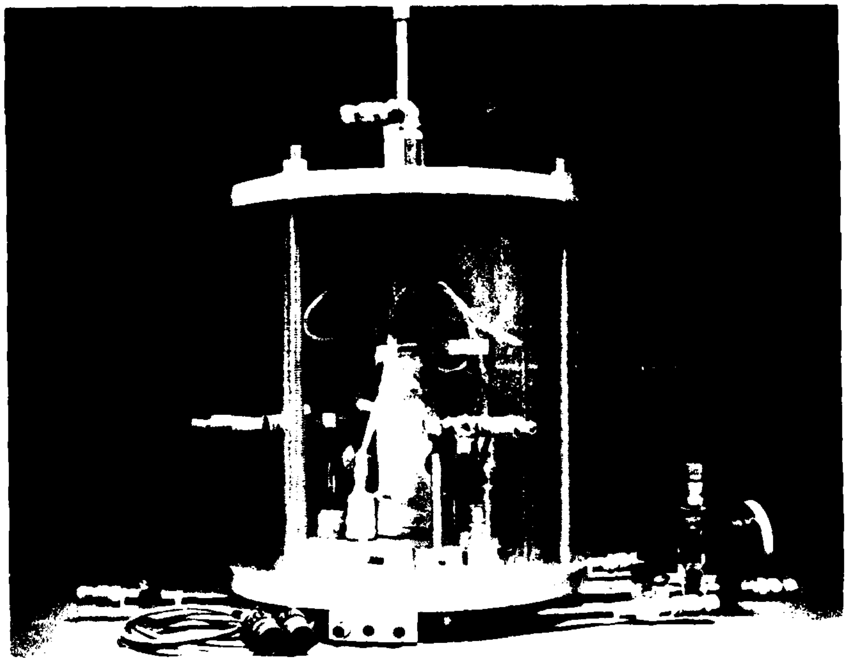

Figure A7. Fully assembled cell.

Moisture tension regulation

Thawed specimens are tested at up to four levels of moisture tension. The range of values is determined from field tensiometer data. A vacuum is applied to the cell drainage system and the specimen is drained until the desired level of moisture tension is achieved. Begin at the lowest level of moisture tension (generally upon thaw) and do tests at increasing tension levels. Keep the vacuum applied during load cycling to maintain a constant moisture tension level.

Currently, a manometer calibrated in cm of Hg is used to regulate the vacuum supply. (Note 1 kPa = 0.75 cm of Hg). The 2-in.-diameter, coarse-grained specimens equilibrate within 2-3 hours, while the 6-in. diameter specimens require up to 24 hours.

Test operation

The MTS machine is a very complex system and the operator should become familiar with its operation before installing any samples in the load frame. Prior to placing the triaxial cell in the MTS load frame, the hydraulic fluid must be warmed up. Turn on the MTS console, select "stroke" control, and place the hydraulic supply on high pressure. Adjust the material test generator for a 1-Hz sine wave. Adjust "Span I" for a 1-V cyclic wave and let the piston cycle for 20 minutes to bring the system to operating temperature.

A shearing device is installed on the piston for testing 2-in. samples to protect the load cell. Screw this device on the end of the MTS piston. Position the crosshead (with the piston fully extended) so that the triaxial cell is out of range of the piston, and the only possible contact is with the cell piston. This will prevent any damage to the triaxial cell in the event of error.

With the hydraulic supply off, install the triaxial cell in the load frame so that the MTS piston and the cell piston are offset. Connect the confining pressure supply to the top plate of the triaxial cell by means of the quick-connect coupling. Supply air to the confining pressure regulator and adjust the regulator for the desired pressure by monitoring the pressure gauge. Connect the load cell cable that goes to the MTS console to the connector on the top plate of the triaxial cell. Select load control and adjust the zero pot on the load dc conditioner for 0.00-V output. Place the hydraulic supply on high pressure and adjust the set point to retract the piston. Slide the triaxial cell to align the two pistons. Lower the MTS piston slowly with the "set point" control so that the two pistons come in contact. Adjust the "set point" so that a slight dead load of ½ lb is applied to the sample. Connect the LVDT and multi-VIT cables to their respective mating connectors on the cell base.

Before testing, make a table of all stress levels desired. This is done by converting the deviator stress to a millivolt output.

$$V_{out} = \sigma_d A_s x K$$

where σ_d = deviator stress (lb/in.^{2})
A_s = sample area (in.^{2})
K = load cell sensitivity (mV/lb)
V_{out} = output from load cell (mV).

The table should also include the confining stress σ_3, the strip chart recorder range, and the number of divisions on the strip chart for the desired σ_d (see Table A2). The choice of stress values depends on the type of test and sample to be run. Refer to the stress tables given in the text.

A thawed test on a 2-in. sample will be used as an example. Place the cell in the MTS with σ_3 = 1 lb/in.^{2} and a ½-lb dead load on the sample. Start the strip chart recorder with a chart speed of 0.05 mm/s. From the stress level table, set the recorder range on channel 1 to 250 mV full-scale. Use channel 2 to record the axial deformation (LVDTs). Turn on the no. 1 and no. 2 switches from the adder circuit and turn off the zero-adjust switch. Adjust the position and zero suppression controls for channel 2 on the recorder to bring the signal into range on the chart. If this procedure fails to bring the signal into range, turn the zero-adjust switch on the adder circuit to "on" and adjust the zero pot on the adder circuit. Place the channel 2 range control to 50 mV full-scale, which will give you 1 mV/division on the chart. Have the radial deformation (multi-VITs) on channel 3 on the recorder. Turn on all four switches on the multi-VIT averager circuit. Adjust the zero pot on the averager circuit to bring the signal on scale. Use the channel 3 position and zero suppression controls to zero the signal on the chart. Place channel 3 range switch to 50 mV full-scale. Position all zero signals at the left edge of their corresponding channels on the chart. Label the chart prior to testing, including all pertinent information (Table A3). The RPB and FWD load pulse waveforms are applied to the specimen as follows.

With Span II at zero, and the counter on the MTS at zero, start the Data Trak. Gradually turn the Span II control up to obtain the desired stress: σ_d = 0.5 kPa (see Table A2). For close scrutiny of each load cycle on the chart, press the divide by 100 (÷100) switch and switch on the recorder; this

Table A2. Load for 2-in.-diameter samples using 200-lb load cell (50 mV/lb).

σ_3 Confining stress (lb/in.^{2})	σ_d Deviator stress (lb/in.^{2})	Load for 2-in. samples (lb)	Load cell output (mV)	Recorder range (mV full-scale)	Number of divisions
1	0.5	1.57	78.5	250	15.7
	1	3.14	157.0	500	15.7
	1.5	4.71	235.5	500	23.5
	2	6.28	314.0	1,000	15.7
	2.5	7.85	392.5	1,000	19.6
2	1	3.14	157.0	500	15.7
	2	6.28	314.0	1,000	15.7
	3	9.42	471.0	1,000	23.5
	4	12.57	628.3	2,500	12.5
	5	15.71	785.4	2,500	15.7
4	2	6.28	314.0	1,000	15.7
	4	12.57	628.3	2,500	12.5
	6	18.85	942.5	2,500	18.8
	8	25.13	1256.6	2,500	25.1
	10	31.42	1570.8	5,000	15.7
10	5	15.71	785.4	2,500	15.7
	10	31.42	1570.8	5,000	15.7
	15	42.12	2356.2	5,000	23.6
	20	62.83	3141.6	10,000	15.7
	25	78.54	3927.0	10,000	19.6

Table A3. Strip chart label information.

	Channel		
	1	*2*	*3*
Device	Load cell, 200-lb capacity	LVDTs 0.25-in. range	Multi-VITs
Factor	50 mV/lb	5×10^{-5} in./mV	6.67×10^{-5} in./mV
Chart sensitivity	5 mV/division	1 mV/division	1 mV/division
σ_3 = 1.0 lb/in.^{2}		DATE	
σ_d = 0.5 lb/in.^{2}		TEST NO.	
ψ = 1 cbar		SPECIMEN NO.	

increases the chart speed to 5 mm/s. Allow three or four cycles to pass and press the ÷100 switch again to slow down the chart. (Note: the counter registers 1 count for each 3 cycles of an RPB cycle). Check the chart to see that the signals are all going to the right. Continue the test for 60 counts on the counter, speeding up the chart at 30 and 60 counts to monitor the signals. Stop the Data Trak at zero load.

Program the material test generator as follows to obtain the FWD pulse:

340 module
28 ms — inv 
trig 

341 module — 2 s
off

342 module — 2 s
cont (press start to run test and off to stop)

Start the program and increase the Span I control to obtain σ_d = 0.5 kPa. Run the chart at 1 mm/s and periodically press the ÷100 switch to expand the chart tracings to review the FWD signals. Run the test for 20 pulses, expanding the time scale at the beginning and end of the test, then stop the signal generator. There are filters on the strip chart recorder that must be set on at least 50 Hz during the FWD pulses so that the signals are not attenuated. These filters can be set on 5 Hz for the slower Data Trak pulses to eliminate any noise; noise is common on the LVDT channel.

Data reduction

Data reduction is done during testing. After each axial stress level is applied, reduce the data using the following formulas (1–19) and record the data on the data sheet (Fig. A4). Once some experience is obtained, the next deviator stress can be running while data are being reduced for the preceding test. This saves a considerable amount of time.

The baselines of the LVDT and multi-VIT data correspond to the residual deformations (see Fig. A8), while the pulses' height corresponds to the resilient deformations of the sample.

The circled numbers indicate the numbers on the chart (Fig. A8).

Fill in the top portion of the chart with all pertinent information: L_o, the gauge length between the circumferential clamps; sample diameter d; A_o = sample area $(D_o/2)^2\pi$; LVDT factor = LVDT sensitivity 0.250 in./2500 mV = 0.5×10^{-4} in./mV. σ_d in the left column denotes the nominal deviator stress, whereas items 15 and 16 in chart 2 give the actual deviator stress in lb/in.^{2} and kPa.

1. Divisions of multi-VIT baseline from zero at end of the test times the channel sensitivity: 3 div × 1 mV/div = 3 mV.

2. Multi-VIT sensitivity times baseline voltage: $(0.667 \times 10^{-4}$ in./mV) × 3 mV = 2×10^{-4} in. This number denotes residual radial deformation.

3. D_o plus residual radial deformation: 1.969 in. + 2×10^{-4} in. = 1.969 in.

4. Divisions of multi-VIT pulse at end of test times the channel sensitivity: 1 div × 0.5 mV/div = 0.5 mV.

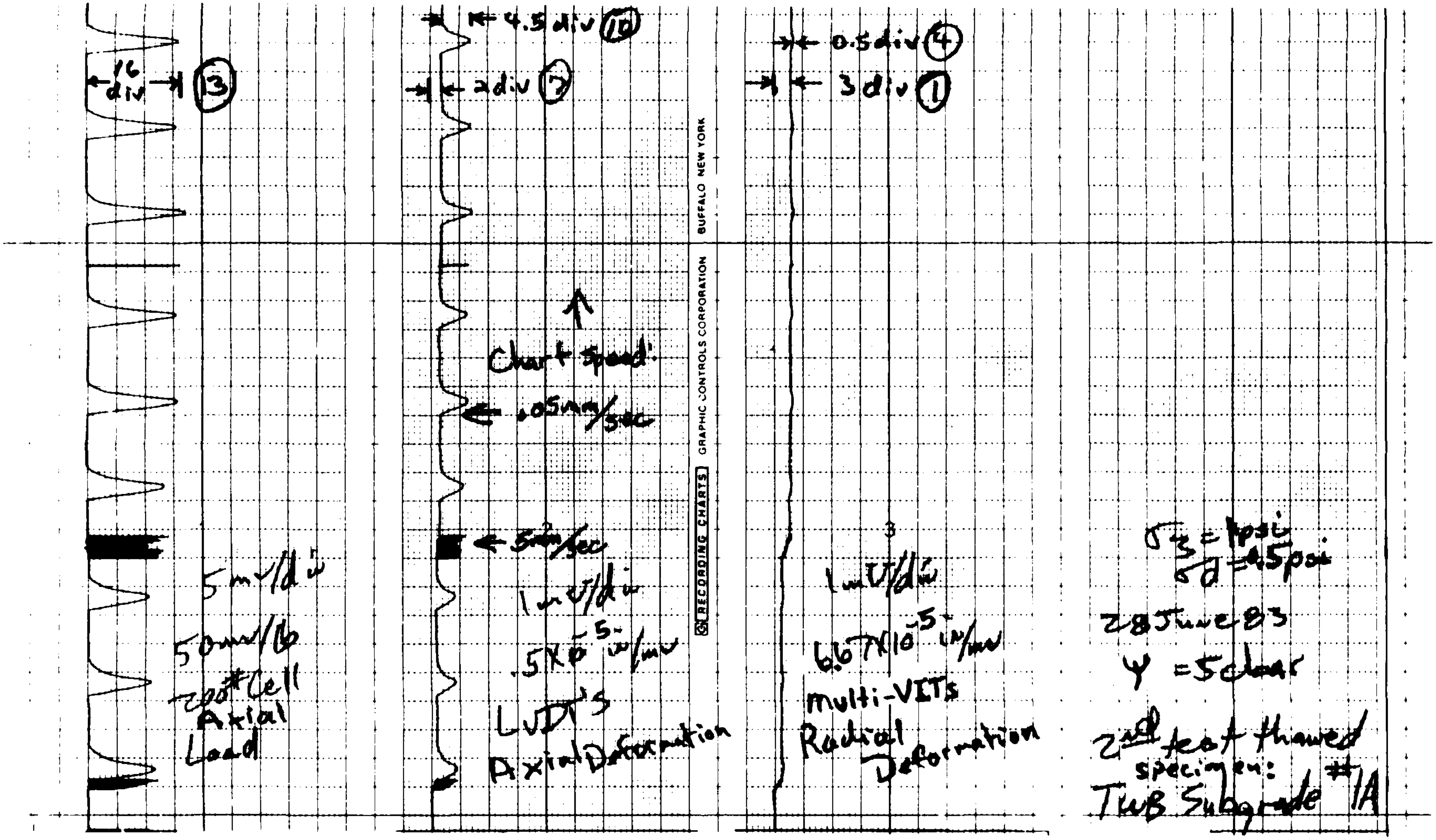

Figure A8. Typical strip chart recording.

5. Multi-VIT sensitivity times pulse voltage: $(0.667 \times 10^{-4}$ in./mV$) \times 0.5$ mV $= 0.333 \times 10^{-4}$ in. This number denotes resilient radial deformation or Δd.

6. $\Delta d/D_o = 0.667 \times 10^{-4}/1.969$ in. $= 0.169 \times 10^{-4}$; this denotes resilient radial strain or ϵ_r.

7. Divisions of LVDT baseline from zero at end of test times the channel sensitivity: 2 div $\times$ 1 mV/div = 2 mV.

8. LVDT sensitivity times baseline voltage: 0.5×10^{-4} in./mV $\times$ 2 mV $= 1.0 \times 10^{-4}$ in. This denotes residual axial deformation.

9. L_o minus residual axial deformation: 3.150 in. $- 1.0 \times 10^{-4}$ in. = 3.150 in.

10. Divisions of LVDT pulse at end of test times the channel sensitivity: 4.5 div $\times$ 1 mV/div = 4.5 mV.

11. LVDT sensitivity times pulse voltage $(0.5 \times 10^{-4}$ in./mV$) \times 4.5$ mV $= 2.250 \times 10^{-4}$ in. This denotes resilient axial deformation ΔL.

12. $\Delta L/L_o = 2.250 \times 10^{-4}$ in./3.150 in. $= 0.714 \times 10^{-4}$. This denotes resilient axial strain, ϵ_A.

13. Load pulse height in divisions times channel sensitivity divided by the load cell sensitivity gives the axial load P: 16 div $\times$ 5 mV/div $\div$ 50 mV/lb = 1.6 lb = P.

14. A_o. Note: If D_o increases during the test, calculate a new A_o.

15. $\sigma_d = P \div A_o$; 1.6 lb $\div$ 3.043 in.^{2} = 0.526 lb/in.^{2} This number is the actual σ_d in lb/in.^{2}

16. $\sigma_{d(kPa)} = \sigma_{d(lb/in.^2)} \times 6.895$: 0.526 lb/in.^{2} $\times$ 6.896 kPa/lb in.$^{-2}$ = 3.625 kPa. This is the actual σ_d in kPa.

17. $\mu_r = \epsilon_r/\epsilon_A$. $0.169 \times 10^{-4} \div 0.714 \times 10^{-4} = 0.237$. μ_r is the resilient Poisson's ratio.

18. $M_{r(lb/in.^2)} = \sigma_d/\epsilon_A$. $0.526/0.714 \times 10^{-4} = 7.36 \times 10^3$ lb/in.^{2} $M_{r(lb/in.^2)}$ denotes the resilient modulus in lb/in.^{2}

19. $M_{r(kPa)} = M_{r(lb/in.^2)} \times 6.895$. 7.36 lb/in.^{2} $\times$ 6.895 kPa/lb in.$^{-2}$ = 50.75 MPa. $M_{r(MPa)}$ denotes the resilient modulus in MPa.

This data reduction must be done for each set of applied stresses and the same procedure is followed regardless of the load waveform.

CONVERSION FACTORS: U.S. CUSTOMARY TO METRIC (SI) UNITS OF MEASUREMENT

These conversion factors include all the significant digits given in the conversion tables in the ASTM *Metric Practice Guide* (E 380), which has been approved for use by the Department of Defense. Converted values should be rounded to have the same precision as the original (see E 380).

Multiply	*By*	*To obtain*
inches	25.4	millimetres
square inches	0.00064516	square metres
pounds (mass)	0.4535924	kilograms
pounds (force) per square inch	0.006894757	megapascals

APPENDIX B: MOISTURE RETENTION CURVES FOR THE SIX WINCHENDON TEST SOILS

(1 cm water = 98.0638 Pa)

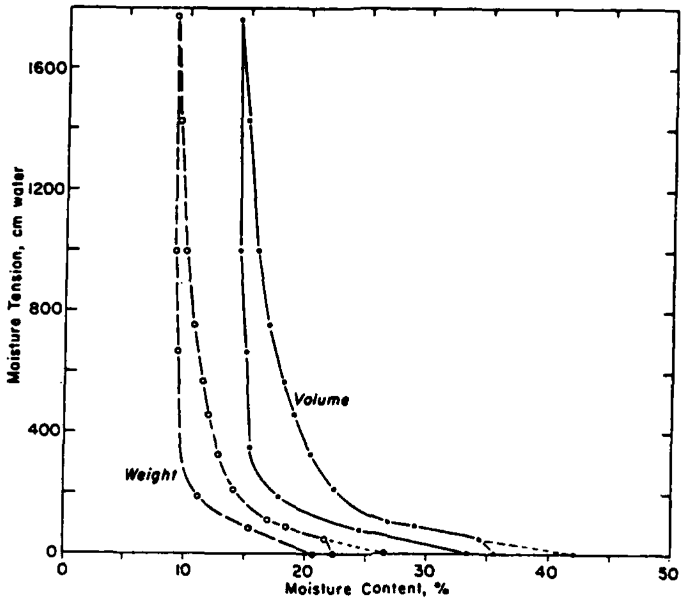

Figure B1. Graves sand (specific gravity = 2.73, dry density = 1.584 g/cm³).

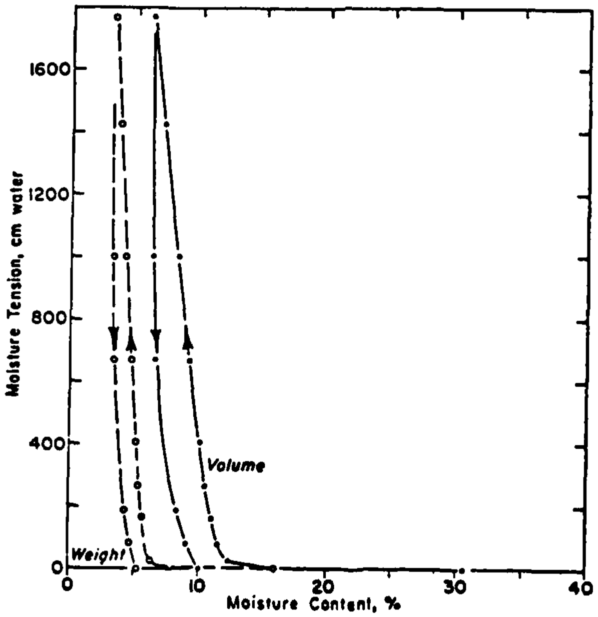

Figure B2. Dense Graded Stone (specific gravity = 2.80, dry density = 1.941 g/cm³).

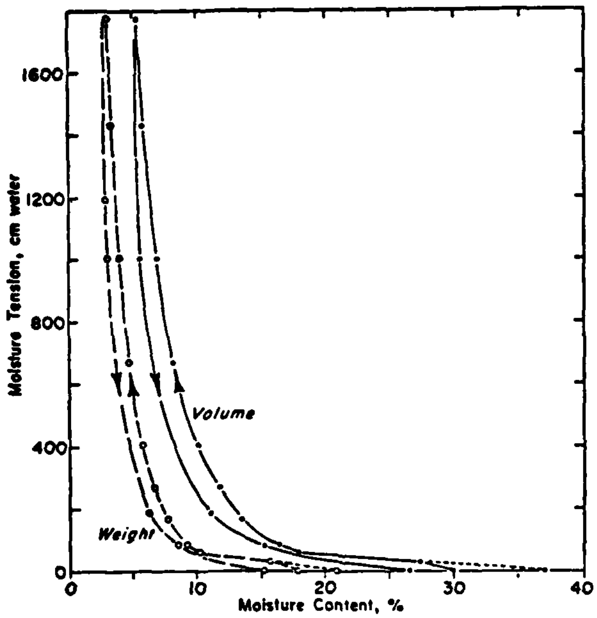

Figure B3. Hart Brothers sand (specific gravity = 2.78, dry density = 1.76 g/cm³).

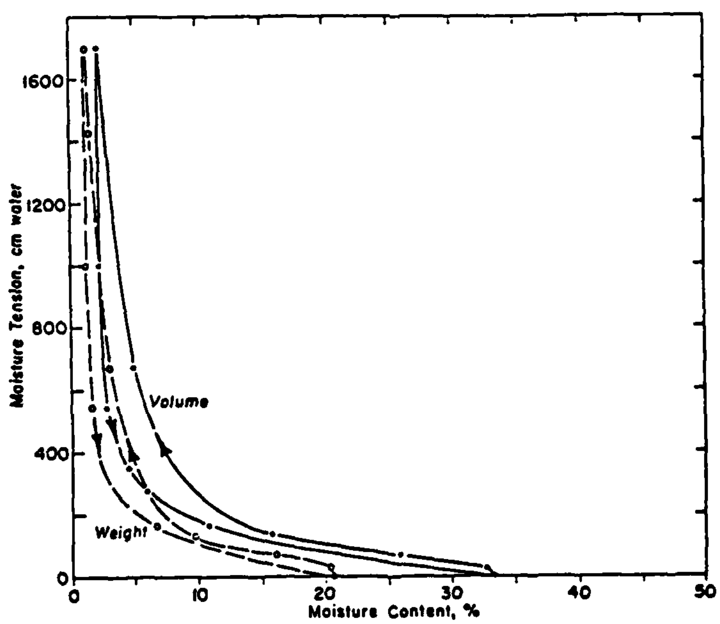

Figure B4. Ikalanian silt (specific gravity = 2.67, dry density = 1.611 g/cm³).

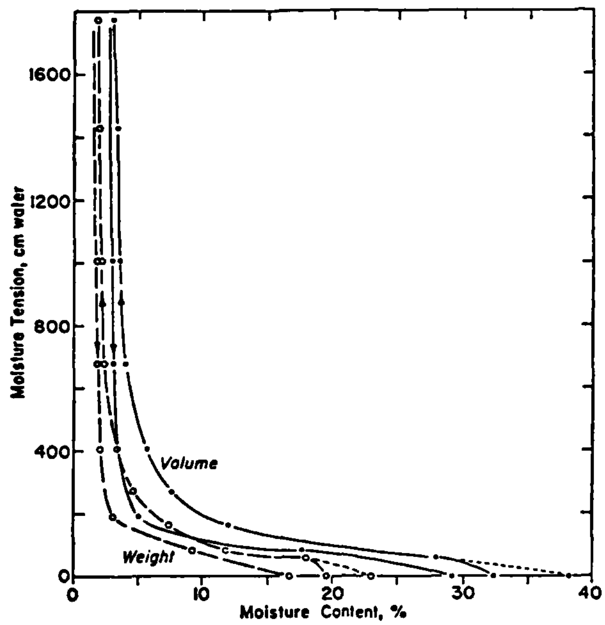

Figure B5. Hyannis sand (specific gravity = 2.67, dry density = 1.652 g/cm³).

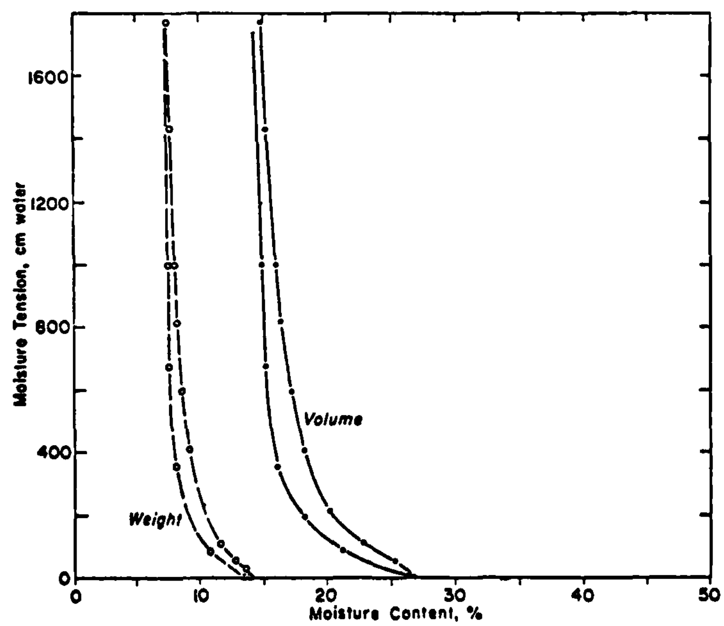

Figure B6. Sibley till (specific gravity = 2.75, dry density = 1.971 g/cm³).

APPENDIX C: REPEATED LOAD TRIAXIAL TEST RESULTS FOR ALL TEST SOILS

Sibley till

Thawed, RPB waveform

Confining pressure (kPa)	Deviator stress (kPa)	Radial strain $\times 10^{-4}$	Axial strain $\times 10^{-4}$	Resilient Poisson's ratio	Resilient modulus (MPa)	Dry density (Mg/m^3)	Moisture content (%)	Moisture tension (kPa)
6.9	3.3	0.220	0.698	0.315	47.8	1.920	12.80	5.0
	7.1	0.659	1.814	0.363	39.4			
	9.5	1.098	2.617	0.420	36.4			
	14.3	2.196	4.538	0.484	31.5			
13.8	7.1	0.549	1.396	0.393	51.1			
	14.3	1.647	3.317	0.497	43.1			
	20.0	3.293	5.416	0.608	36.9			
27.6	14.3	0.549	2.447	0.224	58.3			
	27.3	3.840	5.952	0.645	45.9			
6.9	3.6	0.220	0.591	0.372	60.5	1.930	12.00	8.0
	6.7	0.440	1.391	0.316	48.0			
	10.0	0.879	2.261	0.389	44.3			
13.8	6.7	0.330	1.044	0.316	63.9			
	14.3	1.099	2.784	0.395	51.4			
27.6	13.8	0.550	2.088	0.263	66.2			
	26.2	2.746	5.581	0.492	46.9			
6.9	3.6	0.115	0.333	0.345	109.3	1.920	11.00	16.0
	6.8	0.230	0.767	0.300	88.1			
	10.4	0.459	1.400	0.328	74.3			
	13.5	0.918	2.168	0.423	62.3			
13.8	6.8	0.344	0.734	0.469	92.1			
	13.5	0.689	1.668	0.413	81.0			
	20.8	1.377	3.003	0.459	69.2			
27.6	13.5	0.574	1.168	0.491	115.7			
	26.0	1.262	2.672	0.472	97.2			
6.9	3.4	0.115	0.200	0.575	168.8	1.957	10.40	29.0
	7.0	0.230	0.535	0.430	131.1			
	10.4	0.344	1.002	0.343	103.7			
	13.5	0.574	1.336	0.430	101.1			
13.8	7.0	0.230	0.568	0.405	123.5			
	14.0	0.459	1.236	0.371	113.5			
	20.8	0.803	2.004	0.401	103.7			
	27.3	1.377	3.007	0.458	90.7			
27.6	14.0	0.344	1.002	0.343	140.0			
	27.3	0.918	2.340	0.392	116.6			
	41.5	2.294	4.191	0.547	99.1			
6.9	3.4	0.664	0.416	1.596	81.3	1.696	11.80	9.0
	3.3	0.220	0.276	0.797	121.3	1.880	10.50	25.0
13.8	6.7	0.220	0.346	0.636	193.0			
	13.4	0.770	1.453	0.530	91.9			
27.6	13.4	0.550	1.456	0.378	91.8			
	27.4	2.748	3.825	0.718	71.7			
6.9	3.6	0.795	1.020	0.779	34.9	1.789	12.70	6.0
13.8	6.6	1.133	1.678	0.675	39.6			
6.9	3.6	0.227	0.600	0.378	59.5	1.910	11.30	13.0
	7.0	0.682	1.503	0.454	46.6			
13.8	7.0	0.682	1.172	0.582	59.8			
	13.4	1.590	2.685	0.592	49.8			
27.6	14.0	1.135	2.019	0.562	69.3			
6.9	10.5	0.795	1.501	0.530	69.9	1.939	10.80	18.0
	14.0	1.022	2.609	0.392	53.6			
13.8	20.3	1.815	3.344	0.543	60.8			
27.6	14.0	0.454	1.171	0.388	119.3			
	26.6	1.928	3.691	0.522	72.2			
6.9	3.4	0.113	0.269	0.420	127.4	1.948	10.30	29.0
	7.0	0.227	0.738	0.308	94.6			
	10.5	0.340	1.118	0.304	93.6			
	13.6	0.454	1.679	0.270	81.3			
	17.8	0.800	2.267	0.353	78.4			
	17.8	0.681	2.267	0.300	78.4			
13.8	7.0	0.227	0.638	0.356	109.4			
	6.9	0.227	0.638	0.356	108.0			
	14.0	0.454	1.578	0.288	88.5			
	14.0	0.340	1.578	0.215	88.5			
	20.9	0.681	2.586	0.263	81.0			
	27.9	1.361	3.868	0.352	72.2			
27.6	13.6	0.227	1.245	0.182	109.6			
	27.9	1.020	2.881	0.354	96.9			
6.9	3.4	0.113	0.668	0.169	51.2	1.951	12.80	5.0
	7.0	0.453	1.413	0.321	49.2			
	10.8	1.020	2.907	0.351	37.0			
	3.4	0.227	0.733	0.310	46.7	1.950	14.00	2.0
	7.0	0.680	1.900	0.358	36.7			

PREVIOUS PAGE IS BLANK

Confining pressure (kPa)	Deviator stress (kPa)	Radial strain x10^{-4}	Axial strain x10^{-4}	Resilient Poisson's ratio	Resilient modulus (MPa)	Dry density (Mg/m^3)	Moisture content (%)	Moisture tension (kPa)
	10.5	1.474	3.160	0.465	33.0			
13.8	7.0	0.453	1.567	0.289	44.5			
	13.6	1.587	3.669	0.433	37.2			
	20.5	3.853	6.843	0.563	30.0			
27.6	13.9	0.567	1.836	0.305	75.9			
	27.9	1.813	4.677	0.388	59.6			
6.9	3.5	0.790	1.000	0.790	35.2	1.579	12.70	6.0
	6.9	2.813	3.174	0.886	21.6			
13.8	6.9	1.688	2.073	0.814	33.1			
27.6	13.0	4.480	4.702	0.953	27.6			
6.9	3.5	-----	0.267	-----	130.6	1.595	11.50	11.0
	6.8	-----	1.001	-----	68.4			
	10.3	-----	2.169	-----	47.3			
13.8	6.8	-----	0.834	-----	82.1			
	13.7	-----	2.837	-----	48.3			
27.6	13.4	-----	1.571	-----	85.2			
	26.1	-----	6.033	-----	43.3			
6.9	3.5	-----	0.200	-----	174.3	1.845	11.00	17.0
	6.8	0.225	0.667	0.337	102.7			
	10.6	0.449	1.334	0.337	79.3			
	13.7	0.674	2.168	0.311	63.2			
13.8	6.8	0.112	0.567	0.198	120.8			
	13.7	0.337	1.668	0.202	82.1			
	19.9	1.011	3.003	0.337	66.3			
	19.9	0.899	3.337	0.269	59.7			
27.6	13.7	0.225	1.335	0.169	102.5			
	26.8	1.011	3.341	0.303	80.1			
6.9	6.8	0.225	0.601	0.374	113.9	1.890	10.30	30.0
	10.0	0.337	1.169	0.288	85.2			
	13.7	0.449	1.838	0.244	74.5			
	17.4	0.786	2.841	0.277	61.3			
	17.4	0.674	3.175	0.212	54.9			
13.8	6.8	0.112	0.468	0.239	146.3			
	13.6	0.449	1.571	0.286	86.8			
	20.5	0.899	2.908	0.309	70.6			
	27.4	1.572	4.681	0.336	58.5			
27.6	13.7	0.225	0.836	0.269	163.8			
	27.4	0.786	2.844	0.276	96.2			
6.9	3.4	0.337	0.837	0.403	40.1	1.922	14.00	2.0
	6.8	1.011	2.175	0.465	31.5			
	10.3	1.909	3.515	0.543	29.2			
13.8	6.8	0.449	1.339	0.335	51.1			
	19.9	3.815	6.366	0.599	31.2			
27.6	13.7	0.786	2.010	0.391	68.0			
	27.3	2.917	6.035	0.483	45.3			

Frozen, RPB waveform

Confining pressure (kPa)	Deviator stress (kPa)	Axial strain x10^{-4}	Resilient modulus (GPa)	Dry density (Mg/m^3)	Moisture content (%)	Temperature ($^{\circ}$C)
27.6	27.3	0.029	9.43	1.827	12.52	-0.5
	40.4	0.059	6.85			
	54.7	0.118	4.63			
	68.9	0.177	3.90			
48.3	23.8	0.029	8.20			
	47.5	0.103	4.62			
	71.3	0.206	3.46			
	95.1	0.294	3.23			
68.9	66.6	0.177	3.76			
	133.1	0.530	2.51			
	199.7	0.885	2.26			
	68.4	0.103	6.64	1.827	12.52	-1.0
	136.8	0.324	4.22			
	202.2	0.588	3.44			
48.3	47.5	0.074	6.43			
	71.3	0.118	6.04			
	95.0	0.192	4.95			
27.6	27.3	0.015	18.23			
	40.4	0.044	9.19			
	54.7	0.088	6.21			
68.9	68.4	0.029	23.58	1.827	12.52	-5.2
	101.1	0.059	17.14			
	136.8	0.074	18.49			
	208.1	0.132	15.77			
	273.5	0.147	18.61			
	344.9	0.191	18.06			
	475.7	0.324	14.68			
	624.3	0.515	12.12			
	68.4	0.015	45.59	1.827	12.52	-10.0
	101.1	0.029	34.86			
	136.8	0.059	23.19			
	208.1	0.088	23.65			
	273.5	0.147	18.61			
	333.0	0.191	17.43			
	475.7	0.294	16.18			
	624.3	0.441	14.16			

Confining pressure (kPa)	Deviator stress (kPa)	Axial strain x10^{-4}	Resilient modulus (GPa)	Dry density (Mg/m^3)	Moisture content (%)	Temperature (°C)
27.6	27.7	0.059	4.70	1.886	11.96	-0.4
	41.0	0.177	2.32			
	53.0	0.295	1.80			
	67.5	0.472	1.43			
13.8	13.5	0.022	6.14			
	20.7	0.044	4.71			
	27.7	0.088	3.15			
	37.4	0.148	2.53			
	41.0	0.177	2.32			
48.3	24.1	0.044	5.48			
	48.2	0.251	1.92			
	72.3	0.531	1.36			
	96.4	0.797	1.21			
68.9	33.8	0.181	1.86			
	67.5	0.434	1.56			
	139.8	1.330	1.05			
	103.7	0.916	1.13			
	66.3	0.088	7.54	1.886	11.96	-1.0
	135.7	0.235	5.77			
	205.1	0.412	4.98			
	277.4	0.736	3.77			
	337.8	0.942	3.59			
	482.5	1.916	2.52			
	602.7	2.715	2.22			
48.3	48.2	0.044	10.96			
	72.3	0.088	6.22			
	96.4	0.118	8.17			
	120.5	0.148	8.14			
	144.7	0.207	6.99			
27.6	27.7	0.029	9.56			
	41.0	0.087	4.71			
	55.4	0.118	4.70			
68.9	135.1	0.059	22.90	1.886	11.96	-5.0
	202.7	0.088	23.03			
	265.4	0.118	22.49			
	337.8	0.176	19.19			
	482.5	0.324	14.89			
	603.1	0.441	13.68			
	69.3	0.030	23.10	1.886	11.96	-9.5
	105.5	0.059	17.88			
	138.6	0.074	18.73			
	204.9	0.118	17.36			
	277.2	0.148	18.73			
	349.6	0.207	16.89			
	482.2	0.310	15.55			
	602.7	0.373	16.16			

Graves sand

Thawed, RPB waveform

Confining pressure (kPa)	Deviator stress (kPa)	Radial strain x10^{-4}	Axial strain x10^{-4}	Resilient Poisson's ratio	Resilient modulus (MPa)	Dry density (Mg/m^3)	Moisture content (%)	Moisture tension (kPa)
6.9	3.5	-----	1.430	-----	24.2	1.457	23.50	3.0
	3.5	-----	0.828	-----	41.8	1.496	21.50	6.0
	6.9	0.331	1.641	0.180	37.6			
	10.4	0.828	3.503	0.236	29.6			
	13.8	1.324	5.170	0.256	26.8			
	17.3	1.653	6.479	0.255	26.6			
13.8	6.9	0.165	1.481	0.111	46.6			
	21.6	1.323	5.930	0.223	36.4			
	28.0	2.148	8.371	0.257	33.5			
27.6	43.1	1.818	7.857	0.231	54.9			
6.9	3.5	0.166	0.740	0.224	47.1	1.547	18.50	10.0
	10.4	0.664	2.960	0.224	35.3			
	13.9	0.997	4.255	0.234	32.7			
	17.4	1.495	5.366	0.279	32.5			
13.8	13.9	0.664	3.238	0.205	43.0			
	21.8	1.163	5.183	0.224	42.0			
	28.3	1.827	6.484	0.282	43.6			
	34.8	2.325	8.343	0.279	41.7			
27.6	13.9	0.332	2.039	0.163	68.3			
	28.3	0.997	4.449	0.224	63.6			
	43.5	1.827	7.421	0.246	58.7			
	56.6	2.823	9.683	0.292	58.5			
69.0	34.8	0.499	3.354	0.149	103.8			
6.9	3.5	-----	0.552	-----	62.9	1.550	16.00	15.0
	6.9	0.166	1.379	0.120	50.4			
	10.4	0.332	2.483	0.134	42.0			
	13.9	0.663	3.679	0.180	37.8			
	17.4	0.829	4.601	0.180	37.8			
13.8	13.9	0.332	2.760	0.120	50.3			
	21.7	0.995	4.418	0.225	49.1			
	28.2	1.327	6.080	0.218	46.4			
	34.7	1.658	7.372	0.225	47.1			
27.6	13.9	0.166	1.843	0.090	75.4			
	28.2	0.829	4.055	0.204	69.6			
	43.4	1.327	6.822	0.195	63.6			
	56.4	2.156	9.232	0.234	61.1			
6.9	3.4	-----	1.607	-----	20.9	1.448	25.00	2.0
	10.1	-----	4.663	-----	21.7			
	13.4	3.261	6.305	0.517	21.3			
13.8	13.4	-----	4.326	-----	31.0			
	20.9	3.258	7.260	0.449	28.8			
27.6	13.4	-----	2.179	-----	61.5			
	27.2	-----	6.189	-----	44.0			
6.9	3.4	0.164	1.060	0.155	32.1	1.499	22.50	5.0
	6.8	0.820	2.829	0.290	24.0			
	10.2	1.640	4.423	0.371	23.1			
	13.6	2.132	5.667	0.376	24.0			
	16.9	2.622	7.451	0.352	22.7			
13.8	6.8	0.328	1.952	0.168	34.7			
	13.6	1.147	3.726	0.308	36.4			
	21.2	2.294	7.105	0.323	29.8			
	27.5	3.276	8.903	0.368	30.9			
27.6	13.5	0.655	2.493	0.263	54.4			
	42.3	3.273	9.303	0.352	45.4			
69.0	33.8	0.655	3.584	0.183	94.4			
6.9	6.8	0.494	1.814	0.272	37.7	1.524	19.50	9.0
	10.3	0.658	2.812	0.234	36.5			
	13.7	1.316	3.811	0.345	35.9			
	17.1	1.809	5.265	0.344	32.4			
13.8	6.8	0.329	1.634	0.201	41.8			
	13.7	0.822	3.268	0.252	41.8			
	21.3	1.480	5.085	0.291	42.0			
	27.8	2.631	6.907	0.381	40.2			
	34.1	3.452	8.552	0.404	39.9			
6.9	3.4	-----	1.495	-----	23.1	1.457	26.00	1.0
	6.9	-----	2.991	-----	23.1			
	10.3	-----	4.225	-----	24.5			
	13.8	-----	5.814	-----	23.7			
13.8	13.8	-----	3.704	-----	37.3			
	21.6	-----	6.351	-----	33.9			
	28.0	-----	8.304	-----	33.8			
27.6	13.8	-----	2.390	-----	57.7			
	28.0	-----	4.958	-----	56.5			

Confining pressure (kPa)	Deviator stress (kPa)	Radial strain $\times 10^{-4}$	Axial strain $\times 10^{-4}$	Resilient Poisson's ratio	Resilient modulus (MPa)	Dry density (Mg/m^3)	Moisture content (%)	Moisture tension (kPa)
	43.1	-----	7.975	-----	54.1			
	56.1	-----	10.670	-----	52.5			
6.9	3.5	-----	0.976	-----	35.4	1.517	22.50	5.0
	10.4	-----	3.196	-----	32.4			
	13.8	-----	4.263	-----	32.4			
13.8	34.6	-----	8.357	-----	41.4			
27.6	28.1	-----	4.267	-----	65.8			
	56.2	-----	8.503	-----	63.1			
	69.1	-----	11.600	-----	59.6			
69.0	34.6	-----	3.034	-----	113.9			
	69.1	-----	6.429	-----	107.5			
6.9	3.5	-----	0.787	-----	44.6	1.546	19.50	9.0
	7.0	-----	1.671	-----	42.0			
	10.5	-----	2.557	-----	41.2			
	14.0	-----	3.345	-----	42.0			
13.8	35.1	-----	7.098	-----	49.4			
27.6	14.0	-----	1.873	-----	75.0			
	57.0	-----	7.893	-----	72.2			
	70.2	-----	9.882	-----	71.0			
69.0	35.1	-----	2.768	-----	126.8			
	70.2	-----	5.934	-----	118.3			
6.9	3.5	-----	0.495	-----	69.7	1.523	14.50	20.0
	6.9	0.165	1.188	0.139	58.1			
	10.4	0.330	1.979	0.167	52.3			
	13.8	0.496	2.771	0.179	49.8			
	17.3	0.661	3.563	0.186	48.4			
13.8	6.9	0.165	0.990	0.167	69.7			
	13.8	0.331	2.276	0.145	60.6			
	21.6	0.661	3.761	0.176	57.4			
	28.0	0.992	5.146	0.193	54.5			
	34.5	1.322	6.334	0.209	54.5			
27.6	13.8	-----	1.386	-----	99.6			
	28.0	0.661	3.365	0.196	83.3			
	43.1	1.157	5.542	0.209	77.8			
	69.0	2.148	8.914	0.241	77.4			
69.0	34.5	0.496	2.180	0.228	158.3			
	69.0	0.992	5.155	0.192	133.9			
6.9	10.1	1.307	3.678	0.355	27.5	1.455	26.00	1.0
	13.5	2.123	6.140	0.346	22.0			
	16.8	2.937	6.984	0.421	24.1			
13.8	21.0	2.284	6.178	0.370	34.0			
	27.3	3.588	8.276	0.434	33.0			
27.6	42.0	3.100	8.322	0.373	50.5			
6.9	3.3	0.163	1.104	0.148	30.3	1.470	22.50	5.0
	10.0	0.977	3.403	0.287	29.5			
	16.7	1.790	6.039	0.296	27.7			
13.8	13.4	0.814	3.221	0.253	41.6			
	20.9	1.628	5.236	0.311	40.0			
	33.4	4.227	10.530	0.401	31.7			
27.6	13.3	0.488	2.025	0.241	65.9			
	27.1	1.300	4.455	0.292	60.9			
	41.7	2.600	7.094	0.367	58.8			
69.0	66.7	1.784	6.522	0.274	102.3			
6.9	6.7	0.163	1.809	0.090	37.1	1.501	20.00	8.0
	10.1	0.489	2.980	0.164	33.8			
	13.4	0.652	4.046	0.161	33.1			
	16.8	1.140	5.115	0.223	32.8			
13.8	6.7	0.163	1.492	0.109	44.9			
	13.4	0.489	2.984	0.164	44.9			
	21.0	1.303	4.904	0.266	42.7			
	27.2	1.629	6.829	0.239	39.9			
	33.5	2.607	8.971	0.291	37.4			
27.6	27.2	0.978	4.487	0.218	60.7			
	41.9	1.955	7.268	0.269	57.7			
	54.5	2.933	9.632	0.305	56.6			
	67.0	4.559	12.240	0.372	54.7			
69.0	33.5	0.489	3.006	0.163	111.4			
6.9	3.4	0.164	0.926	0.177	36.4	1.507	26.00	1.0
	6.8	0.491	2.263	0.217	29.9			
	10.1	0.981	3.707	0.265	27.4			
	13.5	1.636	5.359	0.305	25.2			
	16.9	2.453	7.013	0.350	24.1			
13.8	6.8	0.327	1.547	0.211	43.7			
	13.5	0.818	3.300	0.248	41.0			
	21.1	1.799	6.191	0.291	34.1			

Confining pressure (kPa)	Deviator stress (kPa)	Radial strain x10^{-4}	Axial strain x10^{-4}	Resilient Poisson's ratio	Resilient modulus (MPa)	Dry density (Mg/m^3)	Moisture content (%)	Moisture tension (kPa)
	27.4	2.617	8.261	0.317	33.2			
27.6	13.5	0.491	2.069	0.237	65.3			
	27.4	1.308	4.553	0.287	60.3			
	42.2	2.289	7.453	0.307	56.6			
	54.9	3.924	10.360	0.379	53.0			
	67.4	5.228	13.510	0.387	49.9			
69.0	33.7	0.654	2.496	0.262	135.0			
13.8	12.9	0.640	3.400	0.188	38.1			
	20.2	1.280	5.690	0.225	35.5			
27.6	26.3	0.960	4.373	0.220	60.1			
6.9	3.3	-----	0.670	-----	48.9	1.487	20.50	7.0
	6.6	0.322	1.819	0.177	36.0			
	9.8	0.644	3.046	0.211	32.3			
	13.1	0.806	4.023	0.200	32.6			
	16.4	1.128	5.176	0.218	31.7			
13.8	6.6	0.322	1.342	0.240	48.9			
	13.1	0.484	2.876	0.168	45.6			
	20.5	0.967	4.990	0.194	41.1			
	26.6	1.611	6.728	0.239	39.6			
	32.7	1.932	8.671	0.223	37.7			
27.6	13.1	0.322	1.734	0.186	75.5			
	26.6	0.805	4.241	0.190	62.7			
	40.9	1.610	7.722	0.208	53.0			
	53.2	2.736	11.640	0.235	45.7			
69.0	32.7	0.644	3.108	0.207	105.3			
	65.4	1.610	7.201	0.224	90.9			
6.9	3.3	-----	0.498	-----	65.7	1.501	16.50	13.0
	6.5	0.161	1.595	0.101	41.0			
	13.1	0.483	3.291	0.147	39.8			
	16.4	0.644	4.589	0.140	35.7			
13.8	6.5	0.162	1.297	0.125	50.4			
	13.1	0.322	2.694	0.120	48.6			
	26.6	1.127	5.591	0.202	47.5			
	32.7	1.771	7.391	0.240	44.3			
27.6	13.1	0.322	1.798	0.179	72.8			
	26.6	0.805	3.995	0.202	66.5			
	40.9	1.449	6.795	0.213	60.2			
	53.2	2.253	9.000	0.250	59.1			
	65.4	3.218	12.020	0.268	54.4			
6.9	6.6	0.484	1.656	0.292	39.7	1.501	25.00	2.0
	9.9	0.968	3.130	0.309	31.5			
	13.1	1.613	5.158	0.313	25.5			
	16.4	2.259	6.453	0.350	25.5			
13.8	6.6	0.323	0.830	0.389	79.2			
	13.1	0.968	2.581	0.375	50.9			
	20.5	1.613	5.166	0.312	39.7			
	26.7	2.419	7.388	0.327	36.1			
27.6	13.1	0.484	1.386	0.349	94.8			
	26.7	1.290	4.067	0.317	65.6			
	41.1	2.258	7.029	0.321	58.4			

Thawed, FWD waveform

Confining pressure (kPa)	Deviator stress (kPa)	Radial strain x10^{-4}	Axial strain x10^{-4}	Resilient Poisson's ratio	Resilient modulus (MPa)	Dry density (Mg/m^3)	Moisture content (%)	Moisture tension (kPa)
6.9	3.5	-----	1.430	-----	24.2	1.457	23.50	3.0
	6.9	0.662	3.050	0.217	22.7			
	3.5	-----	0.920	-----	37.6	1.496	21.50	6.0
	6.9	0.497	2.209	0.225	31.3			
	10.4	0.828	4.056	0.204	25.6			
	13.8	1.324	5.539	0.239	25.0			
	17.3	1.984	7.405	0.268	23.3			
13.8	6.7	0.165	1.481	0.111	45.3			
	13.8	0.661	3.517	0.188	39.3			
	21.6	1.653	6.672	0.248	32.3			
	28.0	2.479	9.304	0.266	30.1			
27.6	13.8	0.331	2.047	0.162	67.4			
	13.8	1.157	5.585	0.207	24.7			
	43.1	1.983	7.857	0.252	54.9			
6.9	3.5	0.166	0.740	0.224	47.1	1.547	18.50	10.0
	10.4	0.664	2.960	0.224	35.3			
	13.9	0.997	4.440	0.225	31.4			
	17.4	1.495	5.551	0.269	31.4			
13.8	7.0	0.166	1.480	0.112	47.1			
	13.9	0.664	3.146	0.211	44.3			
	21.8	1.163	5.183	0.224	42.0			
	28.3	1.827	6.854	0.267	41.3			
	34.8	2.325	8.343	0.279	41.7			
27.6	13.9	0.332	2.039	0.163	68.3			
	28.3	0.997	4.635	0.215	61.1			
	43.5	1.827	7.421	0.246	58.7			
69.0	34.8	0.499	2.982	0.167	116.8			

Confining pressure (kPa)	Deviator stress (kPa)	Radial strain x10^{-4}	Axial strain x10^{-4}	Resilient Poisson's ratio	Resilient modulus (MPa)	Dry density (Mg/m^3)	Moisture content (%)	Moisture tension (kPa)
6.9	6.9	0.166	1.471	0.113	47.2	1.550	16.00	15.0
	10.4	0.332	2.758	0.120	37.8			
	13.9	0.663	3.863	0.172	36.0			
	17.4	0.995	4.785	0.208	36.3			
13.8	6.9	0.166	1.472	0.113	47.2			
	13.9	0.498	2.944	0.169	47.2			
	21.7	0.995	4.786	0.208	45.4			
	28.2	1.327	6.448	0.206	43.8			
	34.7	1.824	8.109	0.225	42.8			
27.6	13.9	0.166	1.843	0.090	75.4			
	28.2	0.829	4.423	0.187	63.8			
	43.4	1.327	7.375	0.180	58.9			
	56.4	2.322	10.160	0.229	55.6			
6.9	3.4	-----	1.607	-----	20.9	1.448	25.00	2.0
	6.7	-----	3.577	-----	18.8			
	10.1	-----	4.663	-----	21.7			
	13.4	-----	7.205	-----	18.6			
13.8	13.4	-----	4.506	-----	29.8			
	20.9	-----	8.530	-----	24.5			
27.6	13.4	-----	2.723	-----	49.2			
	27.2	-----	6.735	-----	40.4			
6.9	3.4	0.328	1.060	0.309	32.1	1.499	22.50	5.0
	6.8	0.820	2.829	0.290	24.0			
	10.2	1.640	4.600	0.357	22.2			
	13.6	2.132	6.022	0.354	22.6			
	16.9	2.622	7.984	0.328	21.2			
13.8	6.8	0.328	1.952	0.168	34.7			
	13.6	1.147	3.903	0.294	34.7			
	21.2	2.294	7.105	0.323	29.8			
	27.5	3.440	9.793	0.351	28.1			
27.6	13.5	0.655	2.493	0.263	54.4			
	42.3	3.600	9.850	0.365	42.9			
69.0	33.8	0.982	3.402	0.289	99.4			
6.9	3.4	0.164	0.907	0.181	37.7	1.524	19.50	9.0
	6.8	0.329	1.814	0.181	37.7			
	10.3	0.658	2.721	0.242	37.7			
	13.7	1.316	4.174	0.315	32.8			
	17.1	1.809	5.447	0.332	31.4			
13.8	6.8	0.329	1.452	0.227	47.1			
	13.7	0.622	3.268	0.252	41.8			
	21.3	1.644	5.449	0.302	39.2			
	27.8	2.631	7.815	0.337	35.5			
	34.1	3.945	10.010	0.394	34.1			
6.9	3.4	-----	1.407	-----	24.5	1.457	26.00	1.0
	6.9	-----	2.991	-----	23.1			
	10.3	-----	4.401	-----	23.5			
	13.8	-----	6.166	-----	22.4			
	17.3	-----	7.407	-----	23.3			
13.8	13.8	-----	3.704	-----	37.3			
	21.6	-----	6.528	-----	33.0			
	28.0	-----	8.304	-----	33.8			
	34.5	-----	10.620	-----	32.5			
27.6	13.8	-----	2.302	-----	59.9			
	28.0	-----	5.135	-----	54.6			
	43.1	-----	7.975	-----	54.1			
	56.1	-----	11.550	-----	48.5			
6.9	3.5	-----	0.976	-----	35.4	1.517	22.50	5.0
	6.9	-----	2.130	-----	32.5			
	10.4	-----	3.196	-----	32.4			
	13.8	-----	4.263	-----	32.4			
13.8	6.9	-----	1.777	-----	38.9			
	13.8	-----	3.554	-----	38.9			
	34.6	-----	8.890	-----	38.9			
27.6	28.1	-----	4.623	-----	60.8			
	43.2	-----	7.115	-----	60.7			
	56.2	-----	9.793	-----	57.4			
	69.1	-----	12.490	-----	55.4			
69.0	34.6	-----	3.034	-----	113.9			
	69.1	-----	6.607	-----	104.6			
6.9	3.5	-----	0.787	-----	44.6	1.546	19.50	9.0
	7.0	-----	1.573	-----	44.6			
	10.5	-----	2.754	-----	38.2			
	14.0	-----	3.542	-----	39.6			
13.8	7.0	-----	1.378	-----	50.9			
	21.9	-----	4.726	-----	46.4			
	35.1	-----	7.492	-----	46.8			
27.6	14.0	-----	1.873	-----	75.0			
	43.9	-----	6.903	-----	63.5			
	57.0	-----	8.287	-----	68.8			
	70.2	-----	11.860	-----	59.2			

Confining pressure (kPa)	Deviator stress (kPa)	Radial strain $\times 10^{-4}$	Axial strain $\times 10^{-4}$	Resilient Poisson's ratio	Resilient modulus (MPa)	Dry density (Mg/m^3)	Moisture content (%)	Moisture tension (kPa)
69.0	35.1	0.195	2.966	0.066	118.3			
	70.2	-----	6.131	-----	114.5			
6.9	3.5	-----	0.594	-----	58.1	1.523	14.50	20.0
	6.9	0.165	1.188	0.139	58.1			
	10.4	0.330	1.979	0.167	52.3			
	13.8	0.496	2.969	0.167	46.5			
	17.3	0.661	3.959	0.167	43.6			
13.8	6.9	0.165	1.188	0.139	58.1			
	13.8	0.496	2.375	0.209	58.1			
	21.6	0.661	4.157	0.159	51.9			
	28.0	0.992	5.146	0.193	54.5			
	34.5	1.322	6.334	0.209	54.5			
27.6	13.8	-----	1.584	-----	87.1			
	28.0	0.661	3.365	0.196	83.3			
	43.1	1.157	5.983	0.193	72.1			
	56.1	1.653	7.921	0.209	70.8			
	69.0	2.148	9.311	0.231	74.1			
69.0	34.5	0.496	2.180	0.228	158.3			
	69.0	0.992	5.353	0.185	128.9			
6.9	10.1	1.307	4.087	0.320	24.7	1.455	26.00	1.0
	13.5	2.286	6.549	0.349	20.6			
	16.8	3.426	8.217	0.417	20.5			
13.8	13.4	1.142	3.701	0.309	36.3			
	21.0	2.447	6.590	0.371	31.9			
	27.3	3.916	9.309	0.421	29.3			
27.6	27.3	1.632	4.764	0.343	57.3			
	42.0	3.263	10.400	0.314	40.4			
6.9	3.3	0.163	1.205	0.135	27.8	1.470	22.50	5.0
	6.7	0.489	2.410	0.203	27.8			
	10.0	0.977	3.403	0.287	29.5			
	13.4	1.466	5.026	0.292	26.6			
	16.7	1.953	6.039	0.323	27.7			
13.8	13.4	0.814	3.221	0.253	41.6			
	33.4	4.227	10.130	0.417	32.9			
27.6	13.3	0.488	2.228	0.219	59.9			
	27.1	1.300	4.658	0.279	58.2			
	41.7	2.763	8.107	0.341	51.4			
69.0	66.7	1.946	6.726	0.289	99.2			
6.9	3.4	-----	0.851	-----	39.4	1.501	20.00	8.0
	6.7	0.163	1.915	0.085	35.0			
	10.1	0.489	3.193	0.153	31.5			
	13.4	0.815	3.832	0.213	35.0			
	16.8	1.140	5.115	0.223	32.8			
13.8	6.7	0.163	1.492	0.109	44.9			
	13.4	0.489	2.984	0.164	44.9			
	21.0	1.140	5.117	0.223	41.0			
	27.2	1.955	7.256	0.269	37.5			
	33.5	2.770	8.971	0.309	37.4			
27.6	27.2	0.978	4.721	0.208	57.9			
	41.5	1.955	7.696	0.254	54.5			
	54.5	3.421	10.060	0.340	54.2			
	67.0	4.559	13.950	0.327	48.0			
69.0	33.5	0.489	2.791	0.175	120.0			
6.9	3.4	0.164	1.028	0.160	32.8	1.507	26.00	1.0
	6.8	0.654	2.675	0.244	25.3			
	10.1	0.981	3.913	0.251	25.9			
	13.5	1.799	5.359	0.336	25.2			
	16.9	2.617	7.632	0.343	22.1			
13.8	6.8	0.327	1.650	0.198	41.0			
	13.5	0.981	3.507	0.280	38.6			
	21.1	1.799	6.191	0.291	34.1			
	27.4	2.944	8.261	0.356	33.2			
	33.8	4.250	11.380	0.373	29.7			
27.6	13.5	0.327	2.069	0.158	65.3			
	27.4	1.472	4.760	0.309	57.6			
	42.2	2.616	8.282	0.316	51.0			
	54.9	4.250	11.400	0.373	48.1			
	67.4	6.536	15.590	0.419	43.2			
69.0	33.7	0.654	3.120	0.210	108.0			
6.9	6.5	0.640	2.636	0.243	24.6			
	9.7	1.280	4.151	0.308	23.4			
13.8	20.2	1.919	7.018	0.273	28.8			
27.6	26.3	1.280	4.563	0.281	57.5			
6.9	3.3	-----	0.670	-----	48.9	1.487	20.50	7.0
	6.6	0.322	1.914	0.168	34.3			
	9.8	0.644	3.255	0.198	30.2			
	13.1	0.967	4.406	0.219	29.8			
	16.4	1.263	5.560	0.231	29.5			

Confining pressure (kPa)	Deviator stress (kPa)	Radial strain x10^{-4}	Axial strain x10^{-4}	Resilient Poisson's ratio	Resilient modulus (MPa)	Dry density (Mg/m^3)	Moisture content (%)	Moisture tension (kPa)
13.8	6.6	0.322	1.342	0.240	48.9			
	13.1	0.644	3.067	0.210	42.7			
	20.5	1.289	5.374	0.240	38.1			
	26.6	1.933	7.689	0.251	34.6			
	32.7	2.577	10.600	0.243	30.9			
27.6	26.6	0.966	5.204	0.186	51.1			
	40.9	1.932	8.108	0.238	50.5			
	53.2	3.219	11.650	0.276	45.6			
69.0	32.7	0.644	3.302	0.195	99.1			
	65.4	1.610	6.812	0.236	96.1			
6.9	3.3	-----	0.598	-----	54.7	1.501	16.50	13.0
	6.5	0.161	1.396	0.115	46.9			
	9.8	0.483	2.793	0.173	35.1			
	13.1	0.644	3.591	0.179	36.4			
	16.3	0.805	4.589	0.175	35.6			
13.8	6.5	0.161	1.198	0.134	54.6			
	13.1	0.483	2.794	0.173	46.9			
	20.4	0.966	5.190	0.186	39.4			
	26.6	1.288	6.190	0.208	42.9			
	32.7	1.931	7.990	0.242	41.0			
27.6	13.1	0.322	1.798	0.179	72.8			
	26.6	0.966	4.396	0.220	60.5			
	40.9	1.610	6.994	0.230	58.5			
	53.2	2.414	10.000	0.241	53.2			
	65.4	3.539	13.020	0.272	50.2			
6.9	3.3	0.162	0.736	0.220	44.7	1.501	25.00	2.0
	6.6	0.645	2.024	0.319	32.5			
	9.9	1.129	3.866	0.292	25.5			
	13.1	1.775	5.711	0.311	23.0			
	16.4	2.582	7.375	0.350	22.3			
13.8	6.6	0.323	1.291	0.250	50.9			
	13.1	0.968	3.319	0.292	39.6			
	20.5	1.935	6.273	0.308	32.7			
	26.7	2.903	8.312	0.349	32.1			
27.6	13.1	0.324	1.848	0.175	71.1			
	26.7	1.290	4.606	0.268	55.5			
	41.1	2.580	8.324	0.310	49.3			
49.3								

Recovered

Confining pressure (kPa)	Deviator stress (kPa)	Radial strain x10^{-4}	Axial strain x10^{-4}	Resilient Poisson's ratio	Resilient modulus (MPa)	Dry density (Mg/m^3)	Moisture content (%)	Moisture tension (kPa)
6.9	3.5	0.153	1.195	0.128	29.3	1.420	17.45	12.0
27.6	13.7	0.551	3.462	0.162	40.3			
69.0	34.2	0.765	5.257	0.144	64.6			
103.4	51.6	1.069	6.533	0.156	75.8			
6.9	7.2	0.301	3.002	0.100	24.0			
27.6	27.3	1.082	8.398	0.208	33.7			
69.0	70.2	2.997	12.773	0.235	55.0			
103.4	106.8	3.976	14.932	0.266	71.5			
6.9	10.3	0.917	5.042	0.182	20.4			
69.0	103.0	5.736	18.396	0.312	56.0			
6.9	13.4	0.762	6.229	0.122	21.5			
	3.5	0.251	0.940	0.267	37.2			
27.6	14.2	0.314	2.613	0.120	54.3	1.430	16.79	12.8
69.0	35.0	0.628	3.555	0.177	98.5			
103.4	50.6	0.471	4.190	0.112	120.8			
6.9	7.0	0.942	2.093	0.450	33.4			
27.6	27.6	1.569	5.868	0.267	47.0			
69.0	70.3	2.539	9.656	0.211	72.8			
103.4	105.1	2.196	10.097	0.217	104.1			
6.9	11.3	1.316	3.281	0.401	34.4			
27.6	41.7	3.444	11.370	0.303	36.7			
69.0	100.7	3.444	14.340	0.240	70.2			
27.6	13.7	0.543	2.121	0.256	64.6	1.430	21.46	8.5
69.0	34.0	0.706	2.907	0.312	117.0			
103.4	52.2	1.657	4.204	0.251	124.2			
6.9	6.8	0.664	2.013	0.330	33.8			
27.6	27.9	1.660	6.272	0.265	44.5			
69.0	71.3	2.414	10.328	0.234	69.0			
103.4	107.2	3.520	12.168	0.273	88.1			
6.9	10.6	1.266	4.511	0.281	23.5			
69.0	104.7	3.374	15.632	0.216	67.0			
6.9	6.9	0.607	2.169	0.260	31.8	1.490	18.17	11.3
27.6	28.7	1.365	6.082	0.224	47.2			
69.0	70.9	2.124	10.470	0.203	67.7			
103.4	101.9	2.124	12.714	0.167	80.1			
69.0	104.5	3.788	16.837	0.225	62.1			

Frozen, RPB waveform

Confining pressure (kPa)	Deviator stress (kPa)	Axial strain x10^{-4}	Resilient modulus (GPa)	Dry density (Mg/m^3)	Moisture content (%)	Temperature (°C)
69.0	69.0	0.210	3.28	1.290	31.00	-1.2
	137.9	0.526	2.62			
	208.9	0.978	2.14			
	355.1	2.189	1.62			
	480.7	3.263	1.47			
	344.9	1.470	2.35	1.290	31.00	-1.5
	480.7	2.313	2.08			
	141.1	0.262	5.39			
	209.0	0.578	3.62			
	344.9	0.473	7.29	1.290	31.00	-2.8
	627.0	1.472	4.26			
	480.7	0.946	5.08			
	809.9	1.999	4.05			
	209.0	0.210	9.95			
	344.9	0.315	10.95	1.290	31.00	-5.0
	480.7	0.473	10.16			
	627.0	0.736	8.52			
	757.6	1.156	6.55			
	344.9	0.211	16.35	1.290	31.00	-9.2
	480.7	0.316	15.21			
	627.0	0.474	13.23			
	836.0	0.737	11.34			
	67.7	0.506	1.34	1.304	33.35	-0.5
	135.4	1.419	0.95			
	208.2	2.638	0.79			
	343.0	5.090	0.67			
	476.4	7.374	0.65			
	344.1	1.512	2.28	1.304	33.35	-1.5
	208.6	0.605	3.45			
	140.8	0.202	6.97			
	479.0	2.729	1.76			
	208.2	0.101	20.59	1.304	33.35	-3.1
	354.0	0.607	5.83			
	479.0	1.234	3.88	1.304	33.35	-2.7
	624.7	2.226	2.81			
	833.0	3.440	2.42			
	343.6	0.253	13.58	1.309	31.99	-4.6
	479.0	0.606	7.90			
	624.7	1.011	6.18			
	833.0	1.922	4.33			
	135.7	1.471	0.92	1.309	31.99	-0.5
	199.7	2.492	0.80			
	347.1	4.546	0.76			
	457.5	6.278	0.73			
	204.8	0.567	3.61	1.309	31.99	-1.5
	327.6	1.473	2.22			
	470.0	2.952	1.59			
	132.8	0.284	4.68			
	349.6	0.253	13.82	1.309	31.99	-3.5
	472.0	0.902	5.23			
	615.4	0.677	9.09			
	768.2	2.375	3.23			
	348.2	0.283	12.30	1.309	31.99	-5.1
	471.1	0.565	8.34			
	614.5	0.961	6.39			
	793.8	1.584	5.01			
13.8	28.7	0.086	3.34	1.306	29.70	-0.5
	34.7	0.172	2.02			
27.6	27.5	0.086	3.20			
	41.9	0.216	1.94			
	55.0	0.345	1.59			
	67.0	0.388	1.73			
69.0	69.4	0.216	3.21			
	102.8	0.474	2.17			
	138.7	0.776	1.79			
	172.2	1.121	1.54			
	205.7	1.467	1.40			
	239.2	1.812	1.32			
	275.0	2.158	1.27			
13.8	20.6	0.173	1.19	1.306	29.70	-0.2
	27.5	0.259	1.06			
	34.6	0.389	0.89			
27.6	27.5	0.259	1.06			

Confining pressure (kPa)	Deviator stress (kPa)	Axial strain x10^{-4}	Resilient modulus (GPa)	Dry density (Mg/m^3)	Moisture content (%)	Temperature (^{o}C)
	41.8	0.518	0.81			
	55.0	0.777	0.71			
	69.3	1.166	0.59			
69.0	34.6	0.345	1.00			
	69.3	0.950	0.73			
	102.7	1.383	0.74			
	138.6	1.902	0.73			
	172.0	2.423	0.71			
	205.5	2.685	0.77			

Frozen, FWD waveform

Confining pressure (kPa)	Deviator stress (kPa)	Axial strain x10^{-4}	Resilient modulus (GPa)	Dry density (Mg/m^3)	Moisture content (%)	Temperature (^{o}C)
69.0	137.9	[illegible]	[illegible]	1.290	31.00	[illegible]
	[illegible]	0.421	[illegible]			
	[illegible]	[illegible]	[illegible]			
	480.7	1.789	[illegible]			
	344.9	[illegible]	[illegible]	1.290	31.00	-1.5
	[illegible]	[illegible]	4.57			
	627.0	1.052	[illegible]	1.290	31.00	[illegible]
	836.0	1.378	5.30			
	627.0	0.531	[illegible]	1.290	31.00	-5.0
	836.0	[illegible]	[illegible]			
	627.0	0.526	11.92	1.290	31.00	[illegible]
	836.0	0.842	9.93			
	67.7	0.405	1.67	1.304	33.35	-0.5
	135.4	0.709	1.91			
	203.0	1.420	1.43			
	343.0	2.545	1.35			
	476.4	3.587	1.33			
	344.1	0.907	3.79	1.304	33.35	-1.5
	206.6	0.403	5.16			
	479.0	1.415	3.39			
	354.0	0.202	17.50	1.304	33.35	-3.1
	475.0	0.809	5.92	1.304	33.35	-2.7
	624.7	1.416	4.41			
	833.0	2.024	4.12			
	479.0	0.707	6.78	1.304	33.35	-4.6
	624.7	0.910	6.66			
	833.0	1.416	5.88			
	135.7	1.132	1.20	1.309	31.99	-0.5
	199.7	1.359	1.47			
	347.1	[illegible]	1.80			
	467.7	2.654	1.64			
	327.6	0.566	5.79	1.309	31.99	-1.5
	473.0	1.362	3.45			
	472.0	0.564	[illegible]	1.309	31.99	-3.5
	615.4	0.677	9.04			
	819.4	1.696	4.83			
	614.5	0.848	7.25	1.309	31.99	-5.1
	819.4	1.131	7.24			
27.6	41.9	0.216	1.94	1.306	29.70	-0.5
	55.0	0.259	2.12			
	67.0	0.345	1.94			
69.0	102.8	0.345	2.96			
	138.7	0.517	2.68			
	172.2	0.690	2.50			
	205.7	0.863	2.38			
	239.2	1.036	2.31			
	275.0	1.209	2.27			
13.8	20.6	0.173	1.19	1.306	29.70	[illegible]
	27.5	0.216	1.27			
	34.6	0.302	1.15			
27.6	27.5	0.173	1.59			
	41.8	0.389	1.07			
	55.0	0.516	1.07			
	69.3	1.166	0.59			
69.0	34.6	0.302	1.15			
	69.3	0.561	1.24			
	102.7	0.864	1.19			
	138.6	1.211	1.14			
	172.0	1.558	1.10			
	205.5	1.733	1.19			

Hart Brothers sand

Thawed, RPB waveform

Confining pressure (kPa)	Deviator stress (kPa)	Radial strain $x10^{-4}$	Axial strain $x10^{-4}$	Resilient Poisson's ratio	Resilient modulus (MPa)	Dry density (Mg/m^3)	Moisture content (%)	Moisture tension (kPa)
6.9	3.4	-----	1.120	-----	30.0	1.651	17.50	2.0
	6.7	-----	2.808	-----	23.9			
	10.1	0.979	4.697	0.208	21.4			
13.8	6.7	-----	1.692	-----	39.7			
	13.8	-----	4.520	-----	30.6			
	21.0	1.456	7.964	0.246	26.3			
27.6	13.4	-----	2.655	-----	50.5			
	27.3	1.304	5.893	0.221	46.3			
	41.9	3.259	10.540	0.309	39.8			
6.9	3.5	-----	0.954	-----	36.3	1.723	10.00	5.0
	6.9	0.994	2.299	0.432	30.2			
	10.4	1.656	3.840	0.431	27.0			
	13.8	2.646	5.780	0.458	23.9			
13.8	6.9	0.331	1.541	0.215	44.8			
	13.8	0.593	3.471	0.286	39.8			
	21.6	2.996	6.769	0.443	31.9			
	28.0	3.963	8.165	0.485	34.3			
27.6	14.2	0.660	2.139	0.309	66.4			
	28.0	1.981	4.671	0.424	59.9			
	43.0	3.301	7.613	0.434	56.5			
	55.7	4.942	9.815	0.504	56.7			
69.0	34.3	0.659	2.946	0.224	116.3			
	72.8	2.307	6.883	0.335	105.8			
	102.7	3.952	10.860	0.364	94.6			
6.9	10.8	0.994	3.542	0.281	30.6	1.788	8.20	8.0
	13.9	1.325	4.724	0.280	29.4			
	17.3	1.325	5.908	0.224	29.4			
13.8	6.9	-----	1.575	-----	44.0			
	21.7	1.657	4.728	0.350	45.9			
	29.3	1.988	6.899	0.288	42.4			
	34.7	3.313	9.268	0.357	37.4			
27.6	13.9	-----	1.774	-----	78.2			
	29.3	1.325	4.338	0.305	67.5			
	43.3	2.651	6.901	0.384	62.8			
	56.4	3.976	9.275	0.429	60.8			
	69.3	5.299	11.850	0.447	58.4			
69.0	35.7	-----	2.963	-----	120.5			
	71.4	-----	6.323	-----	113.0			
	108.2	1.325	10.290	0.129	105.2			
6.9	3.4	-----	0.766	-----	44.9	1.778	7.10	13.0
	6.9	-----	1.642	-----	41.9			
	10.3	0.660	2.628	0.251	39.2			
	13.6	0.990	3.725	0.266	36.9			
	17.2	1.650	4.822	0.342	35.6			
13.8	6.9	-----	1.206	-----	57.0			
	13.8	0.990	2.959	0.335	46.5			
	21.5	1.650	4.605	0.358	46.7			
	34.4	2.970	8.121	0.366	42.3			
6.9	3.4	0.327	1.097	0.298	30.8	1.793	20.00	1.0
	6.8	0.490	2.394	0.205	28.2			
	10.1	0.981	3.994	0.246	25.4			
	13.5	1.635	5.596	0.292	24.1			
	16.4	2.288	6.601	0.347	24.8			
13.8	6.7	0.327	1.900	0.172	35.5			
	13.5	1.144	3.800	0.301	35.5			
	21.1	1.634	5.402	0.302	39.0			
	27.4	2.288	7.010	0.326	39.1			
	33.7	3.593	9.023	0.398	37.3			
27.6	13.5	-----	2.205	-----	61.1			
	27.4	1.470	4.411	0.333	62.0			
	42.1	2.450	6.822	0.359	61.7			
	54.7	3.920	9.043	0.433	60.5			
	67.3	4.570	11.090	0.412	60.7			
69.0	33.6	0.979	2.823	0.347	119.2			
	67.3	1.959	5.647	0.347	119.2			
6.9	3.4	-----	0.503	-----	67.5	1.820	8.80	6.0
	6.8	0.328	1.610	0.204	42.2			
	10.2	0.656	2.716	0.242	37.5			
	13.6	0.984	3.622	0.272	37.5			
	17.0	1.312	4.829	0.272	35.1			
13.8	6.8	-----	0.805	-----	84.3			
	13.6	0.656	2.213	0.296	61.4			
	21.2	0.984	4.225	0.233	50.2			

Confining pressure (kPa)	Deviator stress (kPa)	Radial strain $\times 10^{-4}$	Axial strain $\times 10^{-4}$	Resilient Poisson's ratio	Resilient modulus (MPa)	Dry density (Mg/m^3)	Moisture content (%)	Moisture tension (kPa)
	27.6	1.640	5.636	0.291	48.9			
	33.9	2.295	6.847	0.335	49.6			
27.6	13.6	-----	1.309	-----	103.7			
	27.6	1.148	3.426	0.335	80.5			
	42.4	1.968	5.844	0.337	72.6			
	55.2	2.951	7.460	0.396	73.9			
	67.9	3.935	9.076	0.434	74.8			
69.0	33.9	0.620	2.219	0.370	153.0			
	70.0	1.476	4.843	0.305	144.6			
6.9	3.4	-----	0.389	-----	87.5	1.828	7.60	10.0
	6.8	-----	1.264	-----	53.8			
	10.2	0.328	2.042	0.161	50.0			
	13.6	-----	2.724	-----	50.0			
	17.0	0.985	3.113	0.316	54.6			
13.8	21.3	0.821	2.918	0.281	72.9			
	27.6	1.149	3.893	0.295	71.0			
	34.0	1.477	5.062	0.292	67.2			
27.6	27.7	0.821	2.434	0.337	113.9			
	42.5	1.313	3.896	0.337	109.1			
	55.3	2.298	6.238	0.368	88.6			
	68.0	2.953	7.806	0.378	87.1			
69.0	34.0	0.492	1.171	0.420	290.3			
	68.0	1.312	3.125	0.420	217.5			
6.9	3.5	-----	0.217	-----	159.3	1.865	7.00	14.0
	6.9	0.165	0.870	0.190	79.5			
	10.4	0.331	1.304	0.254	79.5			
	13.8	0.497	1.739	0.286	79.5			
	17.3	0.662	2.174	0.305	79.5			
13.8	6.9	-----	0.652	-----	106.0			
	13.8	0.497	1.522	0.327	90.9			
	21.6	0.993	2.392	0.415	90.3			
	28.1	1.323	3.262	0.406	86.1			
	34.6	1.820	4.350	0.418	79.5			
27.6	13.8	0.331	1.087	0.305	127.2			
	28.1	0.993	2.392	0.415	117.4			
	43.2	1.654	3.481	0.475	124.2			
	56.2	2.647	5.660	0.468	99.3			
	69.1	3.473	6.972	0.498	99.1			
69.0	34.5	0.661	0.872	0.758	396.1			
	69.1	1.323	2.833	0.467	243.8			
6.9	3.4	-----	0.507	-----	66.5	1.794	10.00	5.0
	6.7	0.327	1.319	0.248	51.2			
	10.1	0.654	2.436	0.268	41.5			
	13.5	1.144	3.249	0.352	41.5			
	16.9	1.308	4.470	0.293	37.7			
13.8	6.7	0.327	0.914	0.358	73.8			
	13.5	0.654	2.438	0.268	55.3			
	21.1	1.308	3.862	0.339	54.6			
	27.4	2.289	5.693	0.402	48.1			
	33.7	2.779	7.324	0.379	46.1			
27.6	27.4	1.308	3.666	0.357	74.8			
	42.2	1.962	5.704	0.344	73.9			
	54.8	2.943	8.155	0.361	67.2			
	67.5	4.250	10.610	0.401	63.6			
6.9	3.4	-----	0.394	-----	85.4	1.794	7.60	10.0
	10.1	0.490	2.069	0.237	48.8			
	13.5	0.816	2.758	0.296	48.8			
	16.8	0.979	3.547	0.276	47.4			
13.8	13.5	0.490	2.266	0.216	59.4			
	21.0	0.979	3.743	0.262	56.2			
	27.3	1.469	5.123	0.287	53.4			
	33.6	1.959	6.112	0.321	55.1			
27.6	13.5	0.327	1.380	0.237	97.5			
	27.3	0.979	3.155	0.310	86.7			
	42.1	1.463	5.126	0.285	82.1			
	54.7	2.285	7.101	0.322	77.0			
	67.3	3.265	8.879	0.368	75.8			
69.0	33.6	0.653	2.960	0.221	113.7			
	67.3	1.306	5.132	0.254	131.2			
6.9	3.4	-----	0.289	-----	117.7	1.815	6.80	16.0
	6.8	0.328	0.867	0.378	78.5			
	10.2	0.657	1.445	0.455	70.7			
	13.6	0.985	2.119	0.465	64.2			
	17.0	0.985	2.504	0.393	67.9			
13.8	6.8	-----	0.867	-----	78.5			

Confining pressure (kPa)	Deviator stress (kPa)	Radial strain x10^{-4}	Axial strain x10^{-4}	Resilient Poisson's ratio	Resilient modulus (MPa)	Dry density (Mg/m^3)	Moisture content (%)	Moisture tension (kPa)
	13.6	0.657	1.733	0.379	78.5			
	21.3	1.313	3.063	0.426	69.0			
	27.6	1.641	4.241	0.387	65.2			
	34.0	2.298	5.206	0.441	65.3			
27.6	13.6	0.657	1.350	0.487	100.1			
	27.6	-----	2.700	-----	102.4			
	42.5	1.313	4.242	0.310	100.2			
	55.3	2.298	6.175	0.372	89.6			
	68.0	3.282	8.111	0.405	83.9			
6.9	3.4	-----	0.723	-----	46.8	1.780	17.50	2.0
	6.8	0.491	1.860	0.264	36.4			
	10.1	0.982	3.102	0.317	32.7			
	13.5	1.473	4.758	0.310	28.5			
	16.9	1.965	5.591	0.351	30.3			
13.8	6.8	0.327	1.449	0.226	46.7			
	13.5	0.819	3.106	0.264	43.6			
	21.1	1.801	5.366	0.334	39.3			
	27.5	2.620	6.633	0.395	41.5			
	33.8	3.602	8.298	0.434	40.8			
27.6	13.5	0.491	1.867	0.263	72.5			
	27.5	0.962	4.568	0.215	62.5			
	42.3	2.456	7.066	0.348	59.9			
	55.0	3.928	8.742	0.449	62.9			
	67.6	5.888	11.890	0.495	56.8			
69.0	33.8	0.654	1.774	0.369	190.4			
	67.6	1.963	5.288	0.371	127.8			

Thawed, FWD waveform

Confining pressure (kPa)	Deviator stress (kPa)	Radial strain x10^{-4}	Axial strain x10^{-4}	Resilient Poisson's ratio	Resilient modulus (MPa)	Dry density (Mg/m^3)	Moisture content (%)	Moisture tension (kPa)
6.9	3.4	-----	1.197	-----	28.2	1.793	20.00	1.0
	6.8	0.490	2.793	0.175	24.2			
	10.1	0.981	4.395	0.223	23.1			
	13.5	1.471	5.596	0.263	24.1			
	16.4	1.961	7.000	0.280	23.4			
13.8	6.7	0.327	2.000	0.163	33.7			
	13.5	0.817	3.800	0.215	35.5			
	21.1	1.307	5.802	0.225	36.3			
	27.4	1.961	7.409	0.265	37.0			
	33.7	2.613	9.423	0.277	35.8			
27.6	13.9	-----	2.205	-----	63.0			
	27.4	1.143	4.611	0.248	59.4			
	42.1	1.960	7.424	0.264	56.7			
	54.7	2.940	10.050	0.293	54.5			
	67.3	3.591	12.500	0.287	53.8			
69.0	33.6	0.653	2.823	0.231	119.2			
27.6	67.3	-----	5.849	-----	115.0			
6.9	6.8	-----	1.811	-----	37.5	1.820	6.80	6.0
	10.2	0.492	2.817	0.175	36.1			
	13.6	0.656	3.823	0.172	35.5			
	17.0	0.984	4.829	0.204	35.1			
13.8	6.8	-----	1.006	-----	67.5			
	13.6	0.492	2.616	0.188	51.9			
	21.2	0.984	4.225	0.233	50.2			
	27.6	1.312	5.837	0.225	47.3			
	33.9	1.640	7.249	0.226	46.8			
27.6	27.6	0.984	3.628	0.271	76.0			
	42.4	1.968	6.046	0.326	70.2			
	55.2	2.295	8.468	0.271	65.1			
	67.9	3.279	10.008	0.328	67.8			
69.0	33.9	0.656	2.219	0.296	153.0			
	70.0	1.148	5.650	0.203	123.9			
6.9	3.4	-----	0.389	-----	87.5	1.828	7.60	10.0
	6.8	-----	1.361	-----	50.0			
	10.2	0.328	2.139	0.153	47.7			
	13.6	0.493	2.918	0.169	46.6			
	17.0	0.656	3.696	0.177	46.0			
13.8	13.6	-----	1.946	-----	69.9			
	21.3	0.657	3.307	0.199	64.3			
	27.6	0.985	4.671	0.211	59.2			
	34.0	1.149	5.841	0.197	58.2			
27.6	27.7	0.493	2.921	0.169	94.9			
	42.5	1.149	4.869	0.236	87.3			
	55.3	1.641	6.823	0.241	81.0			
	68.0	2.297	8.782	0.262	77.4			
69.0	34.0	-----	1.952	-----	174.1			
	68.0	0.820	4.297	0.191	158.2			
6.9	6.9	0.165	0.890	0.185	77.7	1.865	7.00	14.0
	10.4	0.331	1.304	0.254	79.5			
	13.8	0.497	1.739	0.286	79.5			
	17.3	0.827	2.174	0.380	79.5			

Confining pressure (kPa)	Deviator stress (kPa)	Radial strain $\times 10^{-4}$	Axial strain $\times 10^{-4}$	Resilient Poisson's ratio	Resilient modulus (MPa)	Dry density (Mg/m^3)	Moisture content (%)	Moisture tension (kPa)
13.8	6.9	-----	0.652	-----	106.0			
	13.8	0.331	1.739	0.190	79.5			
	21.6	0.827	2.610	0.317	82.8			
	28.1	1.323	3.697	0.358	76.0			
	34.6	1.820	5.002	0.364	69.1			
27.6	13.8	0.331	1.305	0.254	106.0			
	28.1	0.993	2.827	0.351	99.4			
	56.2	2.647	7.836	0.338	71.7			
6.9	3.3	-----	1.307	-----	25.6	1.651	17.50	2.0
	6.7	-----	3.370	-----	19.9			
	10.1	-----	5.637	-----	17.9			
13.8	6.7	-----	2.068	-----	32.5			
	13.8	-----	9.416	-----	14.7			
	21.0	1.956	8.532	0.229	24.6			
27.6	13.4	-----	2.655	-----	50.5			
	27.3	1.304	6.654	0.196	41.0			
	41.9	2.933	10.540	0.278	39.8			
6.9	3.5	-----	0.954	-----	36.3	1.723	10.00	5.0
	7.4	0.663	2.299	0.288	32.0			
	10.4	1.656	3.840	0.431	27.0			
	13.8	1.985	6.744	0.294	20.5			
13.8	6.9	-----	1.541	-----	44.8			
	13.8	0.993	3.471	0.286	39.8			
	21.6	2.315	6.769	0.342	31.9			
	28.0	3.302	9.137	0.361	30.6			
27.6	13.8	-----	2.334	-----	59.0			
	28.0	1.651	5.450	0.303	51.3			
	43.0	2.640	8.782	0.301	49.0			
	55.7	3.955	11.780	0.336	47.3			
69.0	34.3	0.659	2.946	0.224	116.3			
	72.8	1.648	7.275	0.227	100.1			
	102.7	2.964	11.260	0.263	91.2			
6.9	6.9	-----	2.165	-----	32.0	1.788	8.20	8.0
	13.9	0.994	4.724	0.210	29.4			
	17.3	1.325	5.900	0.225	29.4			
13.8	13.9	-----	3.152	-----	44.0			
	21.7	1.325	5.516	0.240	39.3			
	29.3	1.988	7.292	0.273	40.1			
	34.7	2.651	9.858	0.269	35.2			
27.6	13.9	-----	1.972	-----	70.3			
	29.3	1.325	4.929	0.269	59.4			
	43.3	1.988	6.901	0.288	62.8			
	56.4	3.313	9.866	0.336	57.1			
	69.3	-----	13.240	-----	52.3			
69.0	108.2	-----	10.890	-----	99.4			
6.9	3.4	-----	0.875	-----	39.2	1.778	7.10	13.0
	6.9	-----	1.642	-----	41.9			
	10.3	0.660	2.628	0.251	39.2			
	13.8	0.990	3.725	0.266	36.9			
	17.2	0.991	5.261	0.188	32.7			
13.8	6.4	-----	1.096	-----	58.8			
	13.8	0.660	2.850	0.232	48.2			
	21.5	1.320	4.825	0.274	44.5			
27.6	68.8	2.640	12.080	0.219	56.9			
69.0	103.1	-----	9.886	-----	104.3			
6.9	6.7	0.327	1.319	0.248	51.2	1.794	10.00	5.0
	10.1	0.490	2.639	0.186	38.3			
	13.5	0.981	3.656	0.268	36.9			
	16.9	1.144	5.079	0.225	33.2			
13.8	6.7	-----	1.016	-----	66.4			
	13.5	0.491	2.641	0.186	51.1			
	21.1	0.981	4.675	0.210	45.1			
	27.4	1.471	6.100	0.241	44.9			
	33.7	2.289	7.526	0.304	44.8			
27.6	13.5	-----	1.425	-----	94.7			
	27.4	0.981	3.666	0.268	74.8			
	42.2	1.635	6.520	0.251	64.7			
	54.8	2.289	8.561	0.267	64.0			
	67.5	3.270	10.610	0.308	63.6			
6.9	6.7	-----	1.182	-----	56.9	1.794	7.60	10.0
	10.1	0.327	2.167	0.151	46.6			
	13.5	0.653	2.955	0.221	45.5			
	16.8	0.653	3.743	0.174	45.0			
13.8	13.5	0.772	2.364	0.327	56.9			
	21.0	0.653	3.743	0.174	56.2			
	27.3	0.979	5.715	0.171	47.8			
	33.6	1.306	6.309	0.207	53.3			
27.6	13.5	-----	1.380	-----	97.5			
	42.1	0.979	5.718	0.171	73.6			
	54.7	1.632	7.890	0.207	69.3			
	67.3	2.285	9.866	0.232	68.2			

Confining pressure (kPa)	Deviator stress (kPa)	Radial strain $\times 10^{-4}$	Axial strain $\times 10^{-4}$	Resilient Poisson's ratio	Resilient modulus (MPa)	Dry density (Mg/m^3)	Moisture content (%)	Moisture tension (kPa)
69.0	33.6	-----	3.157	-----	106.6			
	67.3	0.816	5.922	0.138	113.7			
6.9	6.8	-----	0.867	-----	78.5	1.815	6.80	16.0
	10.2	0.657	1.733	0.379	58.9			
	13.6	0.657	2.311	0.284	58.9			
	17.0	0.985	2.696	0.365	63.1			
13.8	6.8	-----	0.867	-----	78.5			
	13.6	0.657	1.733	0.379	78.5			
	21.3	1.313	3.468	0.379	61.3			
	27.6	1.641	4.626	0.355	59.7			
	34.0	2.298	5.978	0.384	56.9			
27.6	27.6	-----	2.892	-----	95.6			
	42.5	1.313	5.206	0.252	81.7			
	55.3	1.969	7.140	0.276	77.5			
	68.0	2.954	9.656	0.306	70.5			
6.9	3.4	-----	0.826	-----	41.0	1.780	17.50	2.0
	6.8	0.327	2.067	0.158	32.7			
	10.1	0.655	3.309	0.198	30.7			
	14.0	1.146	4.758	0.241	29.3			
	16.9	1.637	6.211	0.264	27.2			
13.8	6.8	-----	1.656	-----	40.9			
	13.5	0.491	3.313	0.148	40.9			
	21.1	1.473	5.592	0.263	37.6			
	27.5	1.965	7.255	0.271	37.9			
	33.8	2.620	9.336	0.281	36.2			
27.6	13.5	-----	2.075	-----	65.3			
	27.5	-----	5.191	-----	53.0			
	42.3	1.801	7.481	0.241	56.5			
	55.0	2.618	9.784	0.268	56.2			
	67.6	4.253	12.520	0.340	54.0			
69.0	33.9	-----	2.296	-----	147.1			
	67.6	1.636	5.848	0.280	115.5			

Remolded, RPB waveform

Confining pressure (kPa)	Deviator stress (kPa)	Radial strain $\times 10^{-4}$	Axial strain $\times 10^{-4}$	Resilient Poisson's ratio	Resilient modulus (MPa)	Dry density (Mg/m^3)	Moisture content (%)	Moisture tension (kPa)
6.9	7.0	0.500	1.237	0.404	56.6	1.768	17.50	2.0
	10.9	0.995	2.474	0.404	44.3			
	14.0	1.332	3.162	0.419	44.0			
13.8	7.0	0.333	0.884	0.377	79.3			
	14.0	0.833	2.122	0.393	66.0			
	20.8	1.332	3.175	0.420	65.5			
	27.4	1.596	4.956	0.403	55.2			
27.6	14.0	0.333	1.416	0.235	98.9			
	27.4	1.163	3.363	0.346	81.4			
	41.6	1.998	5.491	0.364	75.8			
	54.7	2.998	7.444	0.403	73.5			
6.9	3.5	0.166	0.664	0.250	52.5	1.744	15.00	3.0
	7.0	0.499	1.329	0.375	52.4			
	10.4	0.997	2.327	0.428	44.9			
	13.9	1.495	3.327	0.449	41.9			
13.8	7.0	0.332	1.081	0.307	64.5			
	13.9	0.830	2.496	0.333	55.8			
	20.7	1.495	3.997	0.374	51.8			
	27.2	2.491	5.670	0.439	48.0			
27.6	13.9	0.499	1.502	0.332	92.8			
	27.2	1.163	3.171	0.367	85.8			
	41.4	2.325	6.014	0.387	68.8			
	54.4	3.322	7.871	0.422	69.2			
6.9	7.0	0.333	1.062	0.314	65.8	1.762	8.50	7.0
	10.5	0.665	1.635	0.407	64.1			
	14.0	0.998	2.372	0.421	58.9			
	17.5	1.497	2.945	0.508	59.3			
13.8	14.0	0.665	1.882	0.353	74.2			
	20.7	1.331	2.946	0.452	70.4			
	27.3	1.996	4.746	0.421	57.5			
	33.8	2.661	5.894	0.451	57.4			

Confining pressure (kPa)	Deviator stress (kPa)	Radial strain $\times 10^{-4}$	Axial strain $\times 10^{-4}$	Resilient Poisson's ratio	Resilient modulus (MPa)	Dry density (Mg/m^3)	Moisture content (%)	Moisture tension (kPa)
27.6	27.3	1.164	3.112	0.374	87.7			
	41.5	1.830	4.915	0.372	84.4			
	54.6	2.994	6.885	0.435	79.3			
6.9	3.5	-----	0.434	-----	80.4	1.764	7.30	12.0
	7.0	0.166	1.042	0.159	66.9			
13.8	7.0	0.166	0.695	0.239	100.4			
	13.9	0.499	1.739	0.287	80.2			
	20.9	0.997	2.687	0.371	77.7			
	27.5	1.496	3.795	0.394	72.4			
	35.2	1.828	4.745	0.385	74.1			
27.6	14.1	0.332	1.107	0.300	127.1			
	27.5	0.831	2.532	0.328	108.5			
	41.8	1.495	4.114	0.363	101.5			
	55.0	2.326	5.541	0.420	99.2			
6.9	3.4	-----	0.944	-----	35.8	1.744	28.00	1.0
	7.0	0.338	1.888	0.179	37.0			
	10.4	0.507	2.738	0.185	37.9			
	14.0	0.676	3.778	0.179	37.0			
13.8	7.0	0.169	1.325	0.128	52.7			
	14.0	0.338	2.745	0.123	50.9			
	20.3	0.845	4.167	0.203	48.7			
	27.0	1.352	5.499	0.246	49.2			
27.6	14.0	0.169	1.991	0.085	70.2			
	27.0	0.676	3.794	0.178	71.3			
	41.7	1.183	6.074	0.195	68.7			
6.9	3.6	0.170	0.878	0.194	41.4	1.737	17.50	2.0
	7.3	0.509	1.756	0.290	41.4			
	10.5	0.848	2.460	0.345	44.3			
	14.5	1.017	3.342	0.304	43.4			
13.8	7.3	0.339	1.231	0.275	59.0			
	14.5	0.678	2.551	0.266	56.9			
	20.4	1.356	3.873	0.350	52.7			
	27.2	2.034	5.464	0.372	49.8			
27.6	14.0	0.339	1.763	0.192	79.7			
	27.2	1.017	4.233	0.240	64.3			
	41.9	2.034	6.182	0.329	67.8			
6.9	3.6	-----	0.604	-----	60.4	1.753	8.20	8.0
	7.3	0.340	1.209	0.281	60.3			
	10.5	0.510	1.813	0.281	57.8			
	14.1	0.680	2.620	0.260	53.9			
	17.3	1.019	3.226	0.316	53.7			
13.8	6.8	0.340	0.907	0.375	75.4			
	13.7	0.340	2.016	0.169	67.9			
	20.5	0.850	3.427	0.248	59.8			
	27.3	1.359	4.639	0.243	59.0			
	34.2	1.869	5.652	0.331	60.5			
27.6	13.7	0.340	1.312	0.259	104.3			
	27.3	0.850	2.826	0.301	96.8			
	41.0	1.529	4.847	0.315	84.7			
	54.7	2.209	6.874	0.321	79.6			
6.9	3.4	-----	0.536	-----	63.3	1.761	7.30	12.0
	10.9	0.339	1.966	0.172	55.3			
	14.0	0.508	2.324	0.219	60.4			
	17.2	0.678	3.218	0.211	53.4			
13.8	7.0	0.170	0.983	0.173	71.4			
	14.0	0.339	2.145	0.158	65.4			
	20.4	0.678	3.219	0.211	63.3			
	27.2	1.016	4.113	0.247	66.0			
	35.1	1.355	5.367	0.252	65.4			
27.6	14.0	0.170	1.699	0.100	82.6			
	27.2	0.678	3.309	0.205	82.1			
	41.9	1.016	5.190	0.196	80.7			
	54.3	1.525	6.803	0.224	79.9			
6.9	3.4	-----	0.556	-----	61.0	1.757	8.20	8.0
	7.0	0.169	1.111	0.152	63.1			
	10.4	0.339	2.130	0.159	48.9			
	14.0	0.677	2.778	0.244	50.5			
	17.2	0.846	3.520	0.240	48.9			
13.8	7.0	0.170	1.112	0.153	63.1			
	14.0	0.339	2.408	0.141	58.3			
	20.4	0.677	3.520	0.192	57.9			
	27.1	1.016	4.818	0.211	56.4			
	33.9	2.031	5.933	0.342	57.2			
27.6	41.9	1.354	5.380	0.252	77.8			
	54.3	1.524	6.734	0.226	80.7			
6.9	3.5	0.167	0.660	0.253	53.4	1.743	17.50	2.0
	7.0	0.502	1.321	0.380	53.4			
	10.6	0.835	2.559	0.326	41.3			
	14.1	1.170	3.470	0.337	40.6			
	17.6	1.838	4.300	0.427	41.0			

Confining pressure (kPa)	Deviator stress (kPa)	Radial strain x10^{-4}	Axial strain x10^{-4}	Resilient Poisson's ratio	Resilient modulus (MPa)	Dry density (Mg/m^3)	Moisture content (%)	Moisture tension (kPa)
13.8	7.0	0.334	1.158	0.288	60.9			
	14.1	0.668	2.482	0.269	56.8			
	20.9	1.337	4.138	0.323	50.6			
	27.5	1.838	5.302	0.347	51.9			
27.6	13.7	0.334	1.740	0.192	78.5			
	27.5	1.003	3.646	0.275	75.5			
	41.8	1.838	5.974	0.308	70.1			
6.9	3.5	0.167	0.472	0.354	74.5	1.754	8.20	8.0
	7.0	0.334	1.100	0.304	64.0			
	10.5	0.668	1.965	0.340	53.7			
	14.1	1.002	2.358	0.425	59.7			
	17.6	1.168	3.146	0.371	55.9			
13.8	7.0	0.334	0.786	0.425	89.5			
	14.1	0.668	2.045	0.327	68.8			
	22.0	1.168	3.304	0.354	66.6			
	27.5	1.503	4.092	0.367	67.2			
	34.1	2.003	5.039	0.397	67.6			
27.6	14.1	0.334	1.102	0.303	127.7			
	27.5	0.835	2.836	0.294	96.9			
	41.8	1.502	4.727	0.318	88.4			
	55.0	2.337	6.314	0.370	87.1			
6.9	3.5	0.168	0.564	0.298	62.7	1.774	17.50	2.0
	7.1	0.502	1.289	0.389	54.9			
	10.6	0.669	2.095	0.319	50.6			
	14.1	1.339	3.386	0.395	41.8			
13.8	7.1	0.335	0.887	0.378	79.8			
	14.1	0.669	2.419	0.277	58.5			
	21.0	1.339	3.871	0.346	54.2			
	27.6	1.841	5.163	0.357	53.5			
27.6	14.1	0.335	1.614	0.208	87.7			
	27.6	1.004	3.551	0.283	77.8			
	42.0	1.841	5.652	0.326	74.3			
	55.3	2.677	8.083	0.331	68.4			
6.9	3.5	-----	0.259	-----	136.3	1.767	7.40	11.0
	7.1	0.167	0.865	0.193	81.7			

Remolded, FWD waveform

Confining pressure (kPa)	Deviator stress (kPa)	Radial strain x10^{-4}	Axial strain x10^{-4}	Resilient Poisson's ratio	Resilient modulus (MPa)	Dry density (Mg/m^3)	Moisture content (%)	Moisture tension (kPa)
6.9	7.0	0.500	1.237	0.404	56.6	1.768	17.50	2.0
	10.9	0.999	2.474	0.404	44.3			
	14.0	1.332	3.536	0.377	39.6			
13.8	7.0	0.333	1.061	0.314	66.0			
	14.0	0.666	2.299	0.290	60.9			
	20.8	1.332	3.892	0.342	53.4			
	27.4	1.998	5.487	0.364	49.9			
27.6	14.0	0.333	1.593	0.209	87.9			
	27.4	1.163	3.717	0.313	73.6			
	41.6	1.998	6.199	0.322	67.1			
	54.7	2.998	7.976	0.376	68.6			
6.9	3.5	0.166	0.664	0.250	52.5	1.744	15.00	3.0
	7.0	0.499	1.495	0.334	46.6			
	10.4	0.830	2.327	0.357	44.9			
	13.9	1.329	3.493	0.380	39.9			
13.8	7.0	0.332	1.164	0.285	59.9			
	13.9	0.830	2.662	0.312	52.4			
	20.7	1.329	3.997	0.332	51.8			
27.6	27.2	2.325	6.006	0.387	45.3			
	13.9	0.499	1.668	0.299	83.6			
	27.2	1.163	3.171	0.367	85.8			
	41.4	2.325	6.348	0.366	65.2			
	54.4	3.322	8.375	0.397	65.0			
6.9	3.5	0.167	0.490	0.341	71.3	1.762	8.50	7.0
	7.0	0.333	1.144	0.291	61.1			
	10.5	0.665	1.799	0.370	58.3			
	14.0	0.998	2.453	0.407	57.0			
	17.5	1.497	3.109	0.482	56.2			
13.8	7.0	0.333	0.818	0.407	85.4			
	14.0	0.832	1.963	0.424	71.2			
	20.7	1.331	3.437	0.387	60.3			
	27.3	1.996	4.746	0.421	57.5			
	33.8	2.661	6.058	0.439	55.9			
27.6	14.0	0.499	1.473	0.339	94.8			
	27.3	0.998	3.603	0.277	75.7			
	41.5	1.830	5.242	0.349	79.1			
	54.6	2.828	7.377	0.383	74.0			
6.9	3.5	-----	0.434	-----	80.4	1.764	7.30	12.0
	7.0	0.166	1.042	0.159	66.9			

Confining pressure (kPa)	Deviator stress (kPa)	Radial strain x10^{-4}	Axial strain x10^{-4}	Resilient Poisson's ratio	Resilient modulus (MPa)	Dry density (Mg/m^3)	Moisture content (%)	Moisture tension (kPa)
13.8	13.9	0.499	1.739	0.287	80.2			
	20.9	0.997	2.845	0.350	73.4			
	27.5	1.329	3.953	0.336	69.5			
	35.2	1.828	4.904	0.373	71.7			
27.6	14.1	0.332	1.265	0.262	111.2			
	27.5	0.831	2.690	0.309	102.2			
	41.8	1.495	4.430	0.337	94.3			
	55.0	2.326	5.858	0.397	93.8			
6.9	3.4	-----	0.940	-----	36.0	1.744	28.00	1.0
	7.0	0.338	1.888	0.179	37.0			
	10.4	0.507	2.832	0.179	36.6			
	14.0	0.676	3.778	0.179	37.0			
13.8	7.0	0.169	1.325	0.128	52.7			
	14.0	0.338	2.745	0.123	50.9			
	20.3	0.845	4.167	0.203	48.7			
	27.0	1.352	5.499	0.246	49.2			
27.6	14.0	0.169	1.991	0.085	70.2			
	27.0	0.676	3.794	0.178	71.3			
	41.7	1.183	6.454	0.183	64.6			
6.9	3.6	0.170	0.878	0.194	41.4	1.737	17.50	2.0
	7.3	0.509	1.756	0.290	41.4			
	10.9	0.648	2.636	0.322	41.4			
	14.5	1.187	3.517	0.338	41.3			
13.8	7.3	0.339	1.231	0.275	59.0			
	14.5	0.678	2.639	0.257	55.0			
	20.4	1.356	3.873	0.350	52.7			
	27.2	2.034	5.818	0.350	46.8			
27.6	14.0	0.339	1.763	0.192	79.7			
	27.2	1.017	4.409	0.231	61.7			
	42.0	2.034	6.360	0.320	66.0			
6.9	3.6	-----	0.604	-----	60.4	1.753	8.20	8.0
	7.3	0.340	1.209	0.281	60.3			
	10.5	0.510	1.813	0.281	57.8			
	14.1	0.680	2.620	0.260	53.9			
13.8	6.8	0.340	0.907	0.375	75.4			
	13.7	0.510	2.218	0.230	61.7			
	20.5	0.850	3.427	0.248	59.8			
	27.3	1.359	4.639	0.293	59.0			
	34.2	1.869	5.854	0.319	58.4			
27.6	13.7	0.340	1.413	0.241	96.8			
	27.3	0.850	3.230	0.263	84.7			
	41.0	3.002	5.452	0.551	75.3			
	54.7	2.209	7.683	0.288	71.2			
6.9	3.4	-----	0.536	-----	63.3	1.761	7.30	12.0
	10.9	0.339	1.966	0.172	55.3			
	14.0	0.508	2.503	0.203	56.1			
	17.2	0.678	3.218	0.211	53.4			
13.8	7.0	0.170	0.983	0.173	71.4			
	14.0	0.339	2.145	0.158	65.4			
	20.4	0.678	3.219	0.211	63.3			
	27.2	1.016	4.292	0.237	63.3			
	35.1	1.355	5.367	0.252	65.4			
27.6	14.0	0.170	1.699	0.100	82.6			
	27.2	0.678	3.399	0.199	79.9			
	41.9	1.016	5.190	0.196	80.7			
	54.3	1.525	7.161	0.213	75.9			
6.9	3.4	-----	0.556	-----	61.0	1.757	8.20	8.0
	7.0	0.169	1.111	0.152	63.1			
	10.4	0.339	2.130	0.159	48.9			
	14.0	0.677	2.778	0.244	50.5			
	17.2	0.646	3.520	0.240	48.9			
13.8	7.0	0.170	1.112	0.153	63.1			
	14.0	0.339	2.408	0.141	58.3			
	20.4	0.667	3.520	0.189	57.9			
	27.1	1.016	4.818	0.211	56.4			
	33.9	2.031	5.933	0.342	57.2			
27.6	41.9	1.185	5.566	0.213	75.2			
	54.3	1.693	2.482	0.682	218.8			
6.9	3.5	0.167	0.660	0.253	53.4	1.743	17.50	2.0
	7.0	0.502	1.321	0.380	53.4			
	10.6	0.835	2.642	0.316	40.0			
	14.1	1.170	3.470	0.337	40.6			
	17.6	1.671	4.467	0.374	39.4			
13.8	7.0	0.334	1.158	0.288	60.9			
	14.1	0.668	2.482	0.269	56.8			
	20.9	1.337	4.138	0.323	50.6			
	27.5	1.838	5.799	0.317	47.5			

Confining pressure (kPa)	Deviator stress (kPa)	Radial strain x10^{-4}	Axial strain x10^{-4}	Resilient Poisson's ratio	Resilient modulus (MPa)	Dry density (Mg/m^3)	Moisture content (%)	Moisture tension (kPa)
27.6	13.7	0.344	1.740	0.198	78.5			
	27.5	1.003	3.812	0.263	72.2			
	41.8	1.838	6.472	0.284	64.7			
6.9	3.5	0.169	0.472	0.358	74.4	1.754	8.20	8.0
	7.0	0.334	1.100	0.304	64.0			
	10.5	0.668	2.043	0.327	51.6			
	14.1	0.835	2.358	0.354	59.7			
	17.6	1.168	3.303	0.354	53.3			
13.8	7.0	0.334	0.786	0.425	89.5			
	14.1	0.668	2.045	0.327	68.8			
	22.0	1.002	3.461	0.290	63.5			
	27.5	1.335	4.407	0.303	62.4			
	34.1	1.335	4.885	0.273	69.8			
27.6	14.1	0.334	1.417	0.236	99.3			
	27.5	0.835	2.993	0.279	91.8			
	41.8	1.335	4.885	0.273	85.5			
	55.0	2.003	6.629	0.302	83.0			
6.9	3.5	0.168	0.564	0.298	62.7	1.774	17.50	2.0
	7.1	0.502	1.289	0.389	54.9			
	10.6	0.837	2.257	0.371	47.0			
	14.1	1.339	3.547	0.378	39.9			
13.8	7.1	0.335	0.967	0.346	73.2			
	14.1	0.669	2.580	0.259	54.8			
	21.0	1.171	3.871	0.303	54.2			
	27.6	1.841	5.163	0.357	53.5			
27.6	14.1	0.335	1.614	0.208	87.7			
	27.6	1.004	3.551	0.283	77.8			
	42.0	1.841	6.137	0.300	68.4			
	55.3	2.677	8.083	0.331	68.4			
6.9	3.5	-----	0.346	-----	102.1	1.767	7.40	11.0

Frozen, RPB waveform

Confining pressure (kPa)	Deviator stress (kPa)	Axial strain x10^{-4}	Resilient modulus (GPa)	Dry density (Mg/m^3)	Moisture content (%)	Temperature (°C)
69.0	69.2	1.851	0.37	1.554	19.10	-0.4
	138.5	4.561	0.30			
	204.9	6.516	0.31			
	86.6	0.093	9.31	1.554	19.10	-1.6
	138.3	0.372	3.72			
	204.8	0.745	2.75			
	346.2	1.864	1.87			
	471.0	2.986	1.58			
	613.1	4.210	1.46			
	348.9	0.599	5.82	1.554	18.48	-2.8
	472.0	1.291	3.66			
	615.6	2.125	2.90			
	365.3	0.369	9.89	1.554	18.60	-5.5
	496.6	0.639	7.78			
	615.6	1.016	6.06			
	820.8	1.830	4.49	1.554	18.60	-4.3
	347.4	0.281	12.36	1.554	18.68	-10.0
	490.5	0.421	11.65			
	613.1	0.655	9.36	1.554	18.66	-9.8
	740.8	0.795	9.32			
	69.6	3.426	0.20	1.586	15.66	-0.5
	139.1	7.074	0.20			
	208.1	12.210	0.17			
	139.4	0.449	3.10	1.586	15.98	-1.7
	204.2	1.099	1.86			
	348.4	2.704	1.29			
	487.1	4.222	1.15			
	139.2	0.251	5.53	1.586	16.10	-3.0
	203.8	0.604	3.38			
	344.0	1.650	2.08			
	481.1	2.817	1.71	1.586	16.07	-2.6
	621.3	4.026	1.54			
	139.2	0.151	9.22	1.586	16.19	-5.4
	208.8	0.302	6.91			
	347.9	0.704	4.94			
	487.1	1.206	4.04			
	621.3	1.911	3.25			
	720.7	2.314	3.11			
	65.7	1.742	0.38	1.612	17.90	-0.5
	136.5	3.818	0.36			
	202.2	8.210	0.25			
	136.6	0.378	3.61	1.612	17.19	-1.8
	202.4	0.540	3.75			
	344.1	2.162	1.59			
	485.8	3.359	1.45			
	606.6	5.226	1.16			

Confining pressure (kPa)	Deviator stress (kPa)	Axial strain x10^{-4}	Resilient modulus (GPa)	Dry density (Mg/m^3)	Moisture content (%)	Temperature (°C)
	345.2	1.288	2.68	1.612	17.30	-3.0
	203.0	0.537	3.78			
	487.3	1.934	2.52			
	608.4	2.260	2.69			
	809.7	3.024	2.68			
	202.4	0.324	6.25	1.612	17.38	-4.9
	344.1	0.486	7.08			
	465.6	1.080	4.31			
	607.3	1.674	3.63			
	809.7	2.593	3.12			

Frozen, FWD waveform

Confining pressure (kPa)	Deviator stress (kPa)	Axial strain x10^{-4}	Resilient modulus (GPa)	Dry density (Mg/m^3)	Moisture content (%)	Temperature (°C)
69.0	138.5	1.856	0.75	1.554	19.10	-0.4
	199.7	2.606	0.77			
	264.6	0.466	4.35	1.554	19.10	-1.0
	345.2	0.745	4.67			
	471.0	1.120	4.21			
	613.1	1.684	3.64			
	345.9	0.553	6.31	1.554	19.10	-2.8
	472.0	0.830	5.69			
	615.6	0.924	6.66			
	365.3	0.369	9.89	1.554	19.10	-5.5
	496.6	0.554	5.96			
	641.3	0.739	8.68			
	846.5	1.201	7.05			
	498.5	0.187	26.66	1.554	19.10	-10.0
	613.1	0.374	16.39	1.554	19.10	-9.8
	715.2	0.374	19.12			
	69.6	2.217	0.31	1.586	16.70	-0.5
	139.1	5.558	0.25			
	206.1	8.140	0.26			
	204.2	0.600	3.40	1.586	16.70	-1.7
	348.4	1.402	2.49			
	487.1	2.910	2.42			
	139.2	0.201	6.92	1.586	16.70	-3.0
	208.8	0.402	5.19			
	344.0	0.805	4.27			
	481.1	1.207	3.99	1.586	16.70	-2.6
	621.3	2.013	3.09			
	347.5	0.503	6.92	1.586	16.70	-5.4
	487.1	0.905	5.38			
	621.3	1.207	5.15			
	770.4	1.610	4.79			
	136.5	1.745	0.76	1.612	17.90	-0.5
	202.2	3.940	0.51			
	202.4	0.540	3.75	1.612	17.90	-1.8
	344.1	1.169	2.85			
	465.8	1.734	2.80			
	606.6	2.504	2.42			
	345.2	0.644	5.36	1.612	17.90	-3.0
	203.0	0.322	6.30			
	487.3	1.074	4.54			
	608.4	1.184	5.14			
	809.7	1.836	4.41			
	344.1	0.540	6.37	1.612	17.90	-4.9
	465.6	0.756	6.16			
	607.3	1.080	5.62			
	809.7	1.513	5.35			

Ikalanian silt

Thawed

Confining pressure (kPa)	Deviator stress (kPa)	Radial strain x10^{-4}	Axial strain x10^{-4}	Resilient Poisson's ratio	Resilient modulus (MPa)	Dry density (Mg/m^3)	Moisture content (%)	Moisture tension (kPa)
6.9	3.7	0.803	2.975	0.270	12.4	1.504	25.80	0.0
27.6	13.8	3.051	8.246	0.370	16.7			
69.0	34.5	1.606	7.798	0.206	44.2			
103.4	53.1	0.963	7.809	0.123	68.0			
6.9	6.6	1.927	5.742	0.336	11.5			
27.6	26.2	5.109	20.637	0.248	12.7			
69.0	68.3	9.898	26.634	0.372	25.6			
103.4	102.7	3.191	18.382	0.174	55.9			
6.9	10.4	2.549	12.500	0.204	8.3			
	3.4	0.313	1.830	0.171	18.6	1.609	25.00	4.0
27.6	13.6	0.313	3.269	0.096	42.2			
69.0	34.5	0.474	4.712	0.101	73.2			
103.4	69.0	1.106	7.608	0.145	90.7			
6.9	6.9	0.474	3.620	0.131	19.1			
27.6	26.3	0.948	7.870	0.120	36.0			
69.0	66.9	1.264	9.191	0.138	72.8			
103.4	106.2	1.580	11.146	0.142	95.3			
6.9	11.0	1.263	6.211	0.203	17.7			
27.6	41.4	1.694	11.328	0.167	36.5			
	14.2	-----	1.663	-----	85.4	1.609	14.00	11.5
69.0	35.4	-----	2.973	-----	119.1			
103.4	51.2	-----	4.044	-----	126.6			
6.9	7.1	-----	1.427	-----	49.8			
27.6	27.6	0.158	5.471	0.029	50.4			
69.0	70.9	0.473	9.235	0.051	76.8			
103.4	102.4	0.631	9.835	0.064	104.1			
6.9	11.0	0.316	3.219	0.098	34.2			
	3.7	1.119	3.906	0.286	9.5	1.532	25.80	0.0
27.6	13.8	1.918	8.386	0.229	16.5			
6.9	6.9	3.987	8.051	0.495	8.6			
27.6	27.6	5.733	14.210	0.403	19.4			
69.0	69.6	3.695	13.415	0.275	51.9			
103.4	104.1	4.587	13.998	0.328	74.4			
6.9	10.3	5.731	11.760	0.487	8.8			
27.6	40.0	9.528	18.571	0.513	21.5			
6.9	3.4	0.126	1.417	0.089	24.0	1.640	21.50	7.0
27.6	13.1	0.632	1.803	0.351	72.7			
69.0	33.8	0.631	2.629	0.240	128.6			
103.4	51.0	0.947	4.771	0.198	106.9			
6.9	6.9	0.948	3.096	0.306	22.3			
27.6	27.6	1.895	5.421	0.350	50.9			
69.0	71.0	2.210	9.105	0.243	78.0			
103.4	102.0	4.098	12.980	0.316	78.6			
27.6	40.7	5.152	11.755	0.438	34.6			
6.9	3.5	-----	0.614	-----	57.0	1.640	10.00	15.0
27.6	13.1	0.157	1.481	0.106	88.5			
69.0	34.5	0.471	2.582	0.182	133.6			
103.4	51.0	0.628	2.705	0.232	188.5			
6.9	6.9	0.251	1.699	0.148	40.6			
69.0	70.3	1.099	6.164	0.178	114.0			
103.4	101.4	0.943	6.917	0.136	146.6			
27.6	40.7	0.943	5.929	0.159	68.6			
	13.2	0.614	1.596	0.385	82.7	1.638	23.50	4.0
48.3	23.7	1.228	2.632	0.467	90.0			
69.0	34.1	1.843	2.822	0.653	120.8			
6.9	6.8	0.614	1.693	0.363	40.2			
13.8	13.7	0.615	2.445	0.252	56.0			
27.6	27.9	1.228	3.954	0.311	70.6			
48.3	48.6	1.843	5.283	0.349	92.0			
69.0	68.2	2.457	6.240	0.394	109.3			
27.6	13.6	-----	1.054	-----	129.0	1.638	20.45	7.8
48.3	24.8	-----	1.628	-----	152.3			
69.0	34.1	-----	2.203	-----	154.8			
103.5	51.6	-----	2.683	-----	192.3			
13.8	13.6	-----	1.629	-----	83.5			
27.6	27.9	-----	2.875	-----	97.0			
48.3	49.6	-----	3.634	-----	129.4			
69.0	70.2	-----	4.988	-----	140.7			
103.5	103.3	-----	5.378	-----	192.1			
6.9	3.4	-----	0.981	-----	34.7	1.616	21.40	0.0
13.8	6.7	-----	1.417	-----	47.3			
27.6	13.9	0.620	2.508	0.247	55.4			
48.3	24.6	0.620	3.272	0.189	75.2			

Confining pressure (kPa)	Deviator stress (kPa)	Radial strain $\times 10^{-4}$	Axial strain $\times 10^{-4}$	Resilient Poisson's ratio	Resilient modulus (MPa)	Dry density (Mg/m^3)	Moisture content (%)	Moisture tension (kPa)
6.9	6.7	1.240	3.167	0.392	21.2			
13.8	13.5	1.240	4.591	0.270	29.4			
27.6	27.4	1.661	6.351	0.293	43.1			
6.9	3.6	-----	0.325	-----	110.8	1.690	21.00	5.0
13.8	6.9	-----	0.651	-----	106.0			
27.6	13.9	0.620	1.518	0.408	91.6			
48.3	25.3	0.620	2.386	0.260	106.0			
69.0	33.7	0.620	2.821	0.220	119.5			
6.9	6.9	-----	1.302	-----	53.0			
13.8	13.5	-----	2.387	-----	56.6			
27.6	27.4	0.620	3.472	0.179	78.9			
	14.0	-----	1.013	-----	138.2	1.690	18.24	9.0
48.3	24.1	-----	1.519	-----	158.7			
69.0	34.1	0.605	2.126	0.285	160.4			
103.5	52.2	0.605	2.735	0.221	190.9			
13.8	13.6	0.605	1.621	0.373	83.9			
27.6	28.1	0.605	2.938	0.206	95.6			
48.3	48.1	1.210	4.054	0.298	118.6			
69.0	70.2	1.210	5.273	0.229	133.1			
103.5	102.3	1.015	6.093	0.167	167.9			
138.0	140.4	1.815	8.135	0.223	172.6			
6.9	10.4	0.605	2.237	0.270	46.5			
13.8	21.1	1.210	3.863	0.313	54.6			
27.6	42.2	1.210	5.287	0.229	79.8			
69.0	104.3	2.420	8.147	0.297	128.0			
	140.1	5.441	13.320	0.408	105.2			
27.6	25.5	11.865	20.891	0.568	12.2	1.541	25.80	0.0
6.9	3.6	0.317	0.759	0.418	47.4	1.656	24.50	4.5
27.6	15.2	0.601	2.533	0.237	60.0			
69.0	35.9	0.781	4.310	0.181	83.3			
103.4	51.7	1.012	4.569	0.221	113.2			
6.9	6.9	0.949	2.082	0.456	33.1			
27.6	29.6	1.898	5.587	0.340	53.0			
69.0	69.0	1.581	6.212	0.255	111.1			
103.4	102.7	1.898	7.245	0.262	141.8			
6.9	10.3	2.056	4.703	0.437	21.9			
27.6	40.7	4.105	9.240	0.444	44.0			
69.0	98.6	3.000	15.472	0.194	63.7			
6.9	3.5	0.065	0.656	0.099	53.4	1.656	7.20	21.0
27.6	13.8	0.189	1.287	0.147	107.2			
69.0	35.2	0.316	1.248	0.253	282.1			
103.4	52.4	0.379	2.234	0.170	234.6			
6.9	6.9	0.158	0.921	0.172	74.9			
27.6	27.6	0.316	1.776	0.178	155.4			
69.0	71.0	0.758	3.818	0.199	186.0			
103.4	104.1	0.947	4.476	0.212	232.6			

Recovered

Confining pressure (kPa)	Deviator stress (kPa)	Radial strain $\times 10^{-4}$	Axial strain $\times 10^{-4}$	Resilient Poisson's ratio	Resilient modulus (MPa)	Dry density (Mg/m^3)	Moisture content (%)	Moisture tension (kPa)
6.9	3.6	0.559	0.572	0.103	65.7	1.608	8.27	17.5
27.6	13.8	0.176	2.400	0.073	57.5			
69.0	34.8	0.587	3.416	0.172	101.9			
103.4	51.2	0.586	4.070	0.144	125.8			
27.6	27.6	1.060	4.730	0.224	58.4			
69.0	68.3	1.470	4.650	0.316	146.9			
103.4	102.4	2.060	5.710	0.361	179.3			
6.9	10.2	1.410	3.730	0.378	27.3			
27.6	42.2	2.230	6.270	0.356	67.3			
69.0	102.8	2.642	8.061	0.328	127.5			
6.9	14.6	1.759	5.010	0.351	29.1			
27.6	56.0	2.930	7.870	0.372	71.2			
	13.7	0.472	2.610	0.161	52.5	1.491	12.52	9.0
69.0	34.5	0.590	3.864	0.153	89.3			
103.4	51.5	0.826	5.128	0.161	100.4			
6.9	6.9	0.295	2.166	0.136	31.9			
27.6	28.3	0.826	4.564	0.181	62.0			
69.0	68.7	1.327	8.326	0.159	82.5			
103.4	103.0	1.769	9.195	0.192	112.0			
6.9	10.3	0.648	4.600	0.141	22.4			
27.6	42.8	1.913	8.756	0.218	48.9			
69.0	102.6	3.177	11.944	0.266	85.9			
6.9	14.4	1.530	7.183	0.213	20.0			
27.6	54.7	2.944	11.617	0.253	47.1			
6.9	4.5	1.237	1.603	0.772	28.1	1.508	12.77	11.0
27.6	13.8	0.355	2.747	0.129	50.2			
69.0	34.5	0.592	4.245	0.139	81.3			
103.4	51.9	0.740	4.142	0.179	125.3			
6.9	6.9	0.651	2.994	0.217	23.0			
27.6	27.6	1.331	5.489	0.242	50.3			

Confining pressure (kPa)	Deviator stress (kPa)	Radial strain $\times 10^{-4}$	Axial strain $\times 10^{-4}$	Resilient Poisson's ratio	Resilient modulus (MPa)	Dry density (Mg/m^3)	Moisture content (%)	Moisture tension (kPa)
69.0	69.7	2.070	7.896	0.262	88.3			
103.4	103.6	1.774	7.940	0.223	130.5			
6.9	10.3	0.591	2.570	0.230	40.1			
27.6	42.8	1.774	6.317	0.281	67.8			
69.0	103.4	3.544	10.834	0.327	95.4			
6.9	13.8	1.181	4.008	0.295	34.4			
27.6	55.0	3.246	8.274	0.392	66.5			
69.0	103.1	2.950	9.734	0.303	105.9			

Frozen

Confining pressure (kPa)	Deviator stress (kPa)	Axial strain $\times 10^{-4}$	Resilient modulus (GPa)	Dry density (Mg/m^3)	Moisture content (%)	Temperature (°C)
69.0	212.7	0.746	2.85	1.483	22.70	-0.5
	350.0	1.067	1.68			
	478.5	3.181	1.50			
	638.0	5.167	1.23			
	207.1	0.376	5.51	1.483	22.70	-3.0
	350.5	0.611	5.74			
	488.6	0.893	5.47			
	610.7	1.223	4.99			
	849.7	2.071	4.10			
	350.5	0.168	16.64	1.483	22.70	-5.0
	477.9	0.289	16.54			
	610.7	0.329	18.56			
	823.0	0.564	14.59			
	637.0	0.282	22.55	1.483	22.70	-10.0
	623.0	0.376	21.89			
	213.0	0.283	7.53	1.347	32.46	-6.8
	336.0	0.424	7.92			
	491.0	0.495	9.92			
	640.0	0.707	9.05			
	627.0	0.990	8.35			
	214.0	0.110	19.45	1.347	32.46	-5.6
	341.0	0.220	15.50			
	487.0	0.496	9.82			
	619.0	0.716	8.65			
	827.0	1.101	7.51			
	138.0	0.165	8.36	1.347	32.46	-3.0
	213.0	0.330	6.45			
	331.0	0.901	3.67			
	470.0	1.126	4.17			
	619.0	1.351	4.56			
	843.0	1.689	4.99			
	207.0	0.091	22.75	1.470	24.70	-10.0
	342.0	0.227	15.07			
	477.0	0.454	10.51			
	622.0	0.727	8.56			
	829.0	0.999	8.30			
	207.0	0.136	15.22	1.470	24.70	-5.0
	342.0	0.363	9.42			
	477.0	0.636	7.50			
	622.0	0.818	7.60			
	829.0	1.181	7.02			
	207.0	0.136	15.22	1.470	24.70	-3.0
	342.0	0.454	7.53			
	477.0	0.818	5.83			
	622.0	1.363	4.56			
	829.0	2.092	3.96			
	207.7	2.533	0.82	1.470	24.70	-0.5
	343.0	4.527	0.76			
	477.7	6.347	0.75			
	621.9	9.084	0.66			
	207.0	0.191	10.84	1.475	29.05	-4.5
	342.0	0.429	7.97			
	477.0	0.667	7.15			
	622.0	0.762	8.16			
	207.0	0.571	3.63	1.475	29.05	-3.0
	342.0	1.143	2.99			
	477.0	1.430	3.34			
	622.0	1.812	3.43			
	207.0	1.909	1.08	1.475	29.05	-0.5
	342.0	3.245	1.02			
	477.0	5.264	0.91			
	622.0	7.192	0.86			

Hyannis sand

Remolded, FWD waveform

Confining pressure (kPa)	Deviator stress (kPa)	Radial strain $\times10^{-4}$	Axial strain $\times10^{-4}$	Resilient Poisson's ratio	Resilient modulus (MPa)	Dry density (Mg/m^3)	Moisture content (%)	Moisture tension (kPa)
3.4	3.6	-----	0.648	-----	54.9	1.629	22.20	1.0
6.9	7.1	0.336	1.294	0.260	55.0			
	10.7	0.672	2.024	0.332	52.8			
	14.2	1.007	2.759	0.365	51.6			
13.8	7.1	0.336	0.974	0.345	73.1			
	14.2	0.671	2.272	0.295	62.6			
	20.5	1.007	3.410	0.295	60.0			
	27.8	1.678	4.884	0.344	56.9			
27.6	14.2	0.336	1.465	0.229	97.1			
	27.8	0.839	2.931	0.286	94.8			
	41.1	1.509	6.215	0.289	78.8			
	55.5	2.684	7.685	0.349	72.3			
6.9	7.1	0.335	0.938	0.357	75.7	1.647	13.00	8.0
	10.7	0.503	1.720	0.292	62.0			
	14.2	0.671	2.345	0.286	60.6			
	17.8	0.838	2.815	0.298	63.1			
13.8	7.1	0.168	0.938	0.179	75.7			
	14.2	0.335	1.720	0.195	82.6			
	21.1	0.671	2.815	0.238	74.9			
	28.9	1.174	3.755	0.313	76.9			
	34.4	1.509	4.853	0.311	70.9			
27.6	13.8	0.168	1.096	0.153	125.5			
	27.8	0.671	2.348	0.286	118.2			
	41.1	1.174	3.915	0.300	104.9			
	55.5	1.844	5.954	0.310	93.2			
6.9	7.1	0.168	0.665	0.253	106.9	1.649	7.75	12.0
	10.7	0.336	1.163	0.289	91.7			
	14.2	0.504	1.661	0.303	85.6			
	17.8	0.671	2.159	0.311	82.3			
13.8	7.1	0.168	0.831	0.202	85.5			
	14.2	0.335	1.661	0.202	85.6			
	21.1	0.671	2.326	0.288	90.7			
	27.8	1.007	3.156	0.319	88.0			
	34.4	1.342	4.154	0.323	82.9			
27.6	41.1	1.007	3.656	0.275	112.4			
	55.5	1.510	5.153	0.293	107.7			
	71.1	2.013	7.321	0.275	97.1			
6.9	10.7	0.673	1.472	0.457	72.9	1.659	22.20	1.0
	14.3	1.010	2.127	0.475	67.3			
	17.4	1.346	2.947	0.457	59.1			
13.8	7.2	0.169	0.655	0.258	109.2			
	14.3	0.505	1.637	0.308	87.4			
	21.2	1.010	2.620	0.385	81.0			
	27.9	1.346	3.768	0.357	74.2			
	34.6	2.018	4.921	0.410	70.3			
27.6	14.3	0.336	1.477	0.227	96.8			
	27.9	0.841	2.954	0.285	94.4			
	41.3	1.514	4.760	0.318	86.7			
	55.8	2.523	6.899	0.366	80.9			
	14.0	0.344	1.229	0.280	114.2	1.713	7.75	12.0
	28.1	0.688	2.621	0.262	107.1			
	42.1	1.033	4.096	0.252	102.8			
	56.1	1.721	5.572	0.309	100.7			
	70.1	2.409	6.560	0.367	106.9			
	14.1	0.334	1.957	0.171	72.0	1.675	13.00	8.0
	28.6	0.668	3.203	0.209	89.4			
	41.8	1.336	4.984	0.268	83.9			
	55.0	1.837	6.413	0.286	85.8			
	70.5	2.672	8.030	0.333	87.8			
6.9	3.7	0.172	0.664	0.259	56.4	1.712	22.20	1.0
	7.0	0.344	1.329	0.259	52.8			
	10.3	0.689	1.994	0.346	51.6			
	14.0	1.033	2.993	0.345	46.9			
	17.3	1.377	3.327	0.414	52.0			
13.8	7.0	0.172	0.832	0.207	84.4			
	14.0	0.689	1.996	0.345	70.3			
	20.6	1.033	2.995	0.345	68.7			
	28.1	1.550	4.329	0.358	64.9			
	35.1	2.066	5.002	0.413	70.2			
27.6	14.0	0.344	1.335	0.258	105.2			
	28.1	0.861	2.836	0.304	99.0			
	42.1	1.377	4.339	0.317	97.0			
	56.1	2.238	6.515	0.344	86.2			

Confining pressure (kPa)	Deviator stress (kPa)	Radial strain x10^{-4}	Axial strain x10^{-4}	Resilient Poisson's ratio	Resilient modulus (MPa)	Dry density (Mg/m^3)	Moisture content (%)	Moisture tension (kPa)
	70.2	2.753	7.867	0.350	89.2			
6.9	3.5	-----	0.713	-----	48.6	1.686	13.00	8.0
	6.9	0.354	1.070	0.331	64.8			
	10.4	0.708	1.783	0.397	58.3			
	14.3	0.886	2.496	0.355	57.5			
	17.3	1.240	3.031	0.409	57.1			
13.8	6.9	0.177	0.892	0.198	77.7			
	13.9	0.532	1.872	0.284	74.0			
	20.8	0.886	2.853	0.311	72.9			
	27.2	1.418	3.924	0.361	69.4			
	34.6	1.949	4.996	0.390	69.4			
27.6	13.9	0.354	1.606	0.220	86.3			
13.8	6.9	0.177	0.839	0.211	82.2	1.624	7.75	12.0
	13.8	0.530	1.677	0.316	82.2			
	20.7	0.883	2.516	0.351	82.2			
	27.1	1.236	3.355	0.368	80.8			
	34.5	1.766	4.362	0.405	79.1			
27.6	13.8	0.353	1.174	0.301	117.5			
	27.1	0.707	2.685	0.263	100.9			
	41.9	1.242	4.027	0.308	104.0			
	54.2	1.943	5.373	0.362	100.9			
	68.9	2.826	6.720	0.421	102.6			
6.9	3.5	0.177	0.673	0.263	51.3	1.695	22.00	2.0
	6.9	0.531	1.346	0.395	51.3			
	10.8	0.884	2.020	0.438	53.7			
	13.8	1.237	2.695	0.459	51.2			
	17.2	1.766	3.543	0.498	48.7			
13.8	6.9	0.353	0.844	0.418	81.7			
	13.8	0.707	2.024	0.349	68.1			
	20.6	1.236	3.036	0.407	68.0			
	28.3	1.766	4.220	0.418	67.1			
	34.4	2.472	5.747	0.430	59.9			
27.6	13.8	0.353	1.352	0.261	101.9			
	27.1	0.883	2.872	0.307	94.3			
	41.8	1.765	4.395	0.402	95.2			
	54.1	2.471	6.095	0.405	88.8			
6.9	10.3	0.882	1.881	0.469	54.9	1.637	21.00	4.0
	13.8	1.235	2.621	0.471	52.5			
	17.6	1.762	3.284	0.537	53.7			
13.8	6.9	0.353	0.821	0.430	83.6			
	13.7	0.705	1.970	0.358	69.7			
	20.6	1.234	2.792	0.442	73.7			
	27.0	2.115	4.278	0.494	63.0			
27.6	27.0	1.058	2.962	0.357	91.0			
	41.7	2.115	4.447	0.476	93.7			
	53.9	3.171	6.612	0.480	81.5			
13.8	7.2	0.174	0.742	0.235	97.5	1.686	21.80	2.0
	13.5	0.699	1.856	0.377	72.8			
	20.3	1.049	2.971	0.353	68.2			
	26.5	1.748	4.086	0.428	64.9			
	35.0	2.447	5.203	0.470	67.2			
27.6	13.5	0.350	1.301	0.269	103.8			
	27.7	1.224	2.601	0.471	106.6			
	41.0	1.748	4.461	0.392	91.9			
	55.5	2.971	6.138	0.484	90.4			

Remolded, RPB waveform

Confining pressure (kPa)	Deviator stress (kPa)	Radial strain x10^{-4}	Axial strain x10^{-4}	Resilient Poisson's ratio	Resilient modulus (MPa)	Dry density (Mg/m^3)	Moisture content (%)	Moisture tension (kPa)
3.4	3.6	-----	0.648	-----	54.9	1.625	22.20	1.0
6.9	7.1	0.336	1.213	0.277	58.7			
	10.7	0.672	2.024	0.332	52.8			
	14.2	0.839	2.433	0.345	56.5			
13.8	7.1	0.336	0.893	0.376	79.7			
	14.2	0.671	2.110	0.318	67.4			
	20.5	1.007	3.248	0.310	63.0			
	27.8	1.678	4.231	0.397	65.7			
27.6	14.2	0.336	1.140	0.295	124.7			
	27.8	0.839	2.768	0.303	100.4			
	41.1	1.509	4.562	0.331	90.1			
	55.5	2.684	6.211	0.432	89.4			
6.9	14.2	0.504	1.661	0.303	85.6	1.649	7.75	12.0
	17.8	0.671	2.076	0.323	85.5			
27.6	13.8	0.168	0.914	0.184	150.7			
	27.8	0.671	2.077	0.323	133.7			
	41.1	1.007	3.157	0.319	130.1			
	55.5	1.510	4.488	0.336	123.7			
	71.1	2.013	6.323	0.318	112.4			
6.9	3.3	-----	0.621	-----	53.2	1.675	13.00	8.0
	7.0	0.334	1.420	0.235	49.6			
	10.6	0.501	1.953	0.257	54.1			
	13.6	0.668	2.575	0.259	53.0			
	16.7	0.835	3.197	0.261	52.4			

Confining pressure (kPa)	Deviator stress (kPa)	Radial strain x10^{-4}	Axial strain x10^{-4}	Resilient Poisson's ratio	Resilient modulus (MPa)	Dry density (Mg/m^3)	Moisture content (%)	Moisture tension (kPa)
13.8	7.0	0.167	1.243	0.134	56.7			
	14.1	0.501	2.220	0.226	63.5			
	21.1	0.835	3.197	0.261	66.1			
	27.5	1.169	4.266	0.274	64.5			
	35.2	1.670	5.338	0.313	66.0			
27.6	14.1	0.334	1.779	0.188	79.2			
	28.6	0.668	3.203	0.209	89.4			
	41.8	1.336	4.806	0.278	87.1			
	55.0	1.837	6.057	0.303	90.9			
	70.5	2.505	8.030	0.312	87.8			
6.9	3.3	-----	0.491	-----	66.7	1.713	7.75	12.0
	6.5	0.172	0.901	0.191	72.7			
	10.3	0.344	1.473	0.234	69.9			
	13.1	0.517	1.965	0.263	66.6			
	16.8	0.688	2.456	0.280	68.5			
13.8	6.5	0.172	0.737	0.233	88.8			
	13.1	0.344	1.555	0.221	84.2			
	20.6	0.688	2.538	0.271	81.1			
	28.1	1.033	3.603	0.287	77.9			
	32.7	1.205	4.260	0.283	76.8			
27.6	14.0	0.344	1.229	0.280	114.2			
	28.1	0.688	2.457	0.280	114.2			
	42.1	1.205	3.932	0.306	107.0			
	56.1	1.721	5.572	0.309	100.7			
	70.1	2.237	6.560	0.341	106.9			
6.9	3.5	-----	0.624	-----	55.5	1.686	13.00	8.0
	6.9	-----	0.713	-----	97.2			
	10.4	0.708	1.783	0.397	58.3			
	14.3	0.886	2.406	0.368	59.6			
	17.3	1.240	3.031	0.409	57.1			
13.8	6.9	0.177	0.892	0.198	77.7			
	13.9	0.532	1.872	0.284	74.0			
	20.8	0.886	2.853	0.311	72.9			
	27.2	1.418	3.924	0.361	69.4			
	34.6	1.772	4.640	0.382	74.7			
27.6	13.9	0.354	1.606	0.220	86.3			
	69.3	3.365	7.518	0.448	92.2			
6.9	3.4	-----	0.503	-----	68.6	1.624	7.75	12.0
	6.9	0.353	0.839	0.421	82.2			
	10.8	0.530	1.426	0.372	76.0			
	13.8	0.707	2.013	0.351	68.5			
	17.2	0.883	2.432	0.363	70.9			
13.8	6.9	0.177	0.755	0.234	91.4			
	13.8	0.530	1.510	0.351	91.3			
	20.7	0.883	2.348	0.376	88.1			
	27.1	1.060	3.187	0.333	85.0			
	34.5	1.766	4.195	0.421	82.2			
27.6	13.8	0.353	1.174	0.301	117.5			
	27.1	0.707	2.517	0.281	107.7			
	41.9	1.419	3.691	0.384	113.5			
	54.2	1.943	5.037	0.386	107.6			
	68.9	2.826	6.384	0.443	108.0			
6.9	3.5	0.177	0.673	0.263	51.3	1.695	22.00	2.0
	6.9	0.531	1.178	0.451	58.6			
	10.8	0.884	2.020	0.438	53.7			
	13.8	1.237	2.695	0.459	51.2			
	17.2	1.766	3.540	0.499	48.7			
13.8	13.8	0.707	1.771	0.399	77.9			
	20.6	1.236	2.615	0.473	78.9			
	28.3	1.766	3.714	0.475	76.3			
	34.4	2.472	4.731	0.523	72.8			
27.6	13.8	0.353	1.352	0.261	101.9			
	27.1	0.883	2.872	0.307	94.3			
	41.8	1.765	4.226	0.418	99.0			
	54.1	2.471	5.078	0.487	106.5			
6.9	10.3	0.682	1.881	0.469	54.9	1.637	21.00	4.0
	13.8	1.235	2.457	0.503	56.0			
	17.6	1.762	3.119	0.565	56.6			
13.8	6.9	0.353	0.903	0.391	76.0			
	13.7	0.705	1.888	0.373	72.7			
	20.6	1.234	2.628	0.470	78.3			
	27.0	2.115	3.949	0.536	68.3			
27.6	27.0	1.058	2.633	0.402	102.4			
	41.7	2.115	4.117	0.514	101.2			
	56.3	3.171	5.947	0.533	94.7			
6.9	6.8	0.350	0.557	0.628	121.3	1.686	21.80	2.0
	10.6	0.525	0.926	0.567	114.7			
	13.5	0.700	1.668	0.420	81.0			
	17.4	1.049	2.227	0.471	78.0			

Confining pressure (kPa)	Deviator stress (kPa)	Radial strain x10^{-4}	Axial strain x10^{-4}	Resilient Poisson's ratio	Resilient modulus (MPa)	Dry density (Mg/m^3)	Moisture content (%)	Moisture tension (kPa)
13.8	7.2	0.174	0.557	0.312	129.9			
	13.5	0.525	1.392	0.377	97.1			
	20.3	1.049	2.599	0.404	78.0			
	26.5	1.398	3.715	0.376	71.4			
	35.0	2.097	4.831	0.434	72.4			
27.6	13.5	0.350	0.923	0.379	146.4			
	27.7	1.049	2.415	0.434	114.8			
	41.0	1.748	3.717	0.470	110.3			
	55.5	2.797	5.208	0.537	106.5			

Thawed, RPB waveform

Confining pressure (kPa)	Deviator stress (kPa)	Radial strain x10^{-4}	Axial strain x10^{-4}	Resilient Poisson's ratio	Resilient modulus (MPa)	Dry density (Mg/m^3)	Moisture content (%)	Moisture tension (kPa)
13.8	6.8	0.968	1.571	0.616	43.2	1.389	22.30	-1.0
27.6	13.9	2.895	5.091	0.569	27.3			
6.9	6.9	1.600	2.296	0.697	29.9			
51.7	23.2	5.431	7.559	0.718	30.6	1.389	22.30	1.0
6.9	6.6	0.958	1.980	0.484	33.6			
13.8	13.3	2.554	4.141	0.617	32.1			
27.6	26.9	8.427	10.200	0.826	26.4			
6.9	3.7	0.323	0.792	0.408	46.9	1.511	22.30	0.0
13.8	6.8	0.646	1.584	0.408	42.9			
27.6	13.6	1.291	2.776	0.465	48.8			
6.9	6.8	1.597	2.014	0.793	34.0			
27.6	14.0	0.645	1.866	0.346	74.9	1.511	21.80	2.0
51.7	24.6	0.645	2.489	0.259	98.8			
6.9	6.9	0.966	2.137	0.452	32.5			
13.8	13.9	1.610	3.564	0.452	39.0			
27.6	26.6	1.931	4.458	0.433	59.6			
	13.7	0.320	1.628	0.197	84.3	1.577	13.28	8.0
6.9	7.1	0.320	1.267	0.253	55.8			
13.8	13.7	0.460	2.172	0.221	[illegible]			
27.6	28.3	0.800	3.801	0.210	74.4			
51.7	50.5	1.280	5.435	0.236	92.9			
69.0	68.7	1.600	6.709	0.238	102.4			
6.9	9.6	0.320	1.994	0.160	48.3			
13.8	21.2	1.278	3.629	0.352	58.3			
27.6	41.3	1.917	5.816	0.330	71.0			
51.7	72.5	-----	6.736	-----	107.6			
69.0	104.7	3.194	9.124	0.350	114.8			
6.9	13.7	1.278	3.468	0.369	39.5			
	3.4	-----	0.811	-----	41.7	1.408	22.00	2.0
	6.8	0.491	1.713	0.287	39.5			
	10.1	0.982	2.888	0.340	35.1			
	13.5	1.145	3.615	0.317	37.4			
	16.9	1.800	4.889	0.368	34.6			
13.8	6.8	0.327	1.629	0.201	41.5			
	13.5	0.655	3.077	0.213	43.9			
	21.1	1.636	5.072	0.323	41.7			
	27.5	2.455	6.353	0.386	43.2			
	33.8	3.599	7.647	0.471	44.2			
27.6	13.5	0.491	2.004	0.245	67.5			
	27.5	1.308	4.373	0.299	62.8			
13.8	27.1	2.233	5.481	0.407	49.5	1.577	13.30	8.0
27.6	56.1	3.824	8.603	0.444	65.2			
48.3	96.0	3.821	11.010	0.347	87.2			
6.9	21.0	1.911	6.424	0.297	32.7			
13.8	41.1	6.298	10.570	0.596	38.9			
27.6	77.4	6.187	14.240	0.434	54.4			
	42.3	2.290	6.565	0.349	64.4	1.408	20.50	3.0
	54.9	3.597	8.596	0.418	63.8			
69.0	33.8	0.654	3.111	0.210	108.5			
	67.5	1.798	6.408	0.281	105.4			
6.9	3.4	-----	0.635	-----	53.4	1.434	18.50	5.0
	6.8	0.492	1.632	0.301	41.5			
	10.2	0.983	2.540	0.387	40.0			
	13.6	1.310	3.448	0.380	39.3			
	16.9	1.638	4.720	0.347	35.9			
13.8	6.8	0.328	1.271	0.258	53.3			
	13.6	0.655	2.814	0.233	48.2			
	21.2	1.474	4.359	0.338	48.6			
	27.5	1.802	5.614	0.310	47.4			
	33.9	2.948	6.727	0.438	50.4			
27.6	13.6	0.492	1.818	0.271	74.6			
	27.5	1.147	3.818	0.300	72.1			
	42.4	2.129	6.366	0.334	66.6			
	55.1	3.440	8.194	0.420	67.2			
	67.7	4.583	10.410	0.440	65.0			

Confining pressure (kPa)	Deviator stress (kPa)	Radial strain $\times 10^{-4}$	Axial strain $\times 10^{-4}$	Resilient Poisson's ratio	Resilient modulus (MPa)	Dry density (Mg/m^3)	Moisture content (%)	Moisture tension (kPa)
69.0	33.8	0.655	2.925	0.224	115.7			
	67.7	1.636	6.035	0.271	112.1			
6.9	6.8	0.329	1.294	0.254	52.8	1.451	11.50	9.0
	10.3	0.658	2.219	0.297	46.2			
	13.7	0.823	2.959	0.278	46.2			
	17.1	1.152	3.885	0.297	44.0			
13.8	6.8	0.329	1.017	0.324	67.2			
	13.7	0.658	1.942	0.339	70.4			
	21.4	1.316	3.515	0.374	60.8			
	27.8	1.645	4.811	0.342	57.7			
	34.2	2.139	5.926	0.361	57.7			
27.6	13.7	0.329	1.481	0.222	92.3			
	27.8	0.987	3.426	0.288	81.1			
	42.7	1.810	5.372	0.337	79.5			
	55.5	2.632	7.416	0.355	74.9			
	68.3	3.618	8.912	0.406	76.6			
69.0	34.1	0.658	2.506	0.263	136.3			
	68.3	1.480	5.015	0.295	136.2			
6.9	6.9	-----	0.773	-----	88.8	1.453	8.50	14.0
	13.7	0.659	1.740	0.379	78.9			
	17.1	0.989	2.224	0.445	77.1			
13.8	13.7	0.495	1.160	0.427	118.3			
	21.4	0.989	2.321	0.426	92.4			
	27.9	1.318	3.483	0.378	80.0			
	34.3	1.648	4.839	0.341	70.9			
27.6	13.7	0.329	1.258	0.262	109.1			
	27.9	0.659	3.194	0.206	87.3			
	42.9	1.483	5.035	0.295	85.2			
	55.7	2.307	6.977	0.331	79.9			
	68.6	3.295	8.728	0.378	78.6			
69.0	34.3	0.659	2.424	0.272	141.5			
	68.6	1.483	5.043	0.294	136.0			
48.3	24.7	0.474	5.543	0.086	44.5	1.374	21.00	4.0
13.8	13.8	0.316	3.464	0.091	39.9			
27.6	27.6	0.632	6.487	0.097	42.5			
	13.8	0.316	2.906	0.109	47.5	1.385	18.00	6.0
48.3	24.6	0.632	4.926	0.128	50.0			
69.0	34.4	0.790	5.848	0.135	58.8			
6.9	6.9	-----	0.675	-----	102.0			
13.8	13.8	0.316	2.137	0.148	64.4			
27.6	27.5	0.632	4.950	0.128	55.7			
48.3	48.9	1.890	9.132	0.207	53.6			

Thawed, FWD waveform

Confining pressure (kPa)	Deviator stress (kPa)	Radial strain $\times 10^{-4}$	Axial strain $\times 10^{-4}$	Resilient Poisson's ratio	Resilient modulus (MPa)	Dry density (Mg/m^3)	Moisture content (%)	Moisture tension (kPa)
6.9	3.4	-----	0.901	-----	37.5	1.408	22.00	2.0
	6.8	0.491	1.803	0.272	37.5			
	10.1	0.655	2.888	0.227	35.1			
	13.5	0.491	3.977	0.123	34.0			
	16.9	1.473	5.250	0.281	32.2			
13.8	6.8	-----	1.629	-----	41.5			
	13.5	0.655	3.077	0.213	43.9			
	21.1	1.309	5.616	0.233	37.6			
	27.5	1.964	7.262	0.270	37.8			
	33.8	3.108	9.475	0.328	35.7			
27.6	13.5	0.327	2.004	0.163	67.5			
	27.5	0.818	4.555	0.180	60.3			
	42.3	1.472	7.294	0.202	57.9	1.408	20.50	3.0
	54.9	2.943	10.070	0.292	54.5			
69.0	33.8	0.491	3.294	0.149	102.5			
	67.5	1.308	6.957	0.188	97.1			
6.9	3.4	-----	0.725	-----	46.7	1.434	18.50	5.0
	10.2	0.655	2.358	0.278	43.1			
	13.6	0.983	3.267	0.301	41.5			

Confining pressure (kPa)	Deviator stress (kPa)	Radial strain x10^{-4}	Axial strain x10^{-4}	Resilient Poisson's ratio	Resilient modulus (MPa)	Dry density (Mg/m^3)	Moisture content (%)	Moisture tension (kPa)
13.8	6.8	-----	1.452	-----	46.7	1.434	22.00	2.0
	13.6	0.655	2.905	0.225	46.7	1.430	18.50	5.0
	21.2	0.983	4.541	0.216	46.6			
	27.5	1.474	6.177	0.239	44.6			
	33.9	2.129	7.636	0.279	44.4			
27.6	13.6	0.328	2.182	0.150	62.1			
	27.5	0.819	4.727	0.173	58.3			
	55.1	2.457	9.468	0.260	58.2			
	67.7	3.271	11.880	0.275	57.0			
69.0	33.8	0.491	3.108	0.158	108.8			
	67.7	1.145	6.218	0.184	108.8			
6.9	3.4	-----	0.740	-----	46.2	1.451	11.50	9.0
	6.8	0.329	1.479	0.222	46.2			
	10.3	0.658	2.219	0.297	46.2			
	13.7	0.823	3.143	0.262	43.5			
	17.1	0.987	4.070	0.243	42.0			
13.8	13.7	0.658	2.405	0.274	56.8			
	21.4	1.316	4.070	0.323	52.5			
	27.8	1.642	5.366	0.306	51.8			
27.6	13.7	0.329	1.481	0.222	92.3			
	27.8	0.987	3.519	0.280	78.9			
	42.7	1.810	6.113	0.296	69.9			
	55.5	2.632	8.343	0.315	66.6			
	68.3	3.618	10.210	0.354	66.9			
69.0	34.1	0.658	2.599	0.253	131.4			
	68.3	1.480	5.386	0.275	126.8			
6.9	6.9	-----	0.773	-----	88.8	1.453	8.50	14.0
	10.3	0.495	1.547	0.320	66.5			
	13.7	0.659	2.320	0.284	59.1			
	17.1	1.153	3.894	0.296	44.0			
13.8	6.9	-----	0.773	-----	88.8			
	13.7	0.495	1.740	0.284	78.9			
	21.4	0.989	3.288	0.301	65.2			
	27.9	1.318	4.644	0.284	60.0			
	34.3	1.648	6.194	0.266	55.4			
27.6	13.7	0.329	1.549	0.212	88.6			
	27.9	0.989	3.678	0.269	75.8			
	42.9	1.648	5.809	0.284	73.8			
	55.7	2.636	7.946	0.332	70.1			
	68.6	3.295	9.697	0.340	70.8			
69.0	34.3	0.659	2.521	0.261	136.1			
	68.6	1.318	5.431	0.243	126.3			

Recovered

Confining pressure (kPa)	Deviator stress (kPa)	Radial strain x10^{-4}	Axial strain x10^{-4}	Resilient Poisson's ratio	Resilient modulus (MPa)	Dry density (Mg/m^3)	Moisture content (%)	Moisture tension (kPa)
27.6	13.8	-----	1.329	-----	104.2	1.585	18.00	6.0
69.0	34.6	-----	2.394	-----	144.6			
103.5	51.9	-----	3.193	-----	162.6			
6.9	6.9	-----	0.798	-----	86.8			
27.6	27.7	0.296	3.195	0.093	86.7			
69.0	69.2	0.592	5.061	0.117	136.8			
103.5	103.9	0.592	6.403	0.092	162.2			
6.9	10.4	0.592	2.670	0.222	38.9			
27.6	54.9	0.592	5.879	0.101	93.4			
69.0	138.3	1.480	9.439	0.157	146.5			
103.5	189.9	1.479	11.680	0.127	162.6			
6.9	20.7	0.591	4.899	0.121	42.3			
27.6	82.5	1.771	9.626	0.184	85.7			
69.0	34.9	-----	2.425	-----	144.0	1.546	19.29	5.5
103.5	53.9	0.301	2.697	0.112	200.0			
6.9	7.0	-----	0.944	-----	74.0			
27.6	27.8	0.603	4.191	0.144	66.2			
69.0	71.6	0.603	6.233	0.097	114.9			
103.5	103.9	0.904	8.143	0.111	127.6			
6.9	14.3	0.602	2.450	0.246	58.4			
27.6	55.0	1.499	5.599	0.268	98.2			
69.0	140.5	1.492	5.855	0.255	240.0			
103.5	210.8	1.193	5.879	0.203	358.5			
6.9	3.4	-----	0.859	-----	40.2	1.608	17.59	6.0
27.6	13.8	-----	3.007	-----	45.9			
69.0	34.5	0.296	4.300	0.069	80.2			
103.5	53.5	0.591	4.303	0.137	124.3			
6.9	6.7	-----	2.438	-----	27.6			
69.0	70.7	0.591	5.760	0.103	122.8			
103.5	103.5	1.183	6.367	0.186	162.6			
6.9	14.1	0.591	4.638	0.127	30.5			
69.0	136.3	1.469	15.000	0.098	90.9			
103.5	195.9	2.057	18.130	0.113	108.1			

Frozen, RPB waveform

Confining pressure (kPa)	Deviator stress (kPa)	Axial strain x10^{-4}	Resilient modulus (GPa)	Dry density (Mg/m^3)	Moisture content (%)	Temperature (°C)
69.0	137.1	0.966	1.42	1.366	28.80	-0.5
	211.0	1.127	1.87			
	348.1	2.093	1.66			
	485.3	3.224	1.51			
	633.0	3.634	1.74			
	211.0	0.161	13.10	1.366	28.80	-3.0
	348.1	0.282	12.34			
	485.3	0.403	12.04			
	633.0	0.644	9.83			
	843.9	1.207	6.99			
	474.7	0.121	39.23	1.366	28.80	-5.0
	606.6	0.242	25.07			
	843.9	0.563	14.99			
	485.3	0.040	121.32	1.366	28.80	-10.0
	633.0	0.121	52.31			
	843.9	0.201	41.99			
	346.5	0.506	6.85	1.441	29.10	-0.5
	483.1	0.928	5.21			
	630.1	1.434	4.39			
	840.1	2.027	4.14			
	483.0	0.253	19.09	1.441	29.10	-3.0
	630.1	0.422	14.93			
	840.1	0.549	15.30			
	483.1	0.085	56.84	1.441	29.10	-5.0
	630.1	0.169	37.28			
	840.1	0.253	33.21			
	483.1	0.085	56.84	1.441	29.10	-10.0
	630.1	0.127	49.61			
	840.1	0.169	49.71			
	210.0	1.197	1.75	1.374	29.40	-0.5
	347.0	2.210	1.57			
	483.5	3.316	1.46			
	630.6	4.425	1.43			
	841.0	6.462	1.30			
	210.2	0.092	22.85	1.374	29.40	-3.0
	346.5	0.276	12.55			
	483.5	0.552	8.76			
	630.6	0.920	6.85			
	840.9	1.656	5.08			
	210.2	0.138	15.23	1.374	29.40	-5.0
	346.9	0.230	15.08			
	483.5	0.368	13.14			
	630.6	0.552	11.42			
	841.0	0.920	9.14			
	210.2	0.046	45.70	1.374	29.40	-10.0
	346.9	0.092	37.71			
	483.5	0.184	26.28			
	630.6	0.276	22.85			
	840.9	0.368	22.85			

Dense Graded Stone

Thawed, RPB waveform

Confining pressure (kPa)	Deviator stress (kPa)	Radial strain x10^{-4}	Axial strain x10^{-4}	Resilient Poisson's ratio	Resilient modulus (MPa)	Dry density (Mg/m^3)	Moisture content (%)	Moisture tension (kPa)
13.8	10.3	0.853	1.896	0.450	54.4	1.970	6.25	3.0
	13.5	0.960	2.168	0.443	62.1			
27.6	13.5	0.640	1.491	0.429	90.3			
6.9	6.7	-----	0.433	-----	155.5	1.970	5.50	31.0
	10.3	0.213	0.731	0.291	141.2			
	13.5	0.320	0.947	0.338	142.1			
	16.8	0.320	1.218	0.263	138.2			
13.8	6.7	0.107	0.379	0.282	177.6			
	13.5	0.213	0.866	0.246	155.4			
	20.2	0.320	1.353	0.237	149.2			
	26.9	0.427	1.759	0.243	153.0			
	33.7	0.533	2.220	0.240	151.6			
27.6	13.5	0.107	0.704	0.152	191.2			
	26.9	0.320	1.489	0.215	180.8			
	41.5	0.640	2.302	0.278	180.3			
48.3	48.2	0.640	2.168	0.295	222.5			
	70.1	0.853	3.255	0.262	215.4			
6.9	7.0	0.747	0.946	0.790	73.6	2.112	16.00	0.0
	10.3	1.279	1.353	0.945	76.2			

Confining pressure (kPa)	Deviator stress (kPa)	Radial strain $\times 10^{-4}$	Axial strain $\times 10^{-4}$	Resilient Poisson's ratio	Resilient modulus (MPa)	Dry density (Mg/m^3)	Moisture content (%)	Moisture tension (kPa)
13.8	6.7	0.639	0.596	1.072	112.8			
	13.3	2.124	2.171	0.978	61.5			
6.9	3.3	-----	0.243	-----	137.2	2.112	6.00	10.0
	6.7	-----	0.514	-----	129.8			
	10.2	0.106	0.838	0.126	122.1			
	13.3	0.212	1.216	0.174	109.7			
	16.7	0.319	1.406	0.227	118.6			
13.8	6.7	-----	0.514	-----	129.8			
	13.3	0.212	1.054	0.201	126.6			
	20.0	0.265	1.487	0.178	134.6			
	26.7	0.478	1.893	0.253	140.9			
27.6	13.3	0.106	0.784	0.135	170.2			
	26.7	0.319	1.758	0.181	151.8			
	41.1	0.743	2.569	0.289	160.1			
6.9	3.3	0.106	0.514	0.206	64.8	2.170	8.50	2.0
	6.7	0.212	1.081	0.196	61.6			
	10.2	0.318	1.677	0.190	60.9			
13.8	6.7	0.212	0.757	0.280	88.0			
	13.3	0.424	1.758	0.241	75.8			
27.6	13.3	0.318	1.272	0.250	104.7			
6.9	6.7	0.106	0.460	0.230	144.8	2.170	6.00	16.0
	10.2	0.212	0.785	0.270	130.1			
	13.3	0.318	1.137	0.280	117.2			
	16.6	0.424	1.489	0.285	111.8			
13.8	6.7	0.212	0.379	0.559	175.7			
	13.3	0.318	0.948	0.335	140.5			
	20.5	0.424	1.408	0.301	145.8			
	26.6	0.530	2.085	0.254	127.8			
27.6	13.3	0.318	0.731	0.435	182.2			
	26.6	0.530	1.680	0.315	158.6			
	41.1	0.742	2.710	0.274	151.5			
6.9	10.2	0.212	0.596	0.356	171.3	2.170	5.50	29.0
	13.3	0.318	0.949	0.335	140.4			
	16.6	0.318	1.274	0.250	130.7			
13.8	6.7	0.106	0.407	0.260	163.6			
	13.3	0.212	0.949	0.223	140.4			
	20.5	0.318	1.356	0.235	151.4			
	26.6	0.424	1.898	0.223	140.4			
	34.4	0.636	2.441	0.261	140.9			
27.6	13.3	0.212	0.759	0.279	175.5			
	26.6	0.318	1.681	0.189	158.5			
	41.1	0.636	2.576	0.247	159.4			
	55.5	0.742	3.310	0.224	167.6			
69.0	66.6	0.849	2.986	0.284	223.0			
	133.2	-----	7.070	-----	188.4			

Frozen, RPB waveform

Confining pressure (kPa)	Deviator stress (kPa)	Axial strain $\times 10^{-4}$	Resilient modulus (GPa)	Dry density (Mg/m^3)	Moisture content (%)	Temperature (°C)
69.0	280.6	0.077	36.44	1.788	21.78	-4.1
	348.0	0.129	26.98			
	483.0	0.231	20.91			
	617.4	0.463	13.33			
	841.9	0.514	16.38			
	70.4	0.038	18.54	1.788	21.78	-0.5
	140.9	0.180	7.83			
	202.9	0.333	6.09			
	281.6	0.411	6.85			
	70.3	0.437	1.61	1.788	21.78	-0.1
27.6	40.5	0.437	0.93			
	56.2	0.308	1.83			
	67.4	0.411	1.64			
48.3	47.2	0.218	2.17			
	73.0	0.463	1.58			
	95.5	0.720	1.33			
	123.5	0.951	1.30			
69.0	344.0	0.061	56.39	1.831	16.09	-8.2
	477.2	0.122	39.11			
	610.4	0.195	31.30			
	832.4	0.293	28.41			

A facsimile catalog card in Library of Congress MARC format is reproduced below.

Cole, D.
Resilient modulus of freeze-thaw affected granular soils for pavement design and evaluation. Part 1: Laboratory tests on soil from Winchendon, Massachusetts, test sections / by D. Cole, D. Bentley, G. Durell and T. Johnson. Hanover, N.H.: Cold Regions Research and Engineering Laboratory; Springfield, Va.: available from National Technical Information Service, 1986.
vi, 78 p., illus.; 28 cm. (CRREL Report 86-4.)
Prepared for Office of the Chief of Engineers by Corps of Engineers, U.S. Army Cold Regions Research and Engineering Laboratory under DA Project 4A762730AT42.
Bibliography: p. 21.

(continued on Card 2)

Cole, D. (CARD 2)
Resilient modulus of freeze-thaw.... (1986)

1. Airfields. 2. Freezing-thawing. 3. Laboratory tests. 4. Repeated-load triaxial tests. 5. Resilient moduli. 6. Roads. 7. Soil tests. 8. Subgrade soils. I. Bentley, D. II. Durell, G. III. Johnson, T. IV. United States. Army. Corps of Engineers. V. Cold Regions Research and Engineering Laboratory, Hanover, N.H. VI. Series: CRREL Report 86-4/.

END

10-86

DTIC